www.cardiol.br

www.dicsbc.org

ABC Imagem Cardiovascular

Sociedade Brasileira de Cardiologia • ISSN 2675-312X • Volume 35, N° 1, January/February/March 2022

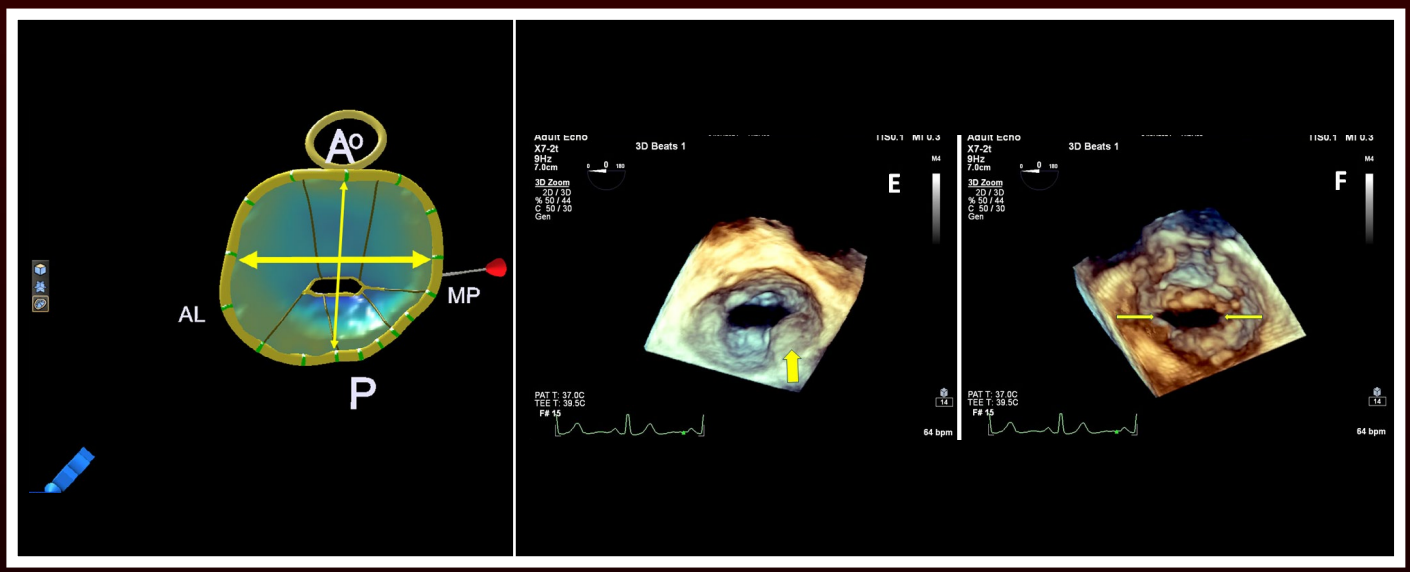

Arquivos Brasileiros de Cardiologia - Imagem Cardiovascular

Volume 35, Nº 1, January/February/March 2021

Indexing source: LILACS - Literatura Latino-Americana e do Caribe em Ciências da Saúde - www.bireme.br, LATINDEX - Sistema Regional de Información en Línea para Revistas Científicas de América Latina, El Caribe, España y Portugal - www.latindex.unam.mx

Department of Cardiovascular Imaging/ Brazilian Society of Cardiology
Rua Barata Ribeiro nº 380 cj.54
01308-000 - São Paulo - SP - Brasil
Fone/Fax: +55 (11) 3259-2988
Fones: +55 (11) 3120-3363
+55 (11) 3259-2988 / +55 (11) 2589-4168

Editorial Coordination
Atha Comunicação e Editora
Rua Machado Bittencourt, 190 - conj. 409
São Paulo, SP, Brasil
Tel.: (11) 50879502

Editorial Support
revista@dicsbc.com

The journal Arquivos Brasileiros de Cardiologia — Imagem Cardiovascular is the official body of the Department of Cardiovascular Imaging of the Brazilian Society of Cardiology.

www.cardiol.br
www.dicsbc.org
ABC Imagem Cardiovascular

Contents - *Sumário*

Click on the title to read the article

www.cardiol.br
www.dicsbc.org
ABC Imagem Cardiovascular

Review article - Artigo de Revisão

Case Reports - Relatos de Caso

Images - Imagens

www.cardiol.br
www.dicsbc.org
ABC Imagem Cardiovascular

Editorial Board Imagem Cardiovascular

National Editorial Board

Brivaldo Markman Filho - Hospital das Clínicas da Universidade Federal de Pernambuco – PE

Bruna Morhy Borges Leal Assunção - Hospital Sírio Libanês e Instituto do Câncer do Estado de São Paulo (ICESP), São Paulo - SP

Caio Cesar Jorge Medeiros - Hospital São Luiz, São Paulo - SP

Carlos Eduardo Rochitte - Instituto do Coração do Hospital das Clínicas da Faculdade de Medicina da Universidade de São Paulo (INCOR/FMUSP), São Paulo - SP

Carlos Eduardo Suaide Silva - DASA (Diagnósticos da América) São Paulo - SP

Carlos Eduardo Tizziani Oliveira Lima - Hospital Casa de Saúde de Campinas, Campinas – SP

Cecília Beatriz Bittenciurt Viana Cruz - Instituto do Coração Hospital das Clínicas da Faculdade de Medicina da Universidade de São Paulo (INCOR/FMUSP), Hospital Sírio Libanês e Instituto do Câncer do Estado de São Paulo (ICESP), São Paulo - SP

Cintia Galhardo Tressino - Instituto Dante Pazzanese e Grupo DASA, São Paulo - SP

Claudia Cosentino Gallafrio - Hospital do GRAACC - Universidade Federal de São Paulo/Hospital Israelita Albert Einstein/Grupo DASA São Paulo - Alta diagnósticos, São Paulo – SP

Claudia Pinheiro de Castro Grau - Instituto do Coração Hospital das Clínicas da FMUSP e Hospital e Maternidade São Luiz, São Paulo - SP

Claudia Gianini Monaco - Hospital Israelita Albert Einstein, São Paulo - SP

Cláudio Henrique Fischer – Universidade Federal de São Paulo (UNIFESP) e Hospital Israelita Albert Einstein, São Paulo - SP

Cláudio Leinig Pereira da Cunha - Universidade Federal do Paraná, Curitiba - PR

Claudio Tinoco Mesquita - Universidade Federal Fluminense (UFF), Rio de Janeiro - RJ

Clerio Francisco de Azevedo Filho - Universidade do Estado do Rio de Janeiro (UERJ), Rio de Janeiro – RJ

David Costa de Souza Le Bihan - Instituto Dante Pazzanese da Cardiologia, São Paulo - SP

Djair Brindeiro Filho - Serviço de Ecocardiografia do Recife Ltda. e Real Hospital Português de Beneficência em Pernambuco - PE

Edgar Bezerra Lira Filho - Hospital das Clínicas, FMUSP; Hospital Israelita Albert Einstein, São Paulo – SP

Edgar Daminello - Hospital Israelita Albert Einstein, São Paulo – SP

Eliza de Almeida Gripp - Hospital Pró Cardíaco e do Hospital Universitário Antônio Pedro (UFF), Rio de Janeiro - RJ

Eliza Kaori Uenishi - Instituto do Coração do Hospital das Clínicas da Faculdade de Medicina da Universidade de São Paulo (INCOR/FMUSP), São Paulo - SP

Estela Suzana Kleiman Horowitz - Fundação Universitária de Cardiologia, Porto Alegre – RS

Fabio de Cerqueira Lario - Hospital Alemão Oswaldo Cruz, São Paulo – SP

Fabio Villaça Guimarães Filho - Faculdade de Medicina de Marília/Instituto do Coração de Marília, Marília – SP

Fernando Antônio de Portugal Morcerf - Ecor Ecocardiografia Ltda, Rio de Janeiro – RJ

Frederico José Neves Mancuso - Escola Paulista de Medicina - Universidade Federal de São Paulo (UNIFESP/EPM), São Paulo - SP

Gabriel Leo Blacher Grossman - Hospital Moinhos de Vento e Clínica Cardionuclear, Rio Grande do Sul – RS

Gabriela Liberato - Instituto do Coração do Hospital das Clínicas da Faculdade de Medicina da Universidade de São Paulo (INCOR/FMUSP), São Paulo - SP

Gabriela Nunes Leal - Hospital das Clínicas da Faculdade de Medicina da Universidade de São Paulo (HC-FMUSP), São Paulo - SP

Giordano Bruno de Oliveira Parente - Hospital Agamenon Magalhães, Recife - PE

Gláucia Maria Penha Tavares - Instituto do Coração do Hospital das Clínicas da Faculdade de Medicina da Universidade de São Paulo (INCOR/FMUSP) e Hospital Israelita Albert Einstein, São Paulo - SP

Henry Abensur - Departamento de Ecocardiografia, A Beneficência Portuguesa de São Paulo, São Paulo - SP

Ibraim Masciarelli Francisco Pinto - Instituto Dante Pazzanese de Cardiologia, São Paulo - SP

Ilan Gottlieb - Casa de Saúde São José e Clínica São Vicente, Rio de Janeiro - SP

Iran de Castro - Instituto de Cardiologia do Rio Grande do Sul (IC/FUC), Porto Alegre - RS

Isabel Cristina Britto Guimaraes - Hospital Ana Neri, Universidade Federal da Bahia, Bahia - BA

Ivan Romero Rivera - Universidade Federal de Alagoas, Maceió - AL

Jaime Santos Portugal - Proecho - Cardiologia Serviços Médicos Ltda, Rio de Janeiro - RJ

Jeane Mike Tsutsui - Instituto do Coração do Hospital das Clínicas da Faculdade de Medicina da Universidade de São Paulo (INCOR/FMUSP), Fleury Medicina e Saúde, São Paulo – SP

João Marcos Bemfica Barbosa Ferreira - Universidade do Estado do Amazonas, Amazonas - AM

José de Arimatéia Batista Araujo-Filho - Hospital Sírio-Libanês, São Paulo, Brasil. Memorial Sloan-Kettering Cancer Center, Nova Iorque – Estados Unidos.

José Lázaro de Andrade - Hospital Sírio Libanês, São Paulo – SP

José Luis de Castro e Silva Pretto - Hospital São Vicente de Paulo/Hospital de Clínicas de Passo Fundo, Rio Grade do Sul - RS

José Luiz Barros Pena - Hospital Felício Rocho, Belo Horizonte - MG

José Maria Del Castillo - Pronto Socorro Cardiológico de Pernambuco (PROCAPE - UPE), Recife – PE

José Olimpio Dias Júnior - Hospital Mater Dei, Belo Horizonte - MG

José Sebastião de Abreu - Clinicárdio de Fortaleza e Cardioexata, Fortaleza – PE

José Roberto Matos-Souza - Faculdade de Medicina da UNICAMP, São Paulo - SP

Joselina Luzia Menezes Oliveira - Fundação São Lucas, Aracaju – SE

Jorge Andion Torreão - Hospital Cárdio Pulmonar, Bahia – BA

Juliana Fernandes Kelendjian - CDI Centro de Diagnóstico por Imagem, Goiânia - GC

Laise Antonia Bonfim Guimarães - Sociedade Beneficente Israelita Brasileira de Ensino e Pesquisa Albert Einstein, são Paulo – SP

Lara Cristiane Terra Ferreira Carreira - Cardiologia Nuclear de Curitiba e Hospital Nossa Senhora do Pilar, Curitiba, Paraná – PR

Leina Zorzanelli - Instituto do Coração do Hospital das Clínicas da Faculdade de Medicina da Universidade de São Paulo (INCOR/FMUSP), São Paulo - SP

Lilian Maria Lopes - ECOKIDGRAFIA - Serviços Médicos Ecodoppler, São Paulo – SP

Liz Andréa Baroncini - Hospital da Cruz Vermelha e Instituto Saber e Aprender, Paraná - PR

Luciano Aguiar Filho - Hospital Salvaluz, DIAGMED (Tomografia e Ressonância Cardíaca), Hospital Municipal de Barueri e Instituto Dante Pazzanese de Cardiologia, São Paulo -SP

Luciano Herman Juaçaba Belém - Instituto Nacional de Cardiologia, Rio de Janeiro - RJ

Luiz Darcy Cortez Ferreira - OMNI - CCNI - Medicina Diagnóstica, São Paulo - SP

Luiz Felipe P. Moreira - Instituto do Coração do Hospital das Clínicas da Faculdade de Medicina da Universidade de São Paulo (INCOR/FMUSP), São Paulo - SP

Manuel Adán Gil – Universidade Federal de São Paulo – Escola Paulista de Medicina, São Paulo – SP

Marcela Momesso Peçanha - Instituto Dante Pazzanese de Cardiologia, São Paulo – SP

Marcelo Dantas Tavares - Universidade Federal da Paraíba, Paraíba - PB

Marcelo Haertel Miglioranza - Instituto de Cardiologia do Rio Grande do Sul, Rio Grande do Sul - RS

Marcelo Luiz Campos Vieira - Instituto do Coração do Hospital das Clínicas da Faculdade de Medicina da Universidade de São Paulo (InCor-HCFMUSP) e Hospital Israelita Albert Einstein, São Paulo - SP

Marcelo Souza Hadlich - Instituto Nacional de Cardiologia, INC., Hospital da Unimed-Rio, ACSC - Casa de Saúde São José, RioImagem CDI, Rede D´Or de Hospitais, Rede Labs D'Or, Rio de Janeiro – RJ

Marcia Azevedo Caldas - Faculdade de Medicina de Campos, Rio de Janeiro - RJ

Marcia de Melo Barbosa – ECOCENTER, Belo Horizonte – MG

Marcia Ferreira Alves Barberato - CardioEco – Centro de Diagnóstico Cardiovascular, Curitiba - PR

Márcio Silva Miguel Lima - Instituto do Coração do Hospital das Clínicas da Faculdade de Medicina da Universidade de São Paulo (InCor-HCFMUSP), São Paulo – SP

Marcio Sommer Bittencourt - Hospital Universitário de São Paulo/Hospital Israelita Albert Einstein, São Paulo - SP

Márcio Vinícius Lins de Barros - Faculdade de Saúde e Ecologia Humana FASEH, Vespasiano - MG

Marcos Valério Coimbra de Resende - Hospital Samaritano Paulista, São Paulo – SP

Maria Clementina Di Giorgi - Instituto do Coração do Hospital das Clínicas da Faculdade de Medicina da Universidade de São Paulo (InCor-HCFMUSP), São Paulo – SP

International Editorial Board

Department of Cardiovascular Imaging

President
André Luiz Cerqueira de Almeida - BA

Vice President of Echocardiography
Alex dos Santos Félix - RJ

Vice President of Nuclear Cardiology
Simone Cristina Soares Brandão - PE

Vice President of Vascular Echography
José Aldo Ribeiro Teodoro - SP

Vice President of Magnetic Resonance Imaging
Otávio Rizzi Coelho Filho - SP

Vice President of Computed Tomography
Márcio Sommer Bittencourt - SP

Vice President of Congenital Heart Disease and Pediatric Cardiology
Adriana Mello Rodrigues dos Santos - MG

Managing Director
Silvio Henrique Barberato - PR

Financial Director
Mohamed Hassan Saleh - SP

Journal Director
Daniela do Carmo Rassi Frota - GO

Board of Trustees

President
Fábio Villaça Guimarães Filho - SP

Members
Afonso Akio Shiozaki - PR
Bruna Morhy Borges Leal Assunção - SP
David Costa de Souza Le Bihan - SP
Jorge Andion Torreão - BA
José Luiz Barros Pena - MG
José Olimpio Dias Júnior - MG
Rafael Willain Lopes - SP

Scientific Committee

Coordinator
Alex dos Santos Félix - RJ

Members
Simone Cristina Soares Brandão - PE
José Aldo Ribeiro Teodoro - SP
Otávio Rizzi Coelho Filho - SP
Márcio Sommer Bittencourt - SP

Qualification Committee

Coordinator
Andrea de Andrade Vilela - SP

Adult Echo Members
Antônio Amador Calvilho Júnior - SP
Candice Machado Porto - BA
Eliza de Almeida Gripp - RJ
João Carlos Moron Saes Braga - SP
Rafael Modesto Fernandes – BA
Rudyney Eduardo Uchoa de Azevedo – SP
Sandra Nívea dos Reis Saraiva Falcão - CE

Congenital Echo Members
Carlos Henrique de Marchi - SP
Daniela Lago Kreuzig - SP
Halsted Alarcão Gomes Pereira da Silva - SP
Márcio Miranda Brito - TO

Seniors
Fábio Villaça Guimarães Filho - SP
Maria Estefânia Bosco Otto - DF
Solange Bernades Tatani - SP

Communication, Information and Internet Committee

Coordinator
José Roberto Matos Souza - SP

Members
Fabio Roston
Issam Shehadeh

Committee of Institutional Relations, Fees and Advocacy

Coordinator
Marcelo Haertel Miglioranza - RS

Members
Wagner Pires de Oliveira Júnior - DF

Committee of Education and Accreditation

Coordinator
Edgar Bezerra de Lira Filho - SP

Intersociety Committee

Coordinator
Marcelo Luiz Campos Vieira - SP

DIC Youth Committee

Coordinator
Eliza de Almeida Gripp - RJ

Positioning and Guidelines Committee

Coordinator
Marcelo Dantas Tavares de Melo - PB

Consultant
José Luiz Barros Pena - MG

Representatives

ASE
José Luiz Barros Pena - MG

EACVI
Alex dos Santos Félix - RJ

SISIAC
Ana Cristina de Almeida Camarozano - PR

Board of Former Presidents
Jorge Eduardo Assef - SP
Arnaldo Rabischoffsky - RJ
Samira Saady Morhy - SP
Marcelo Luiz Campos Vieira - SP
Carlos Eduardo Rochitte -SP

Board of Directors – Year 2022 (Brazilian Society of Cardiology)

North/Northeast
Nivaldo Menezes Filgueiras Filho (BA)
Sérgio Tavares Montenegro (PE)

East
Denilson Campos de Albuquerque (RJ)
Andréa Araujo Brandão (RJ) – Vice-presidente do Conselho Administrativo

State of São Paulo
Celso Amodeo (SP)
João Fernando Monteiro Ferreira (SP) – Presidente do Conselho Administrativo

Center
Carlos Eduardo de Souza Miranda (MG)
Weimar Kunz Sebba Barroso de Souza (GO)

South
Paulo Ricardo Avancini Caramori (RS)
Gerson Luiz Bredt Júnior (PR)

Editor of ABC Cardiol (2022-2025)
Carlos Eduardo Rochitte

Editor of IJCS (2022-2025)
Claudio Tinoco Mesquita

Presidents of State and Regional Chapters

SBC/AL – Pedro Henrique Oliveira de Albuquerque
SBC/BA – Joberto Pinheiro Sena
SBC/DF – Fausto Stauffer Junqueira de Souza
SBC/ES – Tatiane Mascarenhas Santiago Emerich
SBC/GO – Humberto Graner Moreira
SBC/MA – Francisco de Assis Amorim de Aguiar Filho
SBC/MG – Antônio Fernandino de Castro Bahia Neto
SBC/MS – Mauro Rogério de Barros Wanderley Júnior
SBC/NNE – José Albuquerque de Figueiredo Neto
SBC/PB – Guilherme Veras Mascena
SBC/PE – Carlos Japhet Da Matta Albuquerque
SBC/PI – Jônatas Melo Neto
SBC/PR – Olímpio R. França Neto
SOCERJ – Ronaldo de Souza Leão Lima
SBC/RN – Antônio Amorim de Araújo Filho
SOCERGS – Fábio Cañellas Moreira
SOCESP – Ieda Biscegli Jatene

Departments and Study Groups

SBC/DA – Marcelo Heitor Vieira Assad
SBC/DCC – Bruno Caramelli
SBC/DCC/CP – Cristiane Nunes Martins
SBC/DCM – Maria Cristina Costa de Almeida
SBC/DECAGE – José Carlos da Costa Zanon
SBC/DEIC – Mucio Tavares de Oliveira Junior
SBC/DEMCA – Álvaro Avezum Junior
SBC/DERC – Ricardo Quental Coutinho
SBC/DFCVR – Elmiro Santos Resende
SBC/DHA – Lucélia Batista Neves Cunha Magalhães
SBC/DIC – André Luiz Cerqueira de Almeida
SBCCV – João Carlos Ferreira Leal
SOBRAC – Fatima Dumas Cintra
SBHCI – Ricardo Alves da Costa
DCC/GECIP – Marcelo Luiz da Silva Bandeira
DCC/GECOP – Maria Verônica Câmara dos Santos
DCC/GEPREVIA – Isabel Cristina Britto Guimarães
DCC/GAPO – Luciana Savoy Fornari
DCC/GEAT – Carlos Vicente Serrano Junior
DCC/GECETI – João Luiz Fernandes Petriz
DCC/GEDORAC – Sandra Marques e Silva
DCC/GEECG – Nelson Samesima
DCC/GERTC – Adriano Camargo de Castro Carneiro
DEIC/GEICPED – Estela Azeka
DEIC/GEMIC – Marcus Vinicius Simões
DEIC/GETAC – Silvia Moreira Ayub Ferreira
DERC/GECESP – Marconi Gomes da Silva
DERC/GECN – Lara Cristiane Terra Ferreira Carreira
DERC/GERCPM – Pablo Marino Corrêa Nascimento

Message from the President

André L. C. Almeida
President, DIC 2022-2023

Dear associates of the Cardiovascular Imaging Department of the Brazilian Society of Cardiology (Departamento de Imagem Cardiovascular da Sociedade Brasileira de Cardiologia - DIC/SBC)

I have been a member of DIC/SBC since 1991, at the time called the SBC Department of Echocardiography. I had the opportunity and pleasure to contribute to the administrations of presidents Dr. Samira Saady Morhy (2016–17), Dr. Marcelo Luiz Campos Vieira (2018–19), and Dr. Carlos Eduardo Rochitte (2020–21). I learned a significant amount, especially as a managing director (2018–19) and vice president of echocardiography (2020–21).

In January 2022, I was honored to become DIC president for the 2022–23 year. However, I am not alone in this mission! Several brilliant young people and other amazing colleagues who had already provided important and relevant service to our department formed a determined, hardworking board full of new and great ideas and committed to generating benefits for DIC associates.

Our Executive Committee is in charge of managing this conglomerate of more than 3,500 associates. This board meets every Thursday to discuss the department's issues, analyze associates' suggestions, organize the strategic planning and the administrative and financial aspects, debate with partners, listen to SBC management, and discuss many other subjects and themes that may be of interest to DIC associates. This Executive Committee is formed by the president (Dr. André LC Almeida – BA); the experienced and excellent administrative director (Dr. Silvio Henrique Barberato – PR); the insightful, skillful, and faithful chief financial officer (Dr. Mohamed Hassan Saleh – SP); and the tireless and extremely intelligent vice president of the adult echocardiography area (Dr. Alex Santos Felix – RJ).

We always count on the assistance of our Deliberative Council, chaired by Dr. Fábio Villaça Guimarães Filho (SP), an experienced, sensible, and balanced person with an above-average sense of justice, who has actively participated in the Board's decisions. The Deliberative Council is also formed by other experienced colleagues, along with some young people who have already acquired important recognition in the field of echocardiography and cardiovascular imaging in Brazil, namely Dr. José Luiz Barros Pena (MG), Dr. David Costa de Souza Le Bihan (SP), Dr. Jorge Andion Torreão (BA), Dr. Afonso Akio Shiozaki (PR), Dr. Bruna Morhy Borges L Assunção (SP), Dr. José Olímpio Dias Júnior (MG), and Dr. Rafael Willin Lopes (SP).

As you know, DIC's administrative organization chart has always allowed for the allocation of five vice-presidents (VP), one from each area of activity. Here once again, young colleagues are working together with other experienced professionals, who are available to listen to our associates' suggestions and work to forward the mission, namely Dr. Alex Santos Felix – RJ *(VP of Adult Echocardiography),* Dr. Otávio Rizzi Coelho – SP *(VP of MRI),* Dr. Simone Cristina Soares Brandão – PE *(VP of Nuclear Medicine),* Dr. Márcio Sommer Bittencourt – SP *(VP of Computed Tomography),* and Dr. José Aldo Ribeiro Teodoro – SP *(VP of the Vascular area).* As a novelty, we have one more VP, Dr. Adriana Mello Rodrigues dos Santos – MG, the VP of Congenital Heart Disease and Pediatric Cardiology, an area that has shown significant growth within our department. These VP are also the members of the DIC Scientific Committee.

One of DIC's greatest gems is our journal, the *Brazilian Archives of Cardiology Cardiovascular Imaging*, whose Editor-in-Chief is the brilliant Dr. Daniela do Carmo Rassi Frota, a young cardiologist from the state of Goiás. This journal demands unceasing work! Dr. Daniela counts on the indispensable help of eight excellent associate editors, namely Dr. Alexandre Costa Souza – BA (Professional Defense and Echocardiographer Training), Dr. Karen Saori Shiraishi Sawamura – SP (Pediatric Echocardiography), Dr. Leonardo Sara da Silva – GO (MRI), Dr. Marco S. Lofrano Alves – PR (Innovation and Artificial Intelligence), Dr. Rafael Lopes - SP (Nuclear Medicine), Dr. Simone Nascimento dos Santos – DF (Vascular Echocardiography), Dr. Tiago Senra Garcia dos Santos – SP (MRI and Tomography), and Dr. Viviane Tiemi Hotta – SP (Adult Echocardiography). Former editors-in-chief, especially Dr. Sílvio Barberato, editor-in-chief in the management of Dr. Carlos Rochitte, did such a great job that the *Brazilian Archives of Cardiology Cardiovascular Imaging* will soon be indexed to the *Scielo* and *Medline* databases. It is important to remind you that the journal is already indexed in the *Latindex* and *Lilacs* databases. Dr. Daniela Rassi is continuing this work, aiming to reach the set goal, which will be a remarkable achievement for all professionals working with cardiovascular imaging in Brazil. Nevertheless, it is worth remembering that some previous objectives still must be reached. These administrative goals were managed by our former Boards, and the current Board has also been committed, attentive, and active with them. Other goals, though, are directly related with the active participation of DIC associates. And you, DIC associate, can help a lot! Send your article, in the most diverse formats, for publication in *Brazilian Archives of Cardiology Cardiovascular Imaging*. The journal will

never make an impact without good publications; otherwise, Brazil will be a country of great researchers but weak journals. As an extra stimulus, DIC will exempt the next annual fee charge for the associate who becomes the first author to have an article published in *ABC Cardiovascular Imaging*.

DIC webinars are still going strong! They are part of our platform for continuing medical education. After a great job done by Drs. Ronaldo Leão and Marly Uellendahl, the current coordination is under the responsibility of Dr. Sílvio Barberato, who is dynamically organizing activities with the other VPs. As you may have noticed, we have changed the format somewhat. The current format focuses on clinical cases of interest to imaging professionals and clinicians. We have invited several young associates from different states who gained recognition for CV imaging to participate, and they have brilliantly contributed to this. Another novelty is the implementation of webinars with the participation of other societies, such as ASE, SISIAC, EACVI, and others. We believe that clinician participation will add value to the sessions; thus, it is on our radar.

Our Qualification Commission is another chapter. After the great job of the previous commissions highlighting the last three projects coordinated by our dear Dr. Claudia G Monaco (2016–17), Dr. Adenalva Beck (2018–19), and Dr. Marco S. Lofrano Alves (2020–21), the current Qualification Commission is under the coordination of another brilliant young woman, Dr. Andrea de Andrade Vilela (SP). This commission also performs an intensive job. Dr. Andrade has formed a team of exceptional young people who help her with the most substantial tasks. They must remain updated, as they are responsible for preparing the DIC/SBC Qualification Certificate in Echocardiography. These are very capricious data, as all questions must be updated with their respective references. In addition to preparing the questions, they are responsible for reviewing and responding to applicants' appeals based on the references concerning each question. It is humanly impossible to do this work alone. But Dr. Andrade relies on the assistance of a fantastic group that helps her with the Adult Echo issues: Dr. Rafael Modesto Fernandes (BA), Dr. Eliza de Almeida Grippi (RJ), Dr. Sandra Nívea Saraiva dos Reis Falcão (CE), Dr. Rudyney de Azevedo Uchoa (SP), Dr. Antônio Amador Calvilho Júnior (SP), Dr. João Saes Braga (SP), and Dr. Candice Machado Porto (BA). She has another great team that helps her with congenital Echo issues consisting of Dr. Daniela Lago Kreuzig (SP), Dr. Márcio Miranda Brito (TO), Dr. Carlos Henrique de March (SP), and Dr. Halsted Alarcão Gomes Pereira da Silva (SP). The entire group is supported by three excellent senior colleagues: Dr. Fabio Villaça Guimarães Filho (SP), Dr. Maria Estefânia Bosco Otto (DF), and Dr. Solange Bernades Tatani (SP).

We created DIC's Guidelines and Positioning Committee, which is responsible for coordinating and supporting projects aimed at preparing official documents for our department for subsequent publication. This commission is under the coordination of another young man, who I consider an exception within the reality of Brazilian doctors: Dr. Marcelo Tavares de Melo Dantas (PB), who has postulated amazing ideas which are already being implemented with the help of several colleagues. One such idea is the *Positioning of the DIC-SBC on Noninvasive Assessment of Coronary Syndromes*, which is coordinated by the vibrant Dr. Maria Estefânia Bosco Otto (DF). Other ideas are welcome, such as the *Positioning of the DIC/SBC on Stress Echocardiography*, under the coordination of the no less vibrant and always active Dr. Ana Cristina Camarozano (PR). Moreover, some of these projects will be developed in partnership with some international societies, such as the ASE, SIAC/SISIAC, EACVI, and others. The Guidelines and Positioning Committee relies on the advice of none other than our fantastic and experienced Dr. José Luiz Barros Pena (MG), former DIC president, author of several international publications, and editor of a few books.

The proximity and partnership with the various international CV imaging societies are in full swing due to the consistent performance of the magnanimous Dr. Marcelo Luiz Campos Vieira (SP), another former DIC president and coordinator of the Inter-Corporate Commission. Dr. Vieira has enviable interpersonal relationships in addition to being a friend and associate of many leaders of international societies. He counts on the expressive support of Dr. Ana Cristina Camarozano, DIC representative to the SISIAC, Dr. José Luiz Barros Pena, DIC representative to the ASE, and Dr. Alex Santos Felix, DIC representative to the EACVI. In short, we are very well represented.

DIC continues to offer several continuing medical education courses. The Echocardiography Retraining Course assembles some of the greatest experts in the field and is very useful for those who want to obtain the DIC/SBC Certificate of Performance in Echocardiography. This course, launched in 2021, has been updated with 25% new lessons to complement the already excellent ones. We formed a commission with Dr. Alex Santos Felix, Dr. Marcelo Tavares de Melo Dantas, Dr. Mônica Alcântara (RJ), Dr. Marcelo Miglioranza (RS), and Dr. Rodrigo Bellio Barreto (SP), who is already working on new courses (POCUS, Strain, Eco 3D, Contrast, and others). Another course focused on pediatric cardiology imaging is also under development, coordinated by Dr. Adriana Mello Rodrigues dos Santos, the VP of Congenital Heart Diseases and Pediatric Cardiology. Likewise, the course Echocardiography in Interventions is being developed with the coordination of Dr. David Costa de Souza Le Bihan. Other courses covering CT, MRI, and Nuclear Medicine were launched under the management of Dr. Carlos Rochette in 2021. These courses are still being updated but will be renewed as soon as necessary.

The DIC website requires redevelopment. We are aware of this and have already started working on the design of a new and modern Portal to provide a better and easier contact with our associates. Stay tuned!

The important Fees and Professional Defense Committee, continuing the great work of the remarkable and determined Dr. Marcos Valério Resende, is now under the coordination of the always active and unique Dr. Marcelo Miglioranza (RS) with the support of the tireless and helpful Dr. Wagner Pires de Oliveira Júnior (DF), who has deep knowledge of the subject since, in addition to being a diligent and helpful doctor, he is also a lawyer. At their suggestion, we are encouraging the presence of representatives of this commission in the different states of the Federation. If you are a DIC associate who wants to contribute to this area, please contact us.

Message from the President

DIC has made a great investment, under the management of Dr. Marcelo Vieira and Dr. Carlos Rochitte, to hire a specialized company to place the Strain, 3D Echo, and Calcium Score on the ANS Procedures List. We have not achieved the expected success yet, but our management keeps fighting and, I believe, has a good chance of achieving victory with Strain (a great job under the coordination of the Dr. Marcelo Miglioranza) and with the Calcium Score (another brilliant job under the coordination of Dr. Márcio Sommer Bittencourt).

The Teaching and Accreditation Commission, under the coordination of the ever-present and active Dr. Edgar Bezerra Lira (SP), is continuing the great job of the Accreditation of Echo Services, with the development of two pilot projects at the Echocardiography Laboratories of the Messejana Hospital (CE) and the Hospital of the Federal University of Uberlândia (MG). These pilot projects are already in the advanced stages and will release results soon. When they are ready, we will start the process of Accreditation of Echocardiography Laboratories spread across Brazil. I believe it could become a key differentiator when negotiating with companies that sell health insurance and group medicine.

It is also important to mention that the Assessment of Normality Pattern of Echocardiographic Variables in the Brazilian Population study is still in progress after some difficulties faced due to the COVID-19 pandemic. The coordination of this study is under the excellent Dr. Ana Clara Tude Rodrigues (SP) and counts on the participation of several participants spread across the five regions of Brazil.

Later this year, probably at our Congress in São Paulo, the DIC will be launching an exceptional Atlas of Multimodality Imaging in Cardiology. This fantastic material has been developed since the management of Dr. Carlos Rochitte, and it currently relies on the participation of about 200 colleagues working in all states of the Federation. It is worth mentioning the fundamental collaboration of the Young DIC, under the coordination of the young stars Dr. Elisa de Almeida Gripp (RJ) and Dr. Isabela Bispo Santos da Silva Costa (SP). Reserve your copy of this beautiful project that contains more than 2,000 images, including photos and videos. It is fantastic!

Do not forget that DIC associates have free access to the *Clinical Key* on our website. There you can find several excellent books on echocardiography and cardiovascular imaging as well as practically all of the good journals of this field worldwide. All of this material is yours, DIC associate, to download anytime you want.

Last but not least, I would like to tell you about our greatest scientific event: the annual DIC Congress, which will take place at the Frei Caneca Convention Center in São Paulo. This year, under the presidency of the fantastic Dr. Marly Uellendahl (SP) and scientific coordination of the no less brilliant Dr. Marcio Lima (SP), the Congress will be of hybrid format. Thus, the event will have many face-to-face activities and online sessions. Hands-on activities will be offered face-to-face only, of course. Join us and your friends! Submit your studies. The abstract submission deadline is 05/05/2022. Submission results will be published on 06/13/2022.

The DIC Board and the Congress organizing committee are working tirelessly to make this the best DIC Congress ever. For that to happen, we need your presence. In addition to super up-to-date classes and presentations, we will offer many unique activities, including events scheduled for reunions with former residents of various echocardiography training centers, private conversations with specialists on the most diverse subjects, unique opportunities to conduct business and take advantage of industry promotions that negotiate the equipment, among other novelties. For extra motivation, DIC will offer a special discount to those who wish to become members at the time of registration. Take this opportunity for early bird registration offered by DIC. We have already confirmed the presence of international speakers Dr. Stephen Little (USA), Dr. João Lima (USA), Dr. Nuno Cardim (Portugal), Dr. Salvador Spina (Argentina), and Dr. Viviane Taqueti (USA). The main exponents of the Brazilian Echocardiography and CV Imaging will also be present. Do not miss the opportunity to take part and embrace Brazilian cardiovascular imaging with us. It has been a long time since the last Congress in 2019.

As you can see, DIC is quite busy. This is only possible because we have an amazing group of partners who dedicate themselves to assisting you, our associates. As you know, none of them receive remuneration for their time and dedication to the DIC.

All actions described in the text above must be communicated to DIC associates, the reason our department exists. To this end, we have created a very special Communication, Information, and Internet Commission. The coordination of this commission is under the responsibility of a special person: Dr. José Roberto Souza (SP), known to all as the dear *Beto from EchoTalk*. With his experience and communication skills, he is bringing great new developments to DIC and is directly involved in some important projects, particularly with the design of the new DIC Portal. This will soon be the true channel of communication among Brazilian echocardiography and cardiovascular imaging professionals.

I apologize for the long message, but I aimed to be as transparent as possible and show you the current reality of the DIC. You are the real reason for the existence of the Cardiovascular Imaging Department of the Brazilian Society of Cardiology.

Thank you so much for your attention and support – let's keep going together!

Regards,

Message from the Editor

Daniela do Carmo Rassi Frota
Editor-in-chief, Arquivos Brasileiros de Cardiologia Imagem Cardiovascular

Dear colleagues,

With great honor, I assume the position of editor-in-chief of *Arquivos Brasileiros de Cardiologia* (ABC) *Imagem Cardiovascular*, the official publication of the Cardiovascular Imaging Department of the Brazilian Society of Cardiology, for the next biennium. The journal is part of the ABC Family and indexed in the Lilacs and Latindex databases. Our mission is to publish high-quality material in all areas of cardiovascular imaging, including echocardiography, magnetic resonance imaging, computed tomography, and nuclear imaging.

In recent years, thanks to the efforts of my predecessors – particularly the brilliant performance of my predecessor, Dr. Silvio Henrique Barberato – the journal underwent important transformations, gaining visibility and consolidating the path toward indexing in the main databases, such as the Scientific Electronic Library Online (SciELO), and, in the future, PubMed®.

For this progress to continue, we rely on the continuous support and effort of all associates and the academic community to maintain consistent high-quality submissions, especially original articles.

Our journal publishes the following types of manuscripts: original research article, review articles ("What do cardiologists expect from the echocardiogram…?" and "My approach to"), point of view, brief communication, letter to the editor, editorial, mini-editorial, and systematic analysis and meta-analysis. Case reports and cardiovascular images are also encouraged for publication, as they provide information on the basic mechanisms responsible for cardiovascular disease and highlight the potential role of noninvasive imaging.

We have a wide national and international editorial board consisting of members of recognized competence in addition to a qualified team of associate editors, including Alexandre Costa Souza (professional defense and training of the echocardiographer), Karen Saori Shiraishi Sawamura (pediatric echocardiography), Leonardo Sara da Silva (MRI), Marco S. Lofrano Alves (innovation and artificial intelligence), Rafael Lopes (nuclear medicine), Simone Nascimento dos Santos (vascular echocardiography), Tiago Senra Garcia dos Santos (MRI and computed tomography), and Viviane Tiemi Hotta (adult echocardiography).

Online publication is permanent, and a new issue is released every 3 months. No fees are charged for submission or publication. Authors who wish to submit their articles to *ABC Imagem Cardiovascular* must follow its publication guidelines and submit their manuscripts through its online submission system.

The site is completely redesigned, uses research tools, enables immediate publication, and provides direct links to social media.

I end this message with my special thanks to our current president of the Department of Cardiovascular Imaging, Dr. André Almeida, for his trust, and I invite all colleagues in the area to send their contributions and studies to *ABC Imagem Cardiovascular.*

My Approach to Aortic Stenosis Assessment with Discrepant Quantification

Como eu Faço: Avaliação da Estenose Aórtica com Discordância em sua Quantificação

[1]Institute of Cardiology and Transplantation of the Federal District, University Foundation of Cardiology (ICTDF/FUC), Federal District, DF, Brasília, Brazil. [2]Hospital Sírio-Libanês, Federal District, DF, Brasília, Brazil.

Adenalva Lima de Souza Beck[1,2]

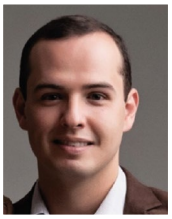

Luiz Carlos Madruga Ribeiro[1]

Introduction

Aortic stenosis (AS) is the most common primary valve disease and an important cause of morbidity and mortality worldwide.[1] Echocardiography is the first-line method for its diagnosis, quantification of severity, prognosis, and determination of intervention timing.[2]

The association of maximum velocity (Vmax) ≥ 4m/s, aortic valve area (AVA) ≤ 1.0 cm², and mean gradient (MG) ≥ 40 mmHg defines the diagnosis of classic severe AS.[3] However, MG and AVA are discrepant (AVA ≤ 1.0 cm², MG < 40 mmHg) in 30–40% of the population with severe AS, leading to low-gradient AS (LGAS),[4] the focus of this article. Less frequently, high-gradient AS can also occur in cases of MG ≥ 40 mmHg and AVA > 1.0 cm² due to high flow situations.[5]

Understanding the factors that lead to this discrepancy is essential to avoiding misdiagnosis and classifying different severe AS phenotypes.

Understanding the discrepancy phenomenon and classifying aortic stenosis

AS with a discrepant valve area and gradient may be due to measurement errors, physiological reasons (small body surface, flow states, and arterial hypertension), and guideline inconsistencies in AVA/MG criteria. Thus, it is important to first correct physiological factors and confirm measurements. If the discrepancy persists, the phenotype must be classified according to the flow state; if the severity remains uncertain, it must be confirmed by other methods.[5] Classically, the flow is evaluated by the ejection fraction and stroke volume index (SVi). All of these aspects are discussed below.

Aortic valve area, stroke volume, or mean aortic transvalvular gradient calculation errors

Measuring errors are usually the main cause of discordant aortic stenosis. The most common error is related to underestimation in left ventricular outflow tract diameter (LVOTd), either due to imaging difficulties, especially if severe calcification is present, or because it is not clear where to measure LVOTd, or a circular LVOT geometry is assumed, whereas it is mostly elliptical. Errors involving just a few millimeters of LVOTd lead to exponential errors in stroke volume (SV) and aortic valve area (AVA) calculation using the continuity equation, leading to misdiagnosis of severe LGAS. To minimize these limitations, AOS grading recommendations (Table 1) also include calculating the ratio between the velocity time integral (VTI) on pulsed Doppler (PW) of the left ventricular outflow tract (LVOT) and on continuous Doppler (CW) of the aortic valve (AOV), which is a dimensionless index. Also, if the patient has a small body surface and is not obese, it is recommended to index AVA to body surface (AVAi)[1], although this indexation method is controversial.[6]

Errors can also occur when obtaining Doppler velocities. According to the Doppler equation, angles greater than 20 degrees between the ultrasound beam and the analyzed jet underestimate the velocity and, consequently, the

Keywords

Aortic Stenosis; Echocardiography; Diagnosis.

Mailing Address: Adenalva Lima de Souza Beck •
SQSW 305, Bloco K, apto 104, Sudoeste, Brasília, DF. CEP 70673462.
E-mail: denalima@yahoo.com.br
Manuscript received 12/16/2021; revised 1/20/2022; accepted 1/30/2022.

DOI: 10.47593/2675-312X/20223501ecom21

gradient. Doppler alignment can be challenging and require multiple windows.

Strict attention to the measurement technique is the first step to reducing errors and avoiding discrepancies (Table 2). Testing measurement reliability involves calculating the predicted LVOT and comparing it with the measured diameter. If the measured LVOT is 2 mm greater or less than the predicted value, measurement error or elliptical geometry is possible. Another measurement that shows an error is an AVAi ≤ 0.6 cm^2/m^2 with a VTI ratio > 0.25. In such cases, complementary measurements and other imaging methods are required to confirm measurement accuracy.

Inconsistent guidelines in the definition of severity by AVA/gradient

Some studies suggested that a gradient ≥ 40 mmHg is related to an area < 0.8 cm^2; thus, areas of 0.8–1.0 cm^2 may be in a gray zone, with intermediate gradients of 30–40 mmHg, which would justify the discrepancy between valve area and gradient.[3]

Table 1 - Aortic stenosis grading recommendations.

Parameter	Aortic sclerosis	Mild	Moderate	Severe
Vmax, m/s	≤ 2.5	2.6-2.9	3-3.9	≥ 4
Mean gradient (mmHg)		< 20	20-39	≥ 40
Valve area (cm^2)		> 1.5	1.0-1.5	≤ 1.0
AVA index (cm^2/m^2)		> 0.85	0.61-0.85	≤ 0.6
DVI		> 0.5	0.26-0.50	≤ 0.25

AVA, aortic valve area; Vmax, maximum aortic valve velocity on continuous Doppler; DVI, ratio between Doppler velocity index integralobtained by pulsed Doppler of the left ventricular outflow tract and continuous Doppler of the aortic valve.[1]

Flow state

Low-flow states can also justify AVA-MG discrepancies for underestimating the gradient even in the presence of severe stenosis. The fluid dynamics principle states that the pressure gradient is directly proportional to the square of the flow and inversely proportional to the square of the valve area.[7] That is, a small flow reduction can lead to large gradient reductions. In this case, two situations are already well described:[1,3,5,8] classic low-flow LGAS (LFLGAS) due to a reduced LV ejection fraction (LVEF) < 50%;[2] and paradoxical LFLGAS with a preserved LVEF (≥50%) but small and remodeled/hypertrophic LV and SVi ≤ 35 mL/m^2.

Another situation representing almost half the cases of "discrepant" AS but still generating much debate is low-gradient stenosis with normal flow LGAS (NFLGAS), where LVEF is also preserved and SVi is > 35 mL/m^2. As it does not seem plausible from a fluid dynamics perspective, it is usually attributed to measurement errors, a small BSA, or inconsistent guidelines. However, some studies showed that when these factors are excluded, up to 50% of such patients have true severe AS, suggesting that it is a real entity.[9,10] Other studies reported that NFLGAS represents an "intermediate" stage between moderate and severe with faster progression and requiring vigilant observation.[11] Assessing transvalvular flow rate (Q) (in addition to SVi) and systemic arterial compliance (SAC) may help explain this entity and refine the LGAS diagnosis and prognosis.[12]

The transvalvular flow rate (Q) is the volume ejected per unit time through the aortic valve during the ejection period and it is measured as SV/ejection time (ET). Q expresses the true energy required to open the valve, making it a more accurate flow parameter.[12,13] In NFLGAS, Q may be low despite a normal SV due to an increased ET. This increased ET is due to increased valve resistance or reduced SAC. On the other hand, a reduced SAC can also reduce the MG under normal flow conditions.[9,14]

Some studies demonstrated that, under normal Q conditions, AVA measured at rest should be considered

Table 2 - Technical measurement aspects for AVA calculation.

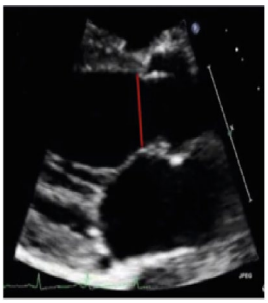

Pay strict attention to the LVOT measurement technique
Longitudinal paraesternal Zoom the image Inner edge to inner edge Measure at mid-systole, parallel and preferably adjacent to the aortic valve
LVOT measurements at ring level or less than 2 mm from the ring are more most accurate for SV and AVA calculations
Use the same LVOT for all tests.
If the measurement is not feasible or the LVOT differs from the predicted diameter[A] (by > or <2 mm), do not use the continuity equation[B]; rather, use the dimension index and other methods
Pay attention when obtaining velocities
Position the PW sample volume in the same place where the LVOT was measured and ensure the best envelope. Obtain unforced expiratory apnea velocities to avoid changing the sample volume location. Interrogate aortic transvalvular velocity with CW using multiple windows. Report the incidence where the highest velocity and gradient was obtained for serial comparison and prognostic assessment. If LVOT PW velocity is >1.5 m/s (fixed subvalvular acceleration[C]), MG, SV, and AVA are not reliable.
Always average three measurements in cases of sinus rhythm and five measurements in cases of arrhythmia

AVA, aortic valve area; CW, continuous wave Doppler; LVOT, left ventricular outflow tract; MG, mean gradient; PW, pulsed wave Doppler; SV, stroke volume; V, velocity. [A]Predicted LVOT = (5.7 × BSA) + 12.1 (do not use in obese patients). [B]VTI: velocity time integral. The continuity equation is calculated as: SV/VTI CW, where SV = (0.785 × LVOT²/2). [C]Sigmoid septum, subvalvular membrane, or obstructive hypertrophic cardiomyopathy can lead to subvalvular acceleration and MG and SV overestimation, with AVA underestimation of AVA even in the absence of significant stenosis (correlate with valve anatomy).

"true" and reflect AS severity rather than SVi or LVEF.[10,13] So, in classic LGAS, differently from what is recommended, flow normalization with echo under stress would only be necessary at a value of Q < 200 mL/s.[15]

Considering the complexity of "discrepant" AS, AVA, MG, and Vmax are insufficient. As seen above, an integrated approach is needed (Figure 1).

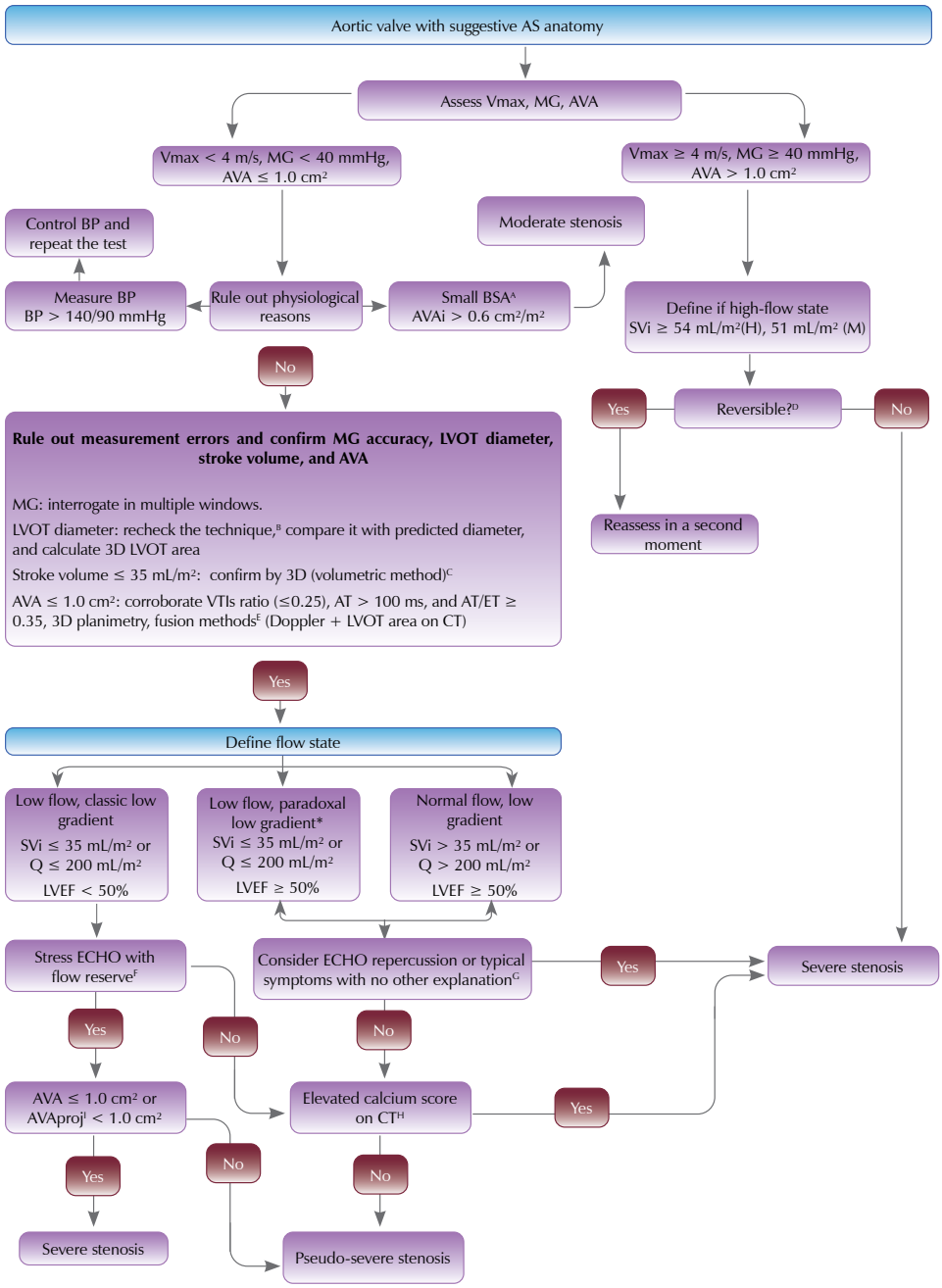

Source: adapted from Vahanian et al.[3]. LVEF: left ventricular ejection fraction; AVAproj = projected aortic valve area; MG: mean gradient; BS: body surface; AVAi: aortic valve area index; SVi: stroke volume index; LVOT: left ventricular outflow tract; VTI: velocity time integral; AT: acceleration time: ET: Ejection time; CT: computed tomography; Vmax: maximum speed; VTI: velocity time integral; Q: flow rate. 3D: three-dimensional; A - Do not index in obese individuals (BMI ≥30 kg/m²) B - Predicted diameter = (5.7 x Body surface) +12.1; C — 3D SV cannot be measured if mitral regurgitation is greater than mild. D - High flow situations may be reversible in patients with anemia, fever, hyperthyroidism or arteriovenous fistula and irreversible in significant aortic regurgitation. E - Use higher limits to define severe AOS: Svi ≥42 ml/m² and AVA <1.2 cm². F - Flow reserve = >20% increase in SV or Q in response to low-dose dobutamine. Pseudosevere aortic stenosis = AVA >1.0 cm2 with increased flow. G - LV hypertrophy (in the absence of coexisting hypertension), LV longitudinal global strain < 16% (no other cause) (if apical sparing pattern, consider associated amyloidosis), Zva (or arterial impedance = MG + systolic blood pressure/SVi) > 4.5 mmHg/ml/m², arterial vascular compliance (SVi/systolic blood pressure - diastolic blood pressure) <0.6 ml/m²/mmHg). H - Thresholds for severe aortic stenosis assessed by aortic valve calcification on CT (Agatston units): men >3,000, women >1,600 = highly likely; men >2000, women >1200 = likely; men < 1600, women < 800 = unlikely. I - Maximum AVA obtained when Q = 250 ml/s calculated as resting AVA +(ΔAVA/ΔQ) x (250-Qrest). SA: aortic stenosis.

Figure 1 – *Adapted "discrepant" AS diagnostic algorithm[3].*

Conclusion

Discrepant AS is a challenging entity that can present as multiple phenotypes and requires an echocardiographic approach integrated with other imaging modalities. The most appropriate combination of methods should be used for each patient with consideration of the clinical context.

Authors' contributions

Research conception and design: Beck ALS, Ribeiro LCM; Manuscript writing: Beck ALS, Ribeiro LCM; Critical review of the manuscript for important intellectual content: Beck ALS; Bibliographic research: Beck ALS, Ribeiro LCM; Table and reference formatting: Ribeiro LCM

Conflict of interest

The authors have declared that they have no conflict of interest.

References

1. Baumgartner H Chair, Hung J Co-Chair, Bermejo J, Chambers JB, Edvardsen T, Goldstein S, et al. Recommendations on the echocardiographic assessment of aortic valve stenosis: a focused update from the European Association of Cardiovascular Imaging and the American Society of Echocardiography. Eur Heart J Cardiovasc Imaging. 2017;18(3):254-75. doi: https://doi.org/10.1093/ehjci/jew335
2. Otto CM. Aortic stenosis progression: Doppler echocardiography shifted the paradigm. J Am Soc Echocardiogr. 2021;34(3):245-7. doi: https://doi.org/10.1016/j.echo.2020.12.012
3. Vahanian A, Beyersdorf F, Praz F, Milojevic M, Baldus S, Bauersachs J, et al.; ESC/EACTS Scientific Document Group. 2021 ESC/EACTS Guidelines for the management of valvular heart disease. Eur J Cardiothorac Surg. 2021;60(4):727-800. doi: https://doi.org/10.1093/ejcts/ezab389. Erratum in: Eur J Cardiothorac Surg. 2022 Jan 13;: PMID: 34453161.
4. Dumesnil JG, Pibarot P, Carabello B. Paradoxical low flow and/or low gradient severe aortic stenosis despite preserved left ventricular ejection fraction: implications for diagnosis and treatment. Eur Heart J. 2010;31(3):281-9. doi: https://doi.org/10.1093/eurheartj/ehp361
5. Otto CM, Nishimura RA, Bonow RO, Carabello BA, Erwin JP 3rd, Gentile F, et al. 2020 ACC/AHA Guideline for the Management of Patients With Valvular Heart Disease: A Report of the American College of Cardiology/American Heart Association Joint Committee on Clinical Practice Guidelines. Circulation. 2021;143(5):e72-e227. doi: https://doi.org/10.1161/CIR.0000000000000923. Epub 2020 Dec 17. Erratum in: Circulation. 2021 Feb 2;143(5):e229. PMID: 33332150
6. Vulesevic B, Kubota N, Burwash IG, Cimadevilla C, Tubiana S, Duval X, et al. Size-adjusted aortic valve area: refining the definition of severe aortic stenosis. Eur Heart J Cardiovasc Imaging. 2021;22(10):1142-8. doi: https://doi.org/10.1093/ehjci/jeaa295
7. Chong A, Senior R, Wahi S. Contemporary imaging of aortic stenosis. Hear Lung Circ. 2019;28(9):1310-9. doi: https://doi.org/10.1016/j.hlc.2019.05.177
8. Tarasoutchi F, Montera MW, Ramos AI, Sampaio RO, Rosa VE, Accorsi TA, et al. Atualização das Diretrizes Brasileiras de Valvopatias – 2020. Arq Bras Cardiol. 2020;115(4):720-75. doi: https://doi.org/10.36660/abc.20201047
9. Clavel M-A, Guzzetti E, Annabi MS, Salaun E, Ong G, Pibarot P. Normal-flow low-gradient severe aortic stenosis: myth or reality? Struct Hear. 2018;2(3):180-7. doi: https://doi.org/10.1080/24748706.2018.1437934
10. Senior R, Khattar RS. Assessment of aortic stenosis: time to go with the flow. J Am Coll Cardiol. 2020;75(15):1770-1. doi: https://doi.org/10.1016/j.jacc.2020.02.042
11. Chadha G, Bohbot Y, Lachambre P, Rusinaru D, Serbout S, Altes A, et al. Progression of normal flow low gradient "severe" aortic stenosis with preserved left ventricular ejection fraction. Am J Cardiol. 2020;128:151-8. doi: 10.1016/j.amjcard.2020.05.003
12. Sen J, Huynh Q, Stub D, Neil C, Marwick TH. Prognosis of severe low-flow, low-gradient aortic stenosis by stroke volume index and transvalvular flow rate. JACC Cardiovasc Imaging. 2021;14(5):915-27. doi: 10.1016/j.jcmg.2020.12.029
13. Namasivayam M, He W, Churchill TW, Capoulade R, Liu S, Lee H, et al. Transvalvular flow rate determines prognostic value of aortic valve area in aortic stenosis. J Am Coll Cardiol. 2020;75(15):175869. doi: 10.1016/j.jacc.2020.02.046
14. Vamvakidou A, Jin W, Danylenko O, Chahal N, Khattar R, Senior R. Low transvalvular flow rate predicts mortality in patients with low-gradient aortic stenosis following aortic valve intervention. JACC Cardiovasc Imaging. 2019;12(9):1715-24. doi: 10.1016/j.jcmg.2018.01.011
15. Chahal NS, Drakopoulou M, Gonzalez-Gonzalez AM, Manivarmane R, Khattar R, Senior R. Resting aortic valve area at normal transaortic flow rate reflects true valve area in suspected low-gradient severe aortic stenosis. JACC Cardiovasc Imaging. 2015;8(10):1133-9. doi: 10.1016/j.jcmg.2015.04.021

My Approach to the Echocardiographic Assessment of Mitral Annular Calcification: Challenges and Particularities

Como eu Faço Avaliação Ecocardiográfica da Calcificação do Anel Mitral: Desafios e Particularidades

[1]*Cardiology Center of the School of Medicine of Ribeirão Preto, University of São Paulo-USP, São Paulo, SP, Brazil.*

Antonio Carlos Leite de Barros Filho[1]

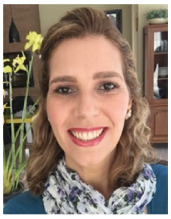

Minna Moreira Dias Romano[1]

Introduction

Mitral annular calcification (MAC) is a chronic degenerative process that affects the fibrous structure supporting the mitral valve. It is present in 8–15% of the general population; however, its prevalence can reach 40% in older people and 50% in patients with chronic kidney disease. Although it was previously classified as a degenerative pathophysiology associated with age or calcium metabolism, other etiological factors have been suggested, such as atherosclerotic disease and its risk factors (hypertension, obesity, dyslipidemia, diabetes mellitus, smoking), exposure to radiation therapy, and conditions that increase mitral valve stress, such as aortic valve stenosis, hypertrophic cardiomyopathy, and mitral valve prolapse.[1-5]

MAC is related to an increased risk of a number of adverse cardiac events, such as acute myocardial infarction, stroke, arrhythmias (conduction disorders and atrial fibrillation), and mitral valve disease (mitral stenosis, mitral regurgitation, and infective endocarditis).[6-8] It is also associated with a higher risk of complications and mortality in patients undergoing mitral valve surgery. Although most cases are not associated with mitral valve dysfunction, some may progress with an increased mitral transvalvular gradient.[4,9]

Normal mitral annulus anatomy and function

The mitral valve apparatus is a complex three-dimensional unit formed by different structures dynamically interacting throughout the cardiac cycle, including the left ventricle (LV), papillary muscles, chordae tendineae, leaflets, and mitral valve annulus. It is not histologically uniform. Its anteromedial portion, called the mitral-aortic curtain, is more rigid and formed by a curved band of connective tissue that connects the aortic annulus at the level of the left and non-coronary leaflet and the junction of the left atrium wall with the anterior leaflet. On the other hand, the posterior portion of the annulus is formed by a semicircle of fibrous tissue connected with the muscular walls (atrial and left ventricular), the mitral leaflets at the level of the hinges, and the epicardial adipose tissue. The mitral annulus is shaped like a bean or a "D"; however, its three-dimensional evaluation appears as a horse saddle, the ideal configuration to minimize leaflet stress and ensure adequate coaptation. In this saddle, the "highest" points correspond to the most anterior portion, visualized on the two-dimensional echocardiogram in the parasternal longitudinal window. Its nadir corresponds to the portion visualized in the apical four-chamber view. The posterior portion of the annulus, which is less fibrotic, shifts during left ventricular systole, increasing the saddle height and decreasing the circumferential area.[4,9-11]

The quantitative analysis of the mitral annulus through linear measurements obtained using tomographic techniques such as two-dimensional echocardiography may not adequately represent its complex non-planar structure, underestimating these measurements; moreover, it is examiner-dependent due to the need for adequate plane alignment for image acquisition.[12,13] In contrast, measurements obtained with the three-dimensional method are not dependent on geometric assumptions and can be obtained even using transthoracic echocardiography; however, this method is less available, expensive, and dependent on a software-dedicated analysis.[14] Important measurements for understanding the mitral annulus, such as its anteroposterior and inter-commissural diameters (Figure 1) or even its circumference and height, are easily quantified by three-dimensional echocardiography and should ideally be acquired transesophageally.

Keywords

Mitral Valve; Echocardiography; Calcinosis.

Mailing Address: Minna Moreira Dias Romano •
Department of Clinical Medicine, Ribeirão Preto School of Medicine, University of São Paulo- FMRP-USP, SP, Brazil.
E-mail: minna@fmrp.usp.br
Manuscript received 12/10/2021; revised 1/13/2022; accepted 2/4/2022.

DOI: 10.47593/2675-312X/20223501ecom19

Echocardiographic evaluation of MAC

MAC can be identified on echocardiography as an irregular hyperechoic structure involving the mitral valve annulus with the formation of a posterior acoustic shadow that most commonly affects its posterior portion (Figure 2).[4]

Calcifications identified on two-dimensional echocardiography are usually already extended beyond the thin portion corresponding to the mitral valve annulus itself; their location must be described in detail as it has prognostic and therapeutic implications. Calcifications involving the base of the valve leaflets can result in calcium mitral stenosis. Unlike rheumatic stenosis, mitral stenosis does not progress with commissural fusion, as it is unresponsive to percutaneous intervention with a balloon catheter. Furthermore, in MAC stenosis, the valve apparatus usually appears more tubular, with the area at the tip of the leaflets closer to the basal portion area; in rheumatic stenosis, the valve apparatus has a funnel-shaped appearance, with the area at the tip of the leaflets smaller than the basal area.[15,16] On the other hand, involvement of the atrial surface of the leaflets can result in valve failure due to reduced mobility and consequent difficult leaflet coaptation. Some patients with LV basal wall involvement (Figure 3) may have mobile deposits that must be described due to the risk of embolization. Finally, patients with calcifications extending to the right fibrous trigone are at increased risk of atrioventricular conduction disorders.[4,9]

MAC is subjectively graded according to the extent of mitral annulus surface calcification. It is considered severe when more than 4 mm thick (measured on the short axis in the anteroposterior direction) (Figure 2), when involving more than 50% of the mitral annulus, or if it reaches the LV inlet. Calcium deposition in less than ⅓ of the annulus is considered mild MAC, while that affecting ⅓ to ½ of the annulus is considered moderate.[4,9,17]

Three-dimensional echocardiography may be useful in the study of annulus dynamics in MAC patients. The annulus is more extended during diastole; however, it is flatter (i.e. loses its height) with an increased anteroposterior dimension. During systole, there is a reduction in saddle conformation and annular contraction (annulus area variation), mainly

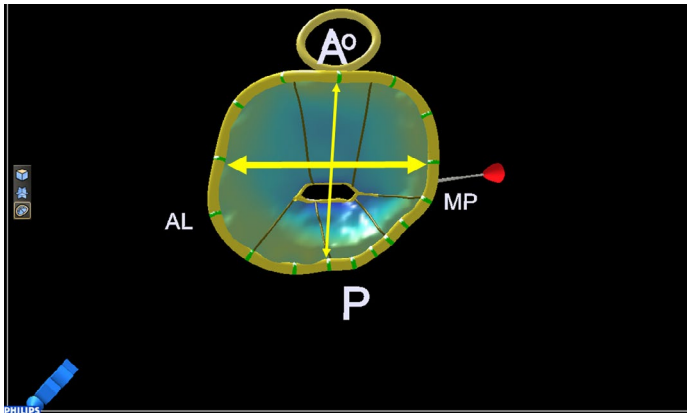

Figure 1 – *Three-dimensional rendering of the mitral valve annulus (yellow outline), which enables measurements such as the inter-commissural (thick arrow) and anteroposterior diameter (thin arrow).*

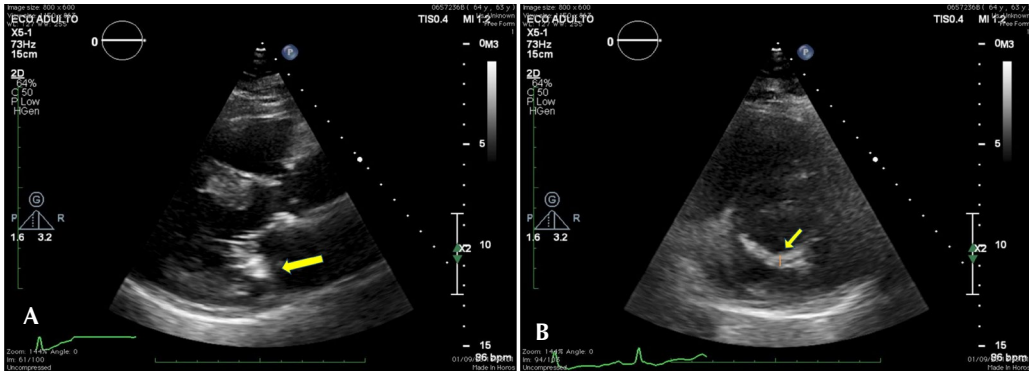

Figure 2 – *Two-dimensional evaluation of mitral annular calcification, which can be identified on the parasternal longitudinal projection as increased brightness intensity in the two-dimensional image (Panel A, yellow arrow). It can be quantified by its extension or its thickness on the parasternal short-axis projection (Panel B, yellow arrow and measurement line).*

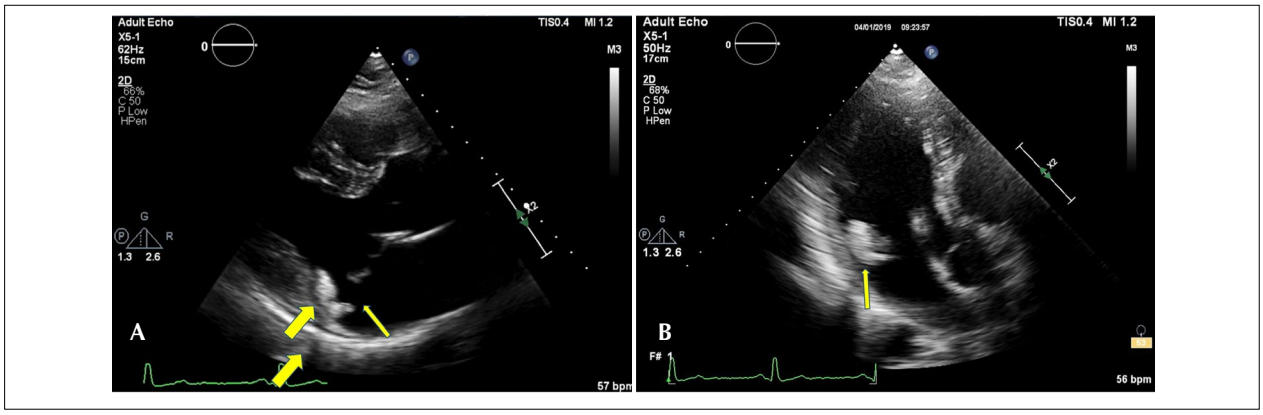

Figure 3 – *Patient with mitral valve prolapse and calcification of part of the posterior portion of the valve annulus. A. The parasternal longitudinal plane showing mitral valve prolapse (thin arrow) and calcification of the valve annulus with formation of posterior acoustic shadow (thick arrows). B. The apical three-chamber plane showing calcification of the valve annulus (thin arrow).*

due to a reduced anteroposterior diameter variation and increased leaflet tenting length and volume without significant inter-commissural diameter variations.[15,18]

Estimating the mitral valve area in such patients can be challenging. The continuity equation can be used as long as mild mitral or aortic regurgitation is not greater than mild. Even so, the estimate may be less accurate due to difficulties in measuring the diameter of the LV outflow tract (due to associated aortic or mitral-aortic curtain calcification). In addition, the LV outflow tract and mitral valve flows are not obtained simultaneously and temporally in the cardiac cycle, which can be even more challenging in patients with an irregular heart rhythm. On the other hand, Doppler estimation using pressure half-time may overestimate the valve area (underestimating stenosis severity) due to decreased LV compliance and increased LV diastolic pressure, which are common in older patients.[9,16,19] Planimetry by two- and three-dimensional echocardiography may be inaccurate due to acoustic shadow formation.[9]

The dimensionless index of the mitral valve can be useful for grading stenosis. It can be obtained by dividing the time-velocity integral value obtained by pulsed-wave Doppler in the LV outflow tract by the time-velocity integral value obtained by continuous-wave Doppler of the mitral inflow. Values lower than 0.35 are correlated with very severe stenosis (mitral valve area < 1 cm²), while those 0.35–0.50 suggest severe stenosis (<1.5 cm²) (Figure 4).[9,19]

The mitral transvalvular gradient should also be cautiously interpreted. In rheumatic mitral stenosis, the relationship between the mean gradient (MG) and the mitral valve area (MVA) is predictable, i.e., when the MG is > 10 mmHg, the MVA is < 1.0 cm². In MAC, this relationship is unpredictable due to a series of confounders. The high flow often present in renal failure and mitral regurgitation may overestimate the MG. On the other hand, the increased LV diastolic pressure caused by advanced age, significant aortic valve disease, or LV systolic dysfunction may underestimate the MG.[20]

These are the predictors of a worse one-year prognosis: MG > 8 mmHg, MVA < 1.5 cm², RV systolic pressure > 50 mmHg, and the presence of atrial fibrillation.[8]

It is important to remember that the transthoracic echocardiogram may underestimate the degree of mitral regurgitation due to the formation of an acoustic shadow posterior to the valve annulus. The regurgitant jet should be analyzed by color Doppler in multiple views, and the power of the subcostal window for this purpose should not be underestimated since it is complemented by transesophageal echocardiography.

In symptomatic patients, interventional procedures may be indicated when symptom control fails after optimized drug treatment; however, the results are dubious and the perioperative risk is often high. Mitral valve replacement surgery with calcium removal is technically challenging due to difficulty obtaining adequate cleavage planes, especially in patients with calcification extending to the LV wall.[21] On the other hand, mitral valve replacement with calcium maintenance can result in paravalvular leak and prosthesis–patient mismatch, common complications in this scenario. In recent years, percutaneous intervention with aortic prosthesis implantation in the mitral position (valve in MAC) has become an alternative in selected cases.[22] The major complications of this procedure involve LV outflow obstruction, atrial embolization of the prosthesis, and paravalvular leak.[21]

Conclusion

MAC is a progressive process with several risk factors and related to a series of adverse cardiovascular events such as arrhythmias, valvular heart disease, heart rhythm disorders, and stroke. In the presence of calcium valve stenosis, stenosis degree grading has some particularities related to rheumatic mitral valve stenosis. The complex anatomy of the mitral valve apparatus can be assessed by two- and three-dimensional echocardiography, and its detailed characterization can add prognostic information that aids the cardiologist with clinical decision-making.

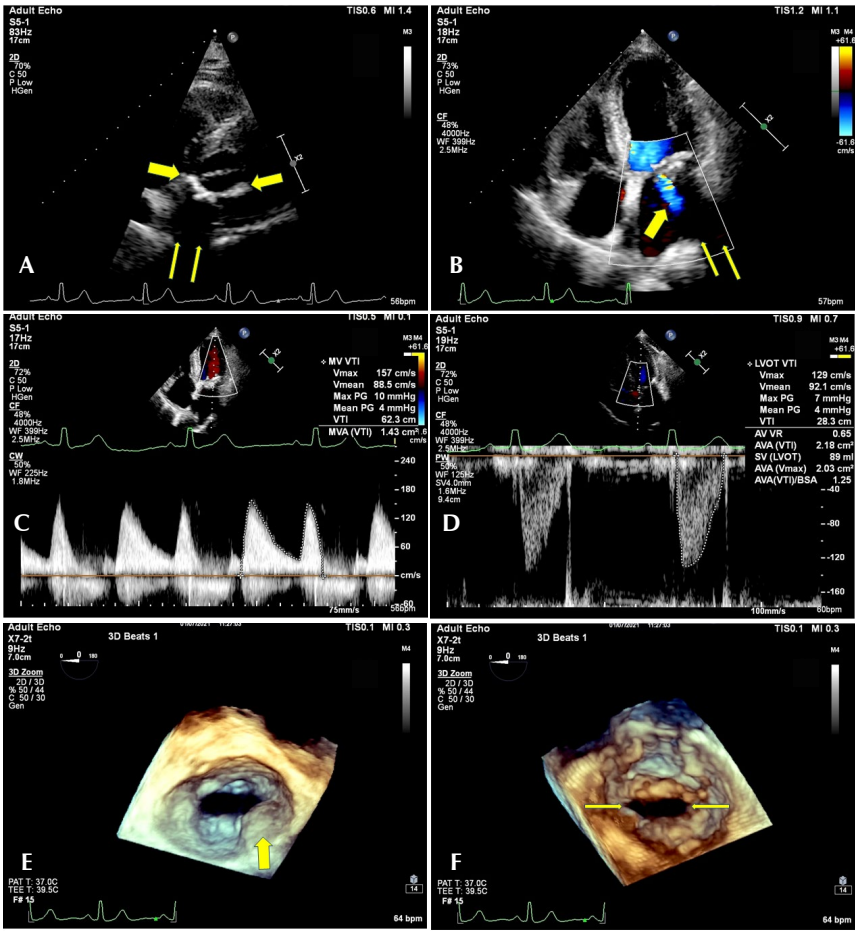

Figure 4 – *Patient with mitral annular calcification (MAC) and a double valve lesion. A. The parasternal short-axis plane at the level of the mitral valve showing calcification of the posterior valve annulus (thick arrow) with formation of a posterior acoustic shadow (thin arrow). B. The apical four-chamber plane with color Doppler showing mitral insufficiency (thick arrow) and the formation of posterior acoustic shadow (thin arrow). C. The time-velocity integral obtained with continuous-wave Doppler of the mitral inflow. D. The time-velocity integral obtained with pulsed-wave Doppler of the LV outflow tract. E. Three-dimensional (3D) transesophageal echocardiogram from the left atrium perspective showing asymmetric MAC distribution (thick arrow). F. The 3D transesophageal echocardiogram from the LV perspective showing a slightly reduced valve opening without commissural involvement (thin arrows).*

Authors' contributions

Manuscript writing: Barros Filho ACL; Literature review: Barros Filho ACL; Image release agreement and figure preparation: Barros Filho ACL, Romano MMD; Manuscript review: Romano MMD; Critical analysis: Romano MMD

Conflict of interest

The authors have declared that they have no conflict of interest.

References

1. Elmariah S, Budoff MJ, Delaney JA, Hamirani Y, Eng J, Fuster V, et al. Risk factors associated with the incidence and progression of mitral annulus calcification: the multi-ethnic study of atherosclerosis. Am Heart J. 2013;166(5):904-12. doi: https://doi.org/10.1016/j.ahj.2013.08.015

2. Fox CS, Larson MG, Vasan RS, Guo CY, Parise H, Levy D, et al. Cross-sectional association of kidney function with valvular and annular calcification: the Framingham heart study. J Am Soc Nephrol. 2006;17(2):521-7. doi: 10.1681/ASN.2005060627.

3. Fusini L, Ghulam Ali S, Tamborini G, Muratori M, Gripari P, Maffessanti F, et al. Prevalence of calcification of the mitral valve annulus in patients undergoing surgical repair of mitral valve prolapse. Am J Cardiol. 2014;113(11):1867-73. doi: 10.1016/j.amjcard.2014.03.013.

4. Abramowitz Y, Jilaihawi H, Chakravarty T, Mack MJ, Makkar RR. Mitral annulus calcification. J Am Coll Cardiol. 2015;66(17):1934-41. doi: https://doi.org/10.1016/j.jacc.2015.08.872

5. Kanjanauthai S, Nasir K, Katz R, Rivera JJ, Takasu J, Blumenthal RS, et al. Relationships of mitral annular calcification to cardiovascular risk factors: the Multi-Ethnic Study of Atherosclerosis (MESA). Atherosclerosis. 2010;213(2):558-62. doi: 10.1016/j.atherosclerosis.2010.08.072.

6. Pressman GS, Rodriguez-Ziccardi M, Gartman CH, Obasare E, Melendres E, Arguello V, et al. Mitral annular calcification as a possible nidus for endocarditis: a descriptive series with bacteriological differences noted. J

Am Soc Echocardiogr. 2017;30(6):572-8. doi: https://doi.org/10.1016/j.echo.2017.01.016.

7. Kizer JR, Wiebers DO, Whisnant JP, Galloway JM, Welty TK, Lee ET, et al. Mitral annular calcification, aortic valve sclerosis, and incident stroke in adults free of clinical cardiovascular disease: the Strong Heart Study. Stroke. 2005;36(12):2533-7. 10.1161/01.STR.0000190005.09442.ad.

8. Kato N, Padang R, Scott CG, Guerrero M, Pislaru SV, Pellikka PA. The Natural History of Severe Calcific Mitral Stenosis. J Am Coll Cardiol. 2020;75(24):3048-57. doi: 10.1016/j.jacc.2020.04.049.

9. Silbiger JJ. Mitral Annular Calcification and Calcific Mitral Stenosis: Role of Echocardiography in Hemodynamic Assessment and Management. J Am Soc Echocardiogr. 2021;34(9):923-31. doi: 10.1016/j.echo.2021.04.007.

10. Faletra FF, Leo LA, Paiocchi VL, Caretta A, Viani GM, Schlossbauer SA, et al. Anatomy of mitral annulus insights from non-invasive imaging techniques. Eur Heart J Cardiovasc Imaging. 2019;20(8):843-57. doi: 10.1093/ehjci/jez153.

11. Silbiger JJ. Anatomy, mechanics, and pathophysiology of the mitral annulus. Am Heart J. 2012;164(2):163-76. doi: 10.1016/j.ahj.2012.05.014.12. Foster GP, Dunn AK, Abraham S, Ahmadi N, Sarraf G. Accurate measurement of mitral annular dimensions by echocardiography: importance of correctly aligned imaging planes and anatomic landmarks. J Am Soc Echocardiogr. 2009;22(5):458-63. doi: 10.1016/j.echo.2009.02.008.

13. Dwivedi G, Mahadevan G, Jimenez D, Frenneaux M, Steeds RP. Reference values for mitral and tricuspid annular dimensions using two-dimensional echocardiography. Echo Res Pract. 2014;1(2):43-50. doi: 10.1530/ERP-14-0050.

14. Mihăilă S, Muraru D, Piasentini E, Miglioranza MH, Peluso D, Cucchini U, et al. Quantitative analysis of mitral annular geometry and function in healthy volunteers using transthoracic three-dimensional echocardiography. J Am Soc Echocardiogr. 2014;27(8):846-57. doi: 10.1016/j.echo.2014.04.017.

15. Pressman GS, Movva R, Topilsky Y, Clavel MA, Saldanha JA, Watanabe N, et al. Mitral Annular Dynamics in Mitral Annular Calcification: A Three-Dimensional Imaging Study. J Am Soc Echocardiogr. 2015;28(7):786-94. doi: 10.1016/j.echo.2015.03.002.16. Pressman GS, Ranjan R, Park DH, Shim CY, Hong GR. Degenerative Mitral Stenosis Versus Rheumatic Mitral Stenosis. Am J Cardiol. 2020;125(10):1536-42. doi: 10.1016/j.amjcard.2020.02.020.

17. Barasch E, Gottdiener JS, Larsen EK, Chaves PH, Newman AB, Manolio TA. Clinical significance of calcification of the fibrous skeleton of the heart and aortosclerosis in community dwelling elderly. The Cardiovascular Health Study (CHS). Am Heart J. 2006;151(1):39-47. doi: 10.1016/j.ahj.2005.03.052.

18. Ben Zekry S, Lang RM, Sugeng L, McCulloch ML, Weinert L, Raman J, et al. Mitral annulus dynamics early after valve repair: preliminary observations of the effect of resectional versus non-resectional approaches. J Am Soc Echocardiogr. 2011;24(11):1233-42. doi: 10.1016/j.echo.2011.08.010.

19. Oktay AA, Riehl R, Kachur S, Khan Z, Tutor A, Chainani V, et al. Dimensionless index of the mitral valve for evaluation of degenerative mitral stenosis. Echocardiography. 2020;37(10):1533-42. doi: 10.1111/echo.14847.

20. Bertrand PB, Churchill TW, Yucel E, Namasivayam M, Bernard S, Nagata Y, et al. Prognostic importance of the transmitral pressure gradient in mitral annular calcification with associated mitral valve dysfunction. Eur Heart J. 2020;41(45):4321-8. doi: 10.1093/eurheartj/ehaa819.

21. El-Eshmawi A, Alexis SL, Sengupta A, Pandis D, Rimsukcharoenchai C, Adams DH, et al. Surgical management of mitral annular calcification. Curr Opin Cardiol. 2020;35(2):107-15. doi: 10.1097/HCO.0000000000000718.

22. Eleid MF, Foley TA, Said SM, Pislaru SV, Rihal CS. Severe Mitral Annular Calcification: Multimodality Imaging for Therapeutic Strategies and Interventions. JACC Cardiovasc Imaging. 2016;9(11):1318-37. doi: 10.1016/j.jcmg.2016.09.001.

My Approach to the Echocardiographic Assessment of Anderson-Fabry Disease

Como Eu Faço Avaliação Ecocardiografica da Doença de Fabry

Hospital de Base do Distrito Federal (HBDF)[1], DF. Brazil

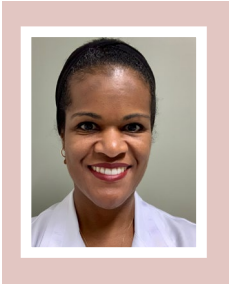

Sandra Marques e Silva[1]

Echocardiographic assessment of anderson-fabry disease

Anderson-Fabry disease (AFD) is a rare lysosomal inborn metabolism error due to changes to the long arm of the X chromosome that result in deficiencies of the alpha-galactosidase enzyme, which is responsible for metabolizing glycosphingolipids. Systemic presentations result from the accumulation of these substances in the cells of organs such as the heart, central and peripheral nervous system, kidneys, eyes, skin, and others.[1] This heart disease, which resembles a sarcomeric hypertrophic cardiomyopathy phenocopy, is a main cause of mortality due to heart failure, arrhythmia, and/or myocardial ischemia in this population in Brazil.[2] The natural disease progression can be changed by an accurate and early diagnosis and the availability of specific intravenous enzyme replacement or oral chaperone therapy, thereby increasing quality of life and life expectancy.[3] Thus, echocardiography plays an essential role as a diagnostic and risk stratification tool in the assessment of therapeutic efficacy and the investigation of cardiac complications.

My approach

A quick anamnesis and precordium auscultation can aid the echocardiographic investigation prior to the test. A detailed history is not always possible, but complaints of intolerance to exertion, chest pain, and palpitations in a young person with no known pathologies should be highlighted. Adolescents and young adults with a history of physical exercise problems in childhood, hypohidrosis, neuropathic pain in the extremities, and/or the presence of reddish nodular lesions on the mucous membranes or in a swimsuit distribution pattern (angiokeratomas) may indicate carriers of the classic form of the disease. Some patients report a family history of AFD and heart disease, chronic kidney disease, and/or cerebral ischemia at an early age; these data are valuable. If an electrocardiogram is available, the presence of ventricular overload signs associated with a short PR interval, arrhythmias, and/or a QTc < 440 ms may help confirm the suspected diagnosis.[4]

The flagship of AFD cardiomyopathy on conventional two-dimensional echocardiography is the presence of hypertrophy. However, it may not be present in the early stages of the disease or might assume unusual aspects. The increased wall thickness is typically concentric, and values greater than 11 mm in women and 12 mm in men are considered pathological by the main international guidelines.[5] Such measures are valid for phenocopy situations and would not work for true hypertrophies such as those in sarcomeric heart diseases, whose values are considered diagnostic if greater than 15 mm in index cases and greater than13 mm in family screening situations.[6] Isolated asymmetric and apical forms are also described; in all cases, left ventricular (LV) outflow tract obstruction is not usually present. More severe cases of hypertrophy are observed concomitantly with chronic renal failure or other outflow tract obstructions, such as rheumatic disease. The right ventricle may be affected by deposits and present 50–70% increased parietal thickness, usually associated with LV hypertrophy.[7]

Papillary muscle hypertrophy is visible even in the first ultrasound sections, but it is not a determinant of the onset of significant intraventricular gradients or severe valvular dysfunction. The latter is often discrete to moderate, and it usually does not progress to severe forms that require correction.[8]

The binary sign, histological correspondent of glycosphingolipid deposits in the endocardium, is visible on two-dimensional images but not currently considered a pathognomonic finding of the disease. It is present in 20–30% of cases, being usually associated with increased ventricular thickness.[9]

The presence of diastolic function changes is usually the earliest AFD cardiomyopathy finding. Cases of patients younger than 40 years of age without underlying diseases such as renal disorders, systemic arterial hypertension, or heart valve disease and presenting decreased tissue Doppler mitral annulus propagation velocities or transmitral flow should be highlighted even if the ventricle is not hypertrophic. Left atrial dilatation indicates advanced disease and is usually present in the final stages of the heart disease progression. This is also true for the development of diastolic dysfunction above grade II and for patterns with restrictive physiology.[10,11]

Systolic function, on the other hand, remains normal over most of the disease course unless other comorbidities such as coronary artery disease, kidney disease, or uncontrolled

Keywords

Fabry Disease; Echocardiography; Diagnosis.

Mailing Address: Sandra Marques e Silva •
Hospital de Base do Distrito Federal (HBDF), DF. Brazil.
E-mail: smarquesmd@gmail.com
Manuscript received 12/10/2021; revised 1/20/2022; accepted 1/23/2022.

DOI: 10.47593/2675-312X/20223501ecom20

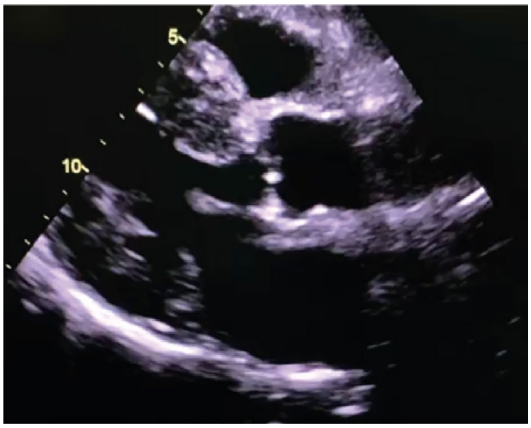

Figure 1 – *Longitudinal parasternal image of the left ventricle showing increased wall thickness, a granulated myocardium (suggestive of deposit disease), increased mitral and aortic valve thickness, and increased endocardial refringence (binary sign).*

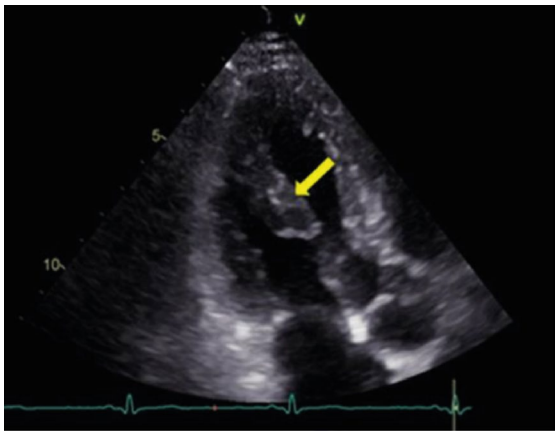

Figure 2 – *Five-chamber apical image of the left ventricle demonstrating increased papillary muscle thickness.*

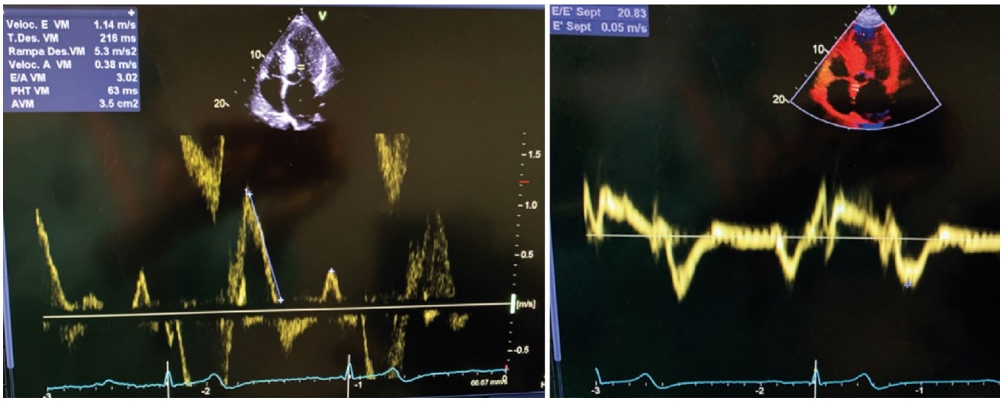

Figure 3 – *Doppler images of the left ventricle of a patient with advanced fabry cardiomyopathy. A. transmitral flow pulsed wave doppler showing an increased e/a ratio. B. mitral ring tissue doppler in the septal position with a decreased propagation velocity and increased e/e' ratio. both changes are compatible with a left ventricle diastolic dysfunction pattern.*

hypertension are present. New assessment techniques such as myocardial strain have detected subclinical changes, even in the presence of preserved ejection fraction. An LV assessment shows a reduced AFD global longitudinal strain due to a characteristic strain change in the basal region of the lower lateral wall. Dysfunction may be more diffuse over the natural course of the disease without adequate clinical treatment. The right ventricle and left atrium may also present decreased strain. These findings add prognostic value and may predict future clinical decompensation with heart failure and arrhythmias, which worsen in the presence of underlying myocardial fibrosis. Although the gold-standard method for this diagnosis is magnetic resonance imaging, this technique may suggest this change.[10,11]

The aorta may present increased proximal portion dimensions determined by the deposits. However, the progression to aneurysmal forms requiring specific treatment is very rare and usually associated with other pathologies.[12]

All of the findings described above should be investigated by the echocardiographer as a possible AFD cardiomyopathy. In many cases, the clinician treating the patient must be informed of this diagnostic hypothesis in the patient's final report. However, echocardiography alone is insufficient to confirm the diagnosis, which requires complementary investigation with magnetic resonance or other diagnostic methods. Genotyping is essential to determining the point of genome change and classifying the disease as classic or late presentation (late onset or cardiac form)[13,14]. The progression of these variants is dissimilar and the findings may have an earlier onset and be more severe in the former than the latter situation. Finally, the process to access the specific treatment (judicially in Brazil) depends on this information.

Conflict of interest

The author declares no conflicts of interest.

References

1. Desnick RJ, Ioannou YA, Eng CM. α-Galactosidase A deficiency: Fabry disease. In: Scriver CR, Beaudet AL, Sly WS, Valle D, eds. The metabolic and molecular bases of inherited disease. 7th ed. New York: McGraw-Hill, 1995. p. 2741-84. v. 2.
2. Martins AM, Kyosen SO, Garrote J, Marques FM, Guilhem JG, Macedo E, et al. Demographic characterization of Brazilian patients enrolled in the Fabry Registry. Genet Mol Res. 2013;12(1):136-42. doi: 10.4238/2013.January.24.5
3. Miller JJ, Kanack AJ, Dahms NM. Progress in the understanding and treatment of Fabry disease. Biochim Biophys Acta Gen Subj. 2020;1864(1):129437. doi: 10.1016/j.bbagen.2019.129437
4. Chaves AV. Doença de Fabry: o que sabemos hoje. Rev Soc Cardiol Estado de São Paulo. 2021 [citado 2022 Fev 9];31(2):198-206. Disponível em: https://socesp.org.br/web-socesp/podcast-revista-socesp/revista-socesp-vol-31-n-02-doencas-raras-em-cardiologia-parte-ii/doenca-de-fabry-o-que-hoje-sabemos/
5. Sirrs S, Bichet DG, Iwanochko M, Khan A, Moore D, Oudit G, et al. Canadian Fabry disease treatment guidelines. Canada; 2016 [cited 2022 Feb 9] Available at: http://www.garrod.ca/wp-content/uploads/Canadian-FD-Treatment-Guidelines-2016.pdf.
6. Maron BJ, McKenna WJ, Danielson GK, Kappenberger LJ, Kuhn HJ, Seidman CE, et al. American College of Cardiology/European Society of Cardiology clinical expert consensus document on hypertrophic cardiomyopathy: a report of the American College of Cardiology foundation task force on clinical expert consensus documents and the European Society of Cardiology committee for practice guidelines. Journal of the American College of Cardiology. 2003;42(9):1687-13.
7. Niemann M, Breunig F, Beer M, Herrmann S, Strotmann J, Hu K, et al. The right ventricle in Fabry disease: natural history and impact of enzyme replacement therapy. Heart. 2010;96(23):1915-9. doi: 10.1136/hrt.2010.204586
8. Ueno H, Yokota Y, Yokoyama M, Itoh H. Comparison of echocardiographic and anatomic measurements of the left ventricular wall thickness. Kobe J Med Sci. 1991;37(6):273-86. PMID: 1840115.
9. Mundigler G, Gaggl M, Heinze G, Graf S, Zehetgruber M, Lajic N, et al. The endocardial binary appearance ('binary sign') is an unreliable marker for echocardiographic detection of Fabry disease in patients with left ventricular hypertrophy. Eur J Echocardiogr. 2011;12(10):744-9. doi: 10.1093/ejechocard/jer112
10. Shanks M, Thompson RB, Paterson ID, Putko B, Khan A, Chan A, et al. Systolic and diastolic function assessment in fabry disease patients using speckle-tracking imaging and comparison with conventional echocardiographic measurements. J Am Soc Echocardiogr. 2013;26(12):1407-14. doi: 10.1016/j.echo.2013.09.005
11. Pieroni M, Moon JC, Arbustini E, Barriales-Villa R, Camporeale A, Vujkovac AC, et al. Cardiac Involvement in Fabry Disease: JACC Review Topic of the Week. J Am Coll Cardiol. 2021;77(7):922-936. doi: 10.1016/j.jacc.2020.12.024
12. Barbey F, Qanadli SD, Juli C, Brakch N, Palacek T, Rizzo E, et al. Aortic remodelling in Fabry disease. Eur Heart J. 2010;31(3):347-53. doi: 10.1093/eurheartj/ehp426
13. Ortiz A, Germain DP, Desnick RJ, Politei J, Mauer M, Burlina A, et al. Fabry disease revisited: Management and treatment recommendations for adult patients. Mol Genet Metab. 2018;123(4):416-427. doi: 10.1016/j.ymgme.2018.02.0
14. Yeung DF, Sirrs S, Tsang MY, Gin K, Luong C, Jue Jet al. Echocardiographic Assessment of Patients with Fabry Disease. J Am Soc Echocardiogr. 2018;31(6):639-649.e2. doi: 10.1016/j.echo.2018.01.016
15. Seydelmann N, Wanner C, Störk S, Ertl G, Weidemann F. Fabry disease and the heart. Best Pract Res Clin Endocrinol Metab. 2015;29(2):195-204. doi: 10.1016/j.beem.2014.10.003

My Approach To Echocardiographic Assessment In Pulmonary Hypertension

Como eu Faço a Avaliação Ecocardiográfica na Hipertensão Pulmonar

Hospital das Clínicas da Universidade Federal de Goiás,[1] Goiânia, GO, Brazil.

João Batista Masson-Silva[1]

Cloves Geraldino da Silva Júnior[1]

Pulmonary hypertension (PH) is a syndrome with a high worldwide prevalence characterized by increased pulmonary circulation pressure that progressively leads to vascular bed and right ventricle component remodeling.[1]

The PH diagnosis is suspected based on clinical signs/symptoms and echocardiographic findings, but it is confirmed only by direct and invasive measurements during right heart catheterization showing a mean pulmonary artery pressure (mPAP) > 20 mmHg. Treatment aims to alleviate symptoms and delay progression to the final disease stage, which presents irreversible micro- and macrovascular changes and right ventricular dysfunction. A delayed diagnosis changes the natural course of the disease, increasing morbidity and mortality.[2,3]

From clinical and hemodynamic points of view, PH can be classified into five groups (Figure 1 e Table 1):[4,5]

Echocardiography plays a fundamental role in the diagnostic screening of PH and in the assessment of right ventricular systolic function.

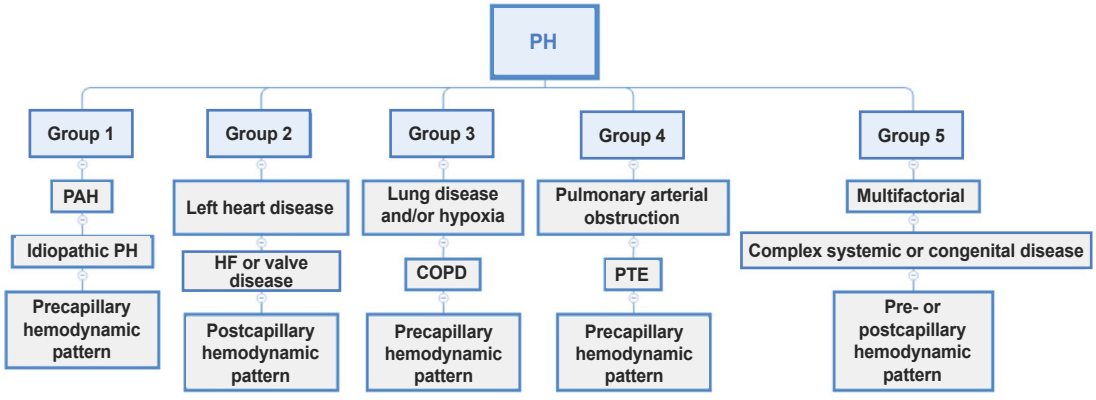

COPD, chronic obstructive pulmonary disease; HF, heart failure; PH, pulmonary hypertension; PTE, pulmonary thromboendarterectomy.

Figure 1 – *Haemodynamic classification of PH Classificação hemodinâmica da Hipertensão pulmonar.*

Keywords

Hypertension, Pulmonary; Diagnosis; Echocardiography.

Mailing Address: João Batista Masson Silva •
Primeira Avenida, quadra 68 lt-AR 1, Setor Leste Universitário.
CEP 74605-020 – Goiânia, GO, Brazil.
E-mail: jbmasson@ufg.br
Manuscript received 12/10/2021; revised 1/16/2022; accepted 2/6/2022.

DOI: 10.47593/2675-312X/20223501ecom18

Table 1 – Clinical and hemodynamic classification of pulmonary hypertension groups.

Grup		Sub-group	Clinical presentation	Hemodynamics
I	PAH	Idiopathic PAH Hereditary PAH PAH associated with connective tissue disease, HIV, portal hypertension, congenital heart disease, schistosomiasis PAH CCB responders Pulmonary capillary hemangiomatosis, pulmonary veno-occlusive disease Persistent PH of the newborn	Dyspnea, syncope, jugular stasis, peripheral edema Specific signs of connective tissue, liver, and HIV disease Echocardiographic signals limited to the right chambers	Precapillary PH: mPAP > 20 mmHg PAOP ≤ 15 mmHg PVR ≥ 3 Wood units
II	PH secondary to left heart disease	PH due to HFpEF PH due to HFrEF Valvar disease Congenital disease or cardiovascular condition leading to postcapillary PH	Left heart and/or valve disease signs and symptoms ECHO: right chamber + left chamber and/or valvular changes	Isolated postcapillary PH: mPAP > 20 mmHg PAOP ≥ 15 mmHg PVR ≤ 3 Wood units Combined pre- and postcapillary PH: mPAP > 20 mmHg PAOP ≥ 15 mmHg PVR ≥ 3 Wood units
III	PH secondary to lung disease and/or hypoxia	COPD Restrictive lung disease Hypoxia without pulmonary disease	Chronic hypoxia at rest and/or on exertion Specific lung function and/or lung imaging test changes Changed polysomnography	Precapillary PH: mPAP > 20 mmHg PAOP ≤ 15 mmHg PVR ≥ 3 Wood units
IV	PH secondary to pulmonary artery obstruction	Chronic PTE	Dyspnea, edema Ventilation/perfusion scintigraphy and/or chest CT angiography changes Association with neoplasia	Precapillary PH: mPAP > 20 mmHg PAOP ≤ 15 mmHg PVR ≥ 3 Wood units
V	Multifactorial and/or uncertain mechanisms	Hematologic disease Metabolic and systemic disorder (pulmonary histiocytosis, Gaucher disease, sarcoidosis, neurofibromatosis, glycogen storage disease) Others (chronic kidney disease with or without hemodialysis, fibrosing mediastinitis) Complex congenital heart disease	Signs and symptoms of underlying disease (anemia, metabolic disease)	Precapillary PH: mPAP > 20 mmHg PAOP ≤ 15 mmHg PVR ≥ 3 Wood units Or Postcapillary PH: mPAP > 20 mmHg PAOP ≥ 15 mmHg PVR ≤ 3 Wood units

CCB, calcium channel blockers; COPD, chronic obstructive pulmonary disease; CT, computed tomography; ECHO, echocardiography; HFpEF, heart failure with preserved ejection fraction; HFrEF, heart failure with reduced ejection fraction; HIV, human immunodeficiency virus; mPAP, mean pulmonary artery pressure; PAH, pulmonary arterial hypertension; PAOP, pulmonary artery occluded pressure; PH, pulmonary hypertension; PVR, pulmonary vascular resistance; PTE, pulmonary thromboembolism.

Clinically suspected patients (symptoms and signs on physical examination suggestive of PH) should be referred for echocardiography to assess the echocardiographic probability of PH, right ventricular function, and the presence of severity criteria.[4,6]

Echocardiographic assessment of PH probability

Echocardiographic PH probability can be classified as low, intermediate, or high. This categorization is based on the assessment of peak tricuspid regurgitation (TR) velocity and the presence of indirect signs suggestive of increased pulmonary vascular bed pressure (Table 2).[4,6]

Peak TR velocity is the key criterion and should be measured by continuous-wave Doppler during smooth respiration according to the following recommendations:[4,6-8] (Table 2).

Indirect echocardiographic signs suggestive of PH may be related to the ventricles (group A), pulmonary artery (group B), inferior vena cava, and RA (group C) and should be evaluated according to the following recommendations (Table 3):[4,6-8]

Assessment of RV systolic function

Due to its anatomical complexity, the RV is the most difficult cardiac chamber to analyze. The architecture of its thin walls (triangular morphology on the long axis, crescent on the short axis) consists of many trabeculations, intertwined longitudinal muscle fibers in the sub-endocardium, and superficial circumferential subepicardial fibers. Its contraction movement resembles a bellows, has a complex mechanism, and occurs predominantly longitudinally from the base to the apex, where the shortening of minor and major axes pulls the tricuspid valve toward the apex. Its thickness does not exceed 5 mm.[7]

Due to this complexity, the functional analysis of the RV has been neglected or evaluated subjectively for years. Studies from the last decade consolidated the importance of the RV in maintaining hemodynamic stability, showing significantly increased morbidity and mortality regardless of the underlying disease in the progression to an advanced stage of RV dysfunction. The clinical need for an accurate RV assessment and the technological advancement of software favored the study of numerous parameters in the search for an earlier diagnosis to delay the disease's natural course.[9]

Cardiac resonance, the gold standard for functional analysis

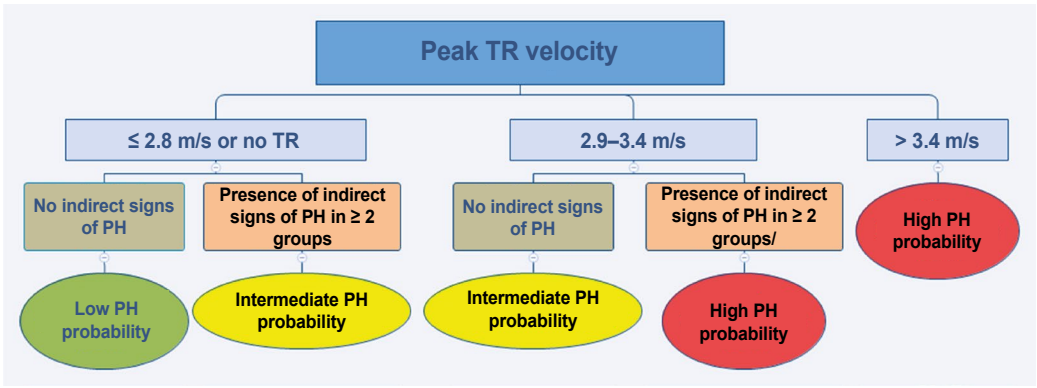

PH, pulmonary hypertension; TR, tricuspid regurgitation.

Figure 2 – *Estimated echocardiographic PH probability based on peak TR velocity and indirect signs of PH.*

Table 2 – Tricuspid regurgitation analysis.

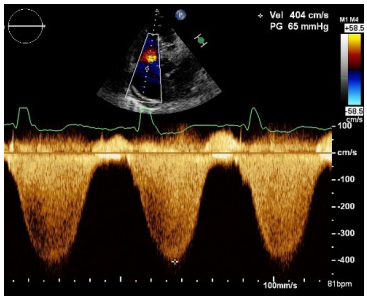

1. Use several windows (apical four-chamber, short-axis, subcostal, or other modified positions) to obtain the best regurgitant jet envelope.
2. Avoid eccentric jets as they may underestimate measurements.
3. Use high scan velocities (100 mm/s) to better differentiate true velocity from artifacts.
4. Report that the velocities may be underestimated in severe regurgitation, especially when associated with annulus dilation and valve leaflet coaptation failure (there is no gradient between the right atrium and the right ventricle; similar to a single chamber)
5. Average five beats in atrial fibrillation.
6. Right ventricular systolic pressure estimation is not recommended due to the high right atrial pressure variability subjectively caused by inferior vena cava variations.

Table 3 – Indirect echocardiographic signs.

Group A – Ventricles	
Ratio of right (RV) and left ventricle (LV) basal diameter measurements 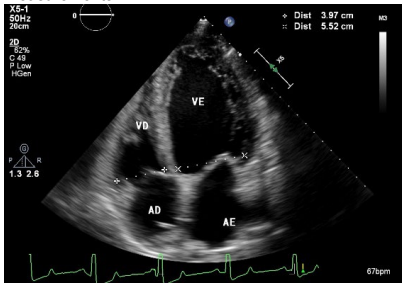	Apical four-chamber plane (avoid shortening) Measure LV and RV basal diameters at end-diastole Consider the ratio of basal RV/LV diameter as an indirect criterion for PH, with a value of >1 indicating RV dilation
LV eccentricity Index (LVEI) 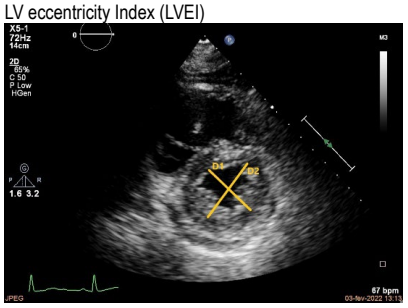	Parasternal short-axis plane – mid-region between papillary muscles and top of mitral valve leaflets End-systole – moment of visualization of the smallest cavity End-diastole – R wave peak Measurement location – D1 is the LV diameter perpendicular to the interventricular septum (IVS), D2 is the LV diameter parallel to the IVS LVEI = D2/D1 Volume overload: changes LVEI only in diastole Pressure overload: changes LVEI in systole and/or diastole Consider as an indirect PH criterion: LVEI > 1.1 in systole or both systole and diastole

Group B - Pulmonary artery	
Pulmonary artery acceleration time 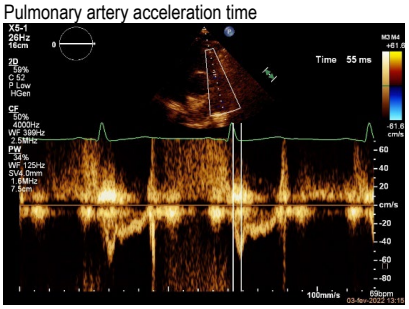	Parasternal short-axis plane Place pulsed Doppler sample volume sample in the RV outflow tract (RVOT) - ventricular face (below the pulmonary valve cusps) Measure time from the beginning to peak pulmonary artery velocity Measure at the end of expiration Use a five-beat average in atrial fibrillation Heart rate (HR) < 70 bpm or > 100 bpm may reduce accuracy – correct with the formula: acceleration time × 75/HR HR does not interfere with acceleration time in patients with an invasive mPAP > 25 mmHg Systolic notching suggests a pattern of high pulmonary circulation resistance Consider as an indirect PH criterion: AT < 105 ms
Initial diastolic pulmonary regurgitant velocity (iPRV) 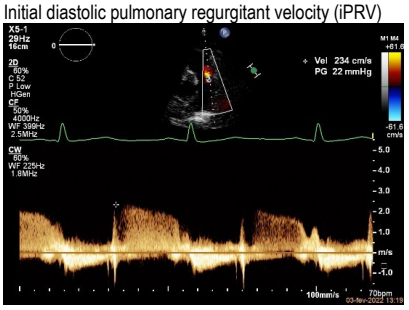	Parasternal short-axis or RVOT plane Align continuous-wave Doppler with the pulmonary reflux jet Measure initial peak velocity Consider as an indirect PH criterion: iPRV > 2.2 m/s
Pulmonary artery diameter (PAD) 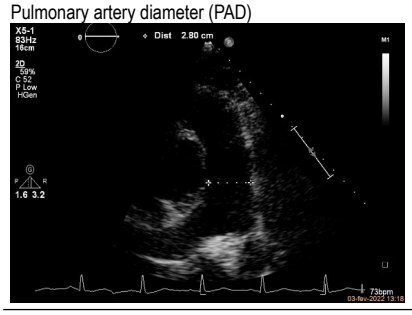	Parasternal short-axis plane Place frame at end-diastole Measure the lung diameter at the midpoint between the pulmonary valve and the bifurcation point (right and left branch emergence) Consider as an indirect PH criterion: PAD > 25 mm
Group C – Inferior vena cava and RA	
Inferior vena cava diameter and respiratory variation 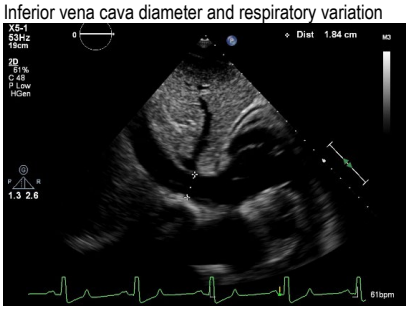	Subcostal plane Measure the diameter 1–2 cm from the junction with the RA Measure at the end of expiration Consider as an indirect PH criterion: diameter > 21 mm with reduced respiratory variability (<50% with deep inspiration or <20% with shallow respiration)
Right atrial area (RAA) 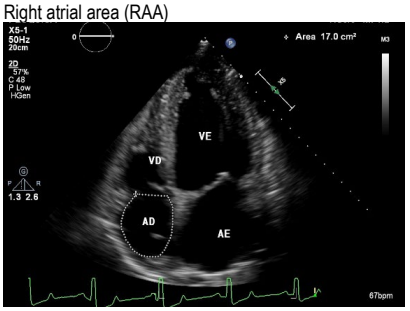	Apical four-chamber plane Measure at the end of ventricular systole (frame before tricuspid valve opening) Consider as an indirect PH criterion: RAA > 18 cm²

LV: left ventricle; RV: right ventricle; LVEI - LV: eccentricity Index; IVS: interventricular septum; RVOT: right ventricle outflow tract; HR: Heart rate; AT: acceleration time; mPAP: mean pulmonary artery pressure; iPRV: Initial diastolic pulmonary regurgitant velocity; PAD: Pulmonary artery diameter; r - IVC: Inferior vena cava; RA: Right atrial; RAA: Right atrial area.

of the RV, is not influenced by technical image acquisition limitations, but its lower availability, impossible portability, time-consuming performance, and high cost hinder its use as a first-choice method for such purposes. On the other hand, echocardiography, which features low cost and no radiation exposure, has become the most attractive method for the initial assessment of global RV function, being the gold standard method for selected cases.[10]

Echocardiography analyzes RV segments by acquiring multiple echocardiographic windows using all the features offered by ultrasound (M-mode, Doppler, 2D, 3D, strain). The first quantitative parameters are derived from basic echocardiography and called classic, conventional, or traditional (Tabela 4). These quantitative parameters aim to detect changes in RV function at an earlier stage but have been criticized for being extremely dependent on pre- and post-load states and inferring that the assessment of a small RV segment may reflect the global function of a highly complex anatomical structure. Despite criticisms and technical difficulties, these parameters are used in clinical practice, being established by both general consensus on chamber quantification and the specific quantification of the right chambers. Technology has brought advanced parameters derived from myocardial deformation and 3D imaging with the advantages of evaluating more than one RV segment and of not being so influenced by hemodynamic conditions. The low availability of software in devices and the few studies of its standardization among manufacturers are real limitations in daily practice.[9,11]

The presence of pericardial effusion and measurements of right ventricular diameters and thickness are additional parameters useful in analyzing the severity of pulmonary hypertension and its hemodynamic repercussion on the right chambers (Table 5).

Final considerations

PH is invasively diagnosed only by right heart catheterization (mPAP > 20 mmHg).

Echocardiography is the main test used to screen patients with suspected PH. It aims to estimate echocardiographic PH probability and assess the morph functionality of the right chambers.

It should not be used to grade PH severity.

Table 4 – Echocardiographic parameters for analysis of right ventricular function.

Classical echocardiographic parameters	
Tricuspid annular plane systolic excursion (TAPSE) 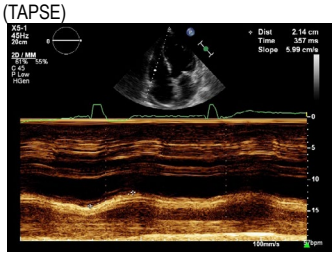	Technique: - Position the unidimensional mode cursor (M) in the basal region of the lateral tricuspid annulus in the apical four-chamber plane. - Measure from the systolic displacement of the tricuspid annulus Advantages: - Easy to perform - Good correlation with cardiac magnetic resonance imaging data Disadvantages and limitations: - Regional segmental changes - Hemodynamic conditions - Angle of insonation - Cardiac translational movement Consider that the measurement of a basal segment represents the global function of a cavity with complex anatomy. It may be normal in patients with cardiac dysfunction (PH) It may be reduced in patients with preserved right ventricular function (post-cardiac surgery) Consider as dysfunction: TAPSE < 17 mm
S' – TDI – Tissue Doppler tricuspid annular systolic velocity 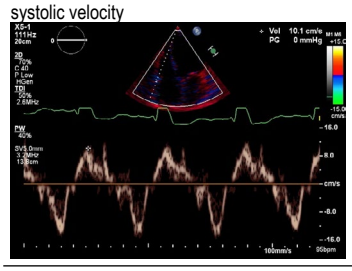	Technique: - Position the tissue Doppler sample volume in the basal region of the lateral tricuspid annulus in the apical four-chamber plane - Measure the peak systolic velocity of lateral tricuspid annular motion Advantages: Easy to perform Disadvantages and limitations: - Dependent on insonation angle - Varies greatly with global cardiac motion - Dependent on correct alignment (as parallel as possible) of the Doppler with the tricuspid annular motion Assesses only the basal segment of the RV free wall Consider as dysfunction: S' - TDI < 9.5 cm/s
MAF/FAC - Fractional area change 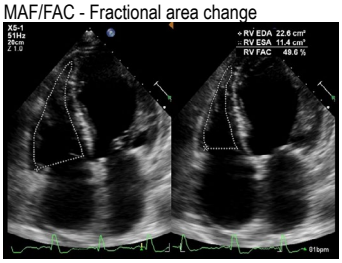	Technique: - Four-chamber apical plane - two-dimensional mode - Trace the endocardial borders of the RV by estimating the area in systole and diastole - Calculate variation using the formula: MAF/FAC = 100 × (RV area in diastole - RV area in systole)/RV area in diastole Advantage: Enables evaluation of a greater number of RV segments Disadvantages and limitations: - Definition of endocardial borders - Does not consider RV outflow in functional analysis Consider as dysfunction: MAF/FAC < 35%

MPI/TEI – myocardial performance index or TEI index 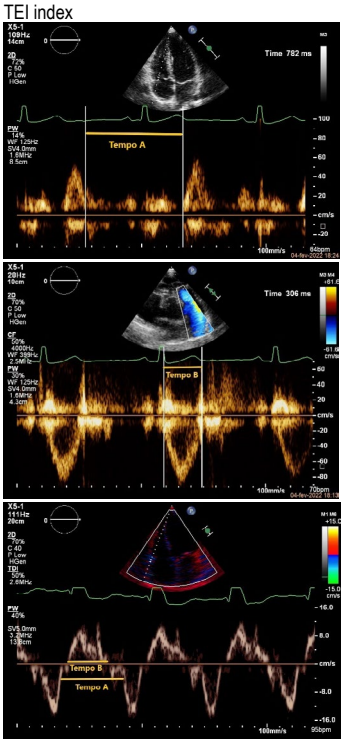	Technique: • Pulsed Doppler: - In 4C apical plane, position the sample volume atop the tricuspid valve leaflets and measure the time between two tricuspid flows (IVRT + ET + IVCT) – Time A - In the short-axis plane, position the sample volume in the RVOT (close to the pulmonary valve leaflets) and measure the pulmonary ejection time – Time B • Tissue Doppler: - In 4C apical plane, position the sample volume in the basal region of the lateral tricuspid annulus - Measure the time between two tricuspid flows (IVRT + ET + IVCT) – Time A - Measure the pulmonary ejection time – Time B Calculated by dividing the sum of isovolumetric contraction and relaxation times by the RV ejection time (MPI = A - B/B). Advantage: Tissue Doppler technique acquires A and B times in a single beat of the cardiac cycle • Disadvantages and limitations: - Pulsed Doppler technique requires beats at different times to acquire A and B times - it can change the results, especially with heart rate variability It is a global index that assesses RV systolic and diastolic function (not possible to distinguish between them) Consider as dysfunction: MPI/TEI > 0.43 on pulsed Doppler and > 0.55 on tissue Doppler
Advanced echocardiographic parameters:	
RV free wall strain (RVFWS) 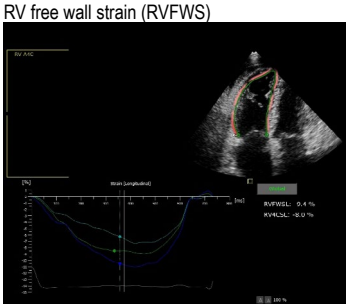	Strain is defined as the change in the length (deformation) of the myocardium under the action of a force (fractional change of a myocardial segment in relation to the initial length after the action of a contraction force) The most common method is speckle tracking using the block matching (region of interest or kernel tracking; Philips and GE) or optical flow techniques (derived from vector velocity; Esaote and Siemens) It can be evaluated globally by left ventricular global strain or only on the RV free wall (RVFWS) – the latter being more specific by excluding interventricular septum analysis (LV fiber interference) Technique: Apical four-chamber plane with optimized image and focused on the RV Frame rate > 50–60 Hz Visualize RV apex throughout the cardiac cycle (request apnea if necessary) Calculate deformation using each manufacturer's own algorithm Automatic methods using artificial intelligence have gained more space due to their agility and good correlation with the gold standard method. Advantages: Reproducible and independent of the angle of insonation and translational movement Disadvantages: Does not consider RVOT, variability between manufacturers, image quality Consider as dysfunction: RVFWS < -20% correlates with a reduced RV ejection fraction
3D RVEF-RV ejection fraction by the 3D method 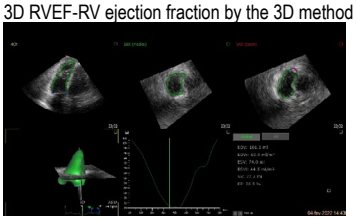	Apical four-chamber plane focused on the RV Use a 3D transducer and acquire the RV full volume encompassing the tricuspid and pulmonary valves Acquire it at the highest possible frame rate – preferably > 20 Hz Reconstruct with specific software (according to the manufacturer) to calculate volumes and ejection fraction Advantages: - Enables better anatomical assessment (includes all RV segments) - Assesses RV longitudinal and radial contraction - Assesses anteroposterior shortening Limitations: - Dependent on pre- and post-load states - Image must be of good quality to enable endocardial border identification - Artifacts produced by arrhythmias - Acquisition and processing time - Availability (of the 3D transducer and quantification software) - Consider as dysfunction: 3D RVEF < 45%

TAPSE = Tricuspid annular plane systolic excursion; TDI - Tissue Doppler; RV = Right ventricle; FAC = Fractional area change; RIMP or Tei index = Right ventricular index of myocardial performance; IVRT = Isovolumic relaxation time; ET = Ejection time; IVCT = Isovolumic contraction time; RVFWS – RV free wall strain; RVGS – RV global strain; 3D RVEF - 3D Right ventricule Ejection fraction; RVOT = Right ventricular outflow tract.

Table 5 – Additional echocardiographic parameters for RV assessment.

Pericardial effusion 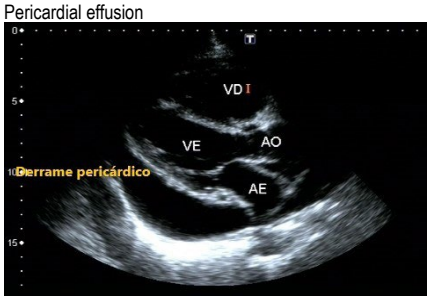	Related to the natural disease course and its prognosis Absence of stroke indicates better prognosis Presence of stroke associated with advanced disease and worse prognosis
RV dimensions 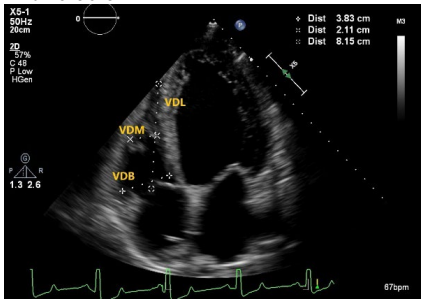 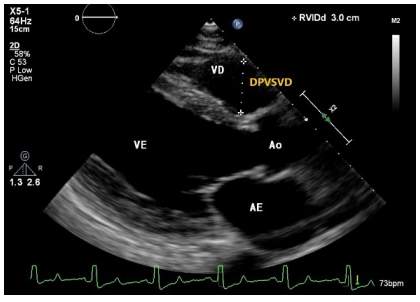 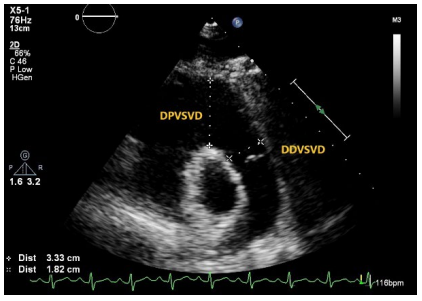	PH increases pre- and post-load with progressive RV dilation RV inflow tract plane: Modified apical four-chamber window for RV Visualize RV apex Avoid RV shortening (can be technically difficult due to crescent shape) Measure the RV at end-diastole Basal diameter of the RV (BRV) - Maximum transverse diameter at the base of the RV - Consider as increased: BRV > 41 mm Mean RV diameter (MRV) - Transverse diameter measured at LV papillary muscle level - Consider increased: MRV > 35 mm Longitudinal RV diameter (LRV) - Longitudinal length from the tricuspid annular plane to the RV apex - Consider increased: LRV > 83 mm RVOT plane: RVOT proximal diameter (RVOTPD): -- Linear measurement taken at end-diastole from the RV anterior wall to the septum-aortic interventricular junction in long-axis parasternal window. Consider as increased: RVOTPD long axis > 30 mm -- Linear measurement taken at end-diastole from the anterior wall of the RV to the aortic valve in sternal short-axis window. Consider increased: RVOTPD short axis > 35 mm RVOT distal diameter (RVOTDD): Linear measurement taken at the close proximal end pulmonary valve diastole in sternal short-axis window. Consider increased: RVOTDD > 27 mm
RV thickness: 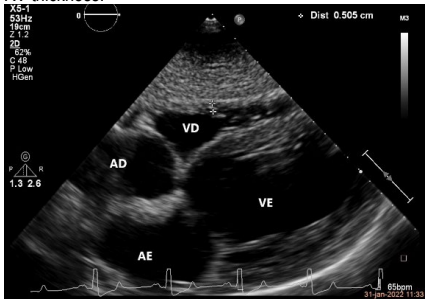	PH causes RV hypertrophy Method: Subcostal or apical four-chamber plane Measure RV thickness using 2D or M-mode at end-diastole Measurement location: RV free wall below the tricuspid annulus (distance from valve plane equivalent to the point at the top of the fully open anterior leaflet and parallel to the free wall) Limitations: Single point measurement Harmonic imaging and angled M-mode may overestimate thickness Technical difficulty in cases of pericardial thickening Consider hypertrophy: thickness > 5 mm

PH: Pulmonary hypertension; RV: right ventricle; BRV: basal diameter of the RV; MRV: mean RV diameter; LV: left ventricle; LRV: longitudinal RV diameter; RVOTPD: right ventricle outflow tract proximal diameter; RVOTDD: right ventricle outflow tract distal diameter.

Authors' contributions

manuscript writing: Masson Silva JB; critical review of the manuscript for important intellectual content: Júnior CGS

Conflict of interest

The authors have declared that they have no conflict of interest.

References

1. Hassoun PM. Pulmonary Arterial Hypertension. N Engl J Med. 2021 Dec 16;385(25):2361-76. doi: https://doi.org/10.1056/NEJMra2000348
2. Mandras SA, Mehta HS, Vaidya A. Pulmonary Hypertension: A Brief Guide for Clinicians. Mayo Clin Proc. 2020;95(9):1978-88. doi: https://doi.org/10.1016/j.mayocp.2020.04.039
3. Yaghi S, Novikov A, Trandafirescu T. Clinical update on pulmonary hypertension. J Investig Med. 2020;68(4):821-7. doi: https://doi.org/10.1136/jim-2020-001291
4. Galiè N, Humbert M, Vachiery JL, Gibbs S, Lang I, Torbicki A, et al.; ESC Scientific Document Group. 2015 ESC/ERS Guidelines for the diagnosis and treatment of pulmonary hypertension: The Joint Task Force for the Diagnosis and Treatment of Pulmonary Hypertension of the European Society of Cardiology (ESC) and the European Respiratory Society (ERS): Endorsed by: Association for European Paediatric and Congenital Cardiology (AEPC), International Society for Heart and Lung Transplantation (ISHLT). Eur Heart J. 2016;37(1):67-119. doi: https://doi.org/10.1093/eurheartj/ehv317
5. Simonneau G, Montani D, Celermajer DS, Denton CP, Gatzoulis MA, Krowka M, et al. Haemodynamic definitions and updated clinical classification of pulmonary hypertension. Eur Respir J. 2019;53(1):1801913. doi: https://doi.org/10.1183/13993003.01913-2018
6. Augustine DX, Coates-Bradshaw LD, Willis J, Harkness A, Ring L, Grapsa J, et al. Echocardiographic assessment of pulmonary hypertension: a guideline protocol from the British Society of Echocardiography. Echo Res Pract. 2018;5(3):G11-G24. doi: https://doi.org/10.1530/ERP-17-0071. PMID: 30012832
7. Rudski LG, Lai WW, Afilalo J, Hua L, Handschumacher MD, Chandrasekaran K, et al. Guidelines for the echocardiographic assessment of the right heart in adults: a report from the American Society of Echocardiography endorsed by the European Association of Echocardiography, a registered branch of the European Society of Cardiology, and the Canadian Society of Echocardiography. J Am Soc Echocardiogr. 2010;23(7):685-713; quiz 786-8. doi: https://doi.org/10.1016/j.echo.2010.05.010
8. Lang RM, Badano LP, Mor-Avi V, Afilalo J, Armstrong A, Ernande L, et al. Recommendations for cardiac chamber quantification by echocardiography in adults: an update from the American Society of Echocardiography and the European Association of Cardiovascular Imaging. J Am Soc Echocardiogr. 2015;28(1):1-39.e14. doi: https://doi.org/10.1016/j.echo.2014.10.003
9. Vijiiac A, Onciul S, Guzu C, Scarlatescu A, Petre I, Zamfir D, et al. Forgotten No More-The Role of Right Ventricular Dysfunction in Heart Failure with Reduced Ejection Fraction: An Echocardiographic Perspective. Diagnostics (Basel). 2021;11(3):548. doi: https://doi.org/10.3390/diagnostics11030548
10. Evaldsson AW, Lindholm A, Jumatate R, Ingvarsson A, Smith GJ, Waktare J, et al. Right ventricular function parameters in pulmonary hypertension: echocardiography vs. cardiac magnetic resonance. BMC Cardiovasc Disord. 2020;20(1):259. doi: https://doi.org/10.1186/s12872-020-01548-4
11. Brugger N, Lichtblau M, Maeder M, Muller H, Pellaton C, Yerly P, Swiss Society For Pulmonary Hypertension Ssph. Two-dimensional transthoracic echocardiography at rest for the diagnosis, screening and management of pulmonary hypertension. Swiss Med Wkly. 2021;151:w20486. doi: https://doi.org/10.4414/smw.2021.20486

My approach to diagnosis of and echocardiographic follow-up for muscular dystrophies

Como Eu Faço Diagnóstico e Seguimento Ecocardiográfico nas Distrofias Musculares

Raphael Henrique Déa Cirino[1], Renata Dal-Prá Ducci[2]

[1]Hospital das Clínicas of the Federal University of Paraná – Department of Clinical Medicine – Cardiology Service, Curitiba, PR, Brazil. [2]Hospital das Clínicas of the Federal University of Paraná – Department of Clinical Medicine – Neuromuscular Disease Service, Curitiba, PR, Brazil

Introduction

Muscular dystrophies (MD) are a group of heterogeneous diseases genetically determined and characterized by progressive muscle atrophy and weakness. Mutations in genes encoding muscle fiber proteins lead to the development of MD. MD types vary by deficient protein, each with its natural history and characteristic clinical presentation. As with other clinical aspects, cardiac involvement is also quite variable.[1,2]

This article will review the most important aspects of the clinical-echocardiographic follow-up of MD types frequently associated with cardiomyopathies, including dystrophinopathy, limb-girdle muscular dystrophy (LGMD), myotonic dystrophy, and Emery-Dreifuss muscular dystrophy (EDMD).

General aspects related to the clinical and echocardiographic diagnosis of MD

The clinical diagnosis of MD considers symptom progression, family history, and, in most cases, a genetic study and/or immunohistochemical analysis for its confirmation and classification (Table 1).[1,2] These patients usually present no cardiomyopathy-related symptoms and signs due to functional limitations caused by muscle weakness. In this context, echocardiography is an essential tool in MD management because, in addition to being widely available and of low cost, it assesses anatomic-functional characteristics of the heart and detects preclinical changes.[3]

Due to the development of new specific therapies, the increased survival of patients with some types of MD has made cardiological complications the leading cause of morbidity and mortality. For this reason, the early detection of cardiac changes and the introduction of cardiomyopathy-directed therapy have become essential.[3,4]

Keywords

Muscular dystrophies; Cardiomyopathy, dilated; Echocardiography.

Mailing Address: Raphael Henrique Déa Cirino •
Rua Herculano Carlos Franco de Souza, 550, apto. 204-A, Água Verde.
CEP 80240-290 – Curitiba, PR, Brazil.
E-mail: rapha_cirino@yahoo.com.br
Manuscript received 2/13/2022; revised 2/14/2022; accepted 2/16/2022.

DOI: 10.47593/2675-312X/20223501eabc292

Dystrophinopathy cardiac presentation and echocardiographic findings

Duchenne MD (DMD) is the most common neuromuscular disease in children and reflects the most severe spectrum of dystrophinopathies, which also include Becker MD and asymptomatic female carriers of the DMD gene mutation[4]. Clinical cardiological presentations are characterized by dilated cardiomyopathy (DCM) and its complications and can occur in any spectrum of dystrophinopathy without a correlation with peripheral muscle involvement severity.[4,5]

In recent years, the role of echocardiography in assessing dystrophinopathies has been questioned, as some studies demonstrated the superiority of cardiac magnetic resonance imaging (cMRI).[6] Despite this, and considering the limitations inherent to cMRI, echocardiography remains valuable in the routine evaluation of these patients for being widely available, being of low cost, and presenting no severe adverse effects.[7,8] Studies comparing echocardiography with cMRI show that left ventricular (LV) fractional shortening[6,9] and LV ejection fraction (LVEF) by the area-length method[6] are the echocardiographic parameters used to assess LV systolic function that best correlate with cMRI.

Typical echocardiographic findings are LV dilation and systolic dysfunction, which define the DCM phenotype (Figure 1).[4,5] Characteristic dystrophinopathy changes include segmental contractility changes with a predilection for LV inferolateral wall involvement.[4,5] Myocardial strain evaluated by speckle tracking also shows changes versus healthy individuals, with reduced global longitudinal (GLS) (Figures 2 and 3),[4,7,10,11] global circumferential,[7,11] and global radial strains, especially the basal segments of the inferior, inferolateral, anterolateral and anterior walls.[7,11] One study also demonstrated reduced three-dimensional myocardial strain in the longitudinal, circumferential, or radial axis.[12] A recent meta-analysis determined that GLS, the most studied and most reliable echocardiographic parameter for the early detection of LV systolic dysfunction,[13] can be reduced in up to to 50% of DMD patients with a normal LVEF.[8] As for LV diastolic dysfunction, DMD patients present lower septal and lateral e' waves values and higher E/e' ratios than controls[11] but do not meet echocardiographic criteria for significant LV diastolic dysfunction. The functions of the right chambers are usually preserved.[7]

Electrocardiography and transthoracic echocardiography are recommended at diagnosis, every two years before 10 years of age, and annually thereafter. Thus, cMRI should always be considered, especially in older patients with poorer echocardiographic image quality, and

Table 1 - Genetic aspects, pathogenesis and typical echocardiographic findings typical of muscular dystrophies most often associated with cardiomyopathy.

	Classification	Inheritance	Gene	Pathogenesis	Non-Cardiac Clinical Manifestations	Typical Echocardiographic Findings
Dystrophinopathies	Duchenne Muscular Dystrophy	X-linked recessive	DMD	Total dystrophin deficiency	Delayed walking Proximal lower limb muscle weakness with onset before 5 years of age and rapid progression to walking disability (usually before 12 years of age) Proximal upper limb muscle weakness	LV dilatation LV systolic dysfunction Predilection towards impairment of the LV inferolateral wall GLS reduction, especially of the basal segments of the inferior, inferolateral, anterolateral, and anterior walls
	Becker Muscular Dystrophy	X-linked recessive	DMD	Partial dystrophin deficiency	Similar to DMD, but with onset around 10 years of age and slower progression	
Myotonic Dystrophies	Type 1	Autosomal dominant	DMPK	CTG repeat expansion	Distal muscular weakness associated with facial muscular weakness, with eyelid ptosis and myotonic phenomenon Systemic manifestations: cataract, insulin resistance, gonadal failure and baldness. It may start at birth (congenital), in childhood or in adulthood	LV systolic function Decreased GLS, especially apical longitudinal strain LV diastolic dysfunction with normal LA Mitral valve prolapse Pericardial effusion
	Type 2	Autosomal dominant	CNBP/ZNF9	CCTG repeat expansion	Proximal muscle weakness Less intense symptoms and slower progression than in myotonic dystrophy type 1. It does not start in childhood	
Limb-girdle Muscular Dystrophies	Laminopathy (LGMD1)	Autosomal dominant	LMNA	Lamin A/C deficiency	Limb-girdle muscle weakness beginning in childhood through the fourth decade of life	LV dilatation LV systolic and diastolic dysfunction
	Sarcoglycanopathies (LGMD2C-F)	Autosomal recessive	SGCG SGCA SGCB SGCD	Beta-sarcoglycan/gamma-sarcoglycan deficiency		
	Fukutinopathy (LGMD2I)	Autosomal recessive	FKRP	Fukutin-related protein deficiency		
Emery-Dreifuss Muscular Dystrophy	Type 1	X-linked recessive	EMD/FHL1	Emerin/FHL1 deficiency	Humerus-peroneal muscle weakness associated with early prominent joint contractures (neck extension, elbow flexion and ankle flexion) with onset in childhood	Predominance of biatrial dilatation over LV dilatation Atrial standstill and increased cardioembolic risk LV systolic and diastolic dysfunction
	Type 2	Autosomal dominant/ recessive	LMNA	Lamin A/C deficiency		

CNBP/ZNF9: Cellular Nucleic Acid-binding Protein/Zinc Finger Protein 9; CTG: Cytosine-Thymine-Guanine; DMD: Duchenne Muscular Dystrophy; DMPK: Myotonic Dystrophy Protein Kinase; FHL1: Four And A Half LIM Domains 1; FKRP: Fukutin Related Protein LGMD: Limb-girdle Muscular Dystrophy; GLS: Global longitudinal strain; CNS: Central Nervous System.

many clinicians advocate annual cMRI, especially in patients who already have dystrophinopathy-related cardiomyopathy.[4,6]

Cardiac presentation and echocardiographic findings in myotonic dystrophy

Myotonic dystrophies are the most common hereditary MD in adults, being characterized by multisystem involvement.[14,15] The most characteristic cardiac presentation is arrhythmia, including conduction disorders, atrial and ventricular tachyarrhythmias, sudden cardiac death, and less frequently DCM.[14,16] These complications are more common in type 1 than in type 2,[1,15,17] accounting for about 30% of deaths in myotonic dystrophy type 1 patients.[14]

Echocardiographic changes vary and may include LV dilation, systolic dysfunction, and excessive trabeculation; LV hypertrophy and diastolic dysfunction; and mitral valve prolapse.[14] Mitral, aortic, and tricuspid valve sclerosis may also be observed in addition to pericardial effusion.[14,15] The prevalence of LV systolic dysfunction is 13.8% in type 1 myotonic dystrophy.[14,15] LV systolic dysfunction presence and severity help in the decision to implant intracardiac devices, such as a pacemaker and implantable cardioverter-defibrillator as they are predictors of conduction disorders and severe tachyarrhythmias.[14] LV GLS is the most reliable parameter for the early detection of systolic dysfunction, with a reduced apical longitudinal strain being the most characteristic finding.[19]

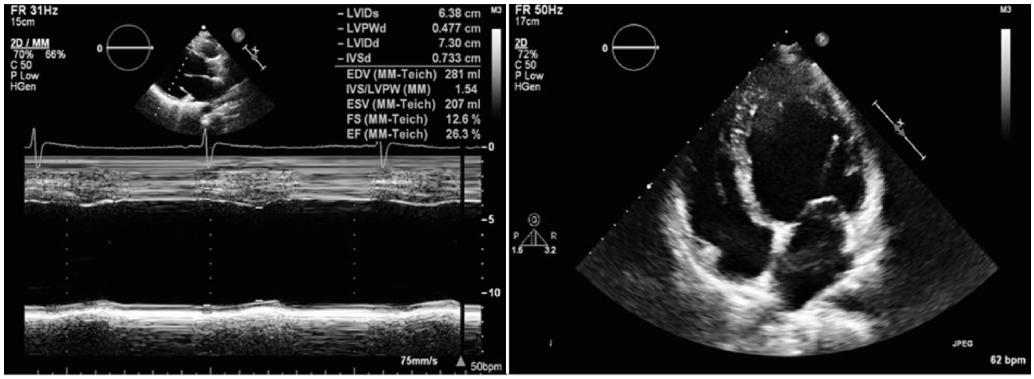

Figure 1 – *Dilated cardiomyopathy phenotype in a 15-year-old ambulatory patient with Becker muscular dystrophy.*

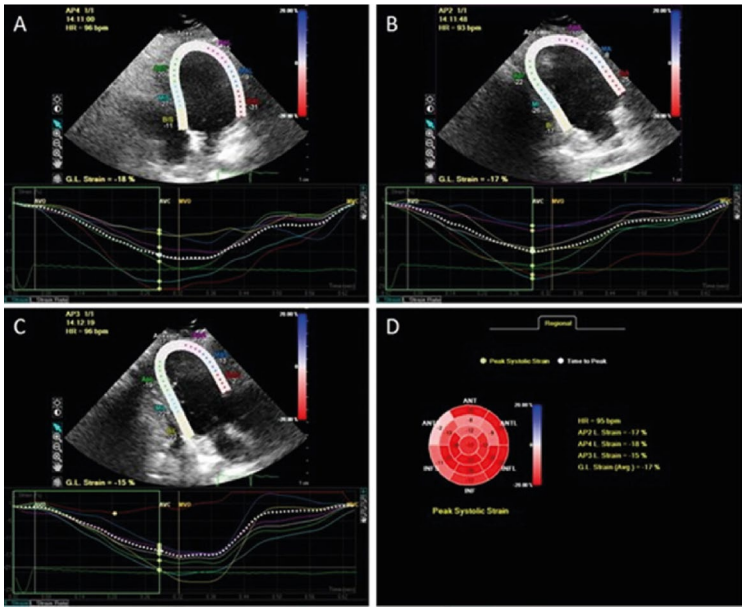

Figure 2 – *Left ventricular (LV) longitudinal strain analysis in apical four- (A), two- (B), and three-chamber (C) views, and LV global longitudinal strain (D) of a patient with Duchenne muscular dystrophy with a normal LV ejection fraction and a reduced global longitudinal strain (-17%).*

Due to the scarcity of symptoms, the high prevalence of subclinical electrocardiographic and echocardiographic changes and the worse prognosis due to these changes, we recommend assessment at the time of diagnosis followed by an annual routine assessment with ECG, 24-hour Holter monitoring, and transthoracic echocardiography and consider early primary prevention with the implantation of intracardiac devices such as a pacemaker and implantable cardioverter-defibrillator.[17,19]

Cardiac presentation and echocardiographic findings in LGMD

LGMD is a group of diseases characterized by pelvic and scapular girdle atrophy and weakness.[1,16,17] Those most frequently associated with cardiomyopathy are laminopathy (LGMD1B), sarcoglycanopathy (LGMD2C-F), and fukutinopathy (LGMD2I).[1,17,20] Cardiac clinical presentations resemble those of other MD, including DCM, cardiac arrhythmias, and sudden cardiac death.[1,17]

DCM is the most characteristic echocardiographic pattern, featuring LV dilation and systolic and diastolic dysfunction,[20] with an LVEF < 50% occurring in about 80%, 50%, and 39–45% of patients with LGMD2E (beta-sarcoglycanopathy), LGMD2C (gamma-sarcoglycanopathy), and LGMD2I, respectively.[17,21,22,23]

Recommendations about the frequency of echocardiographic assessment in LGMD are based on expert consensus.[17] In our practice, we perform ECG and transthoracic echocardiography

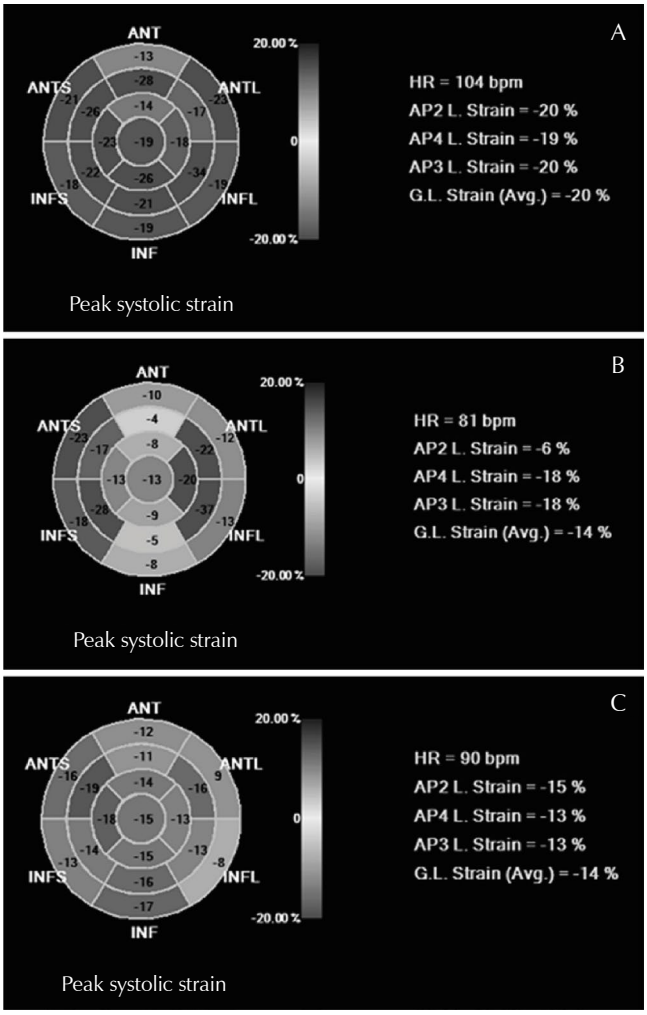

Figure 3 – *Global longitudinal strain (GLS) study of three Duchenne muscular dystrophy patients: (1) Male 10-year-old patient, symptom onset 5 years previous, ambulatory, preserved left ventricular (LV) systolic function, LV ejection fraction (LVEF) of 65%, and GLS of -20%; (2) male 12-year-old patient, symptom onset 10 years previous, wheelchair user, early LV systolic dysfunction, LVEF of 58%, and GLS of -14%; and (3) male 17-year-old patient, symptom onset 15 years prior, wheelchair user, overt LV systolic dysfunction, LVEF of 34%, and GLS of -14%.*

at diagnosis and annually thereafter. More studies are needed to investigate the benefits of myocardial strain and other recent echocardiographic techniques in LGMD.

Cardiac presentation and echocardiographic findings in EDMD

EDMD is a rare disease characterized by a high frequency of cardiac involvement that usually presents as supraventricular and ventricular arrhythmias, conduction disorders, chamber dilation, and systolic dysfunction.[1,2,16,24,25]

The most common echocardiographic findings in EDMD patients characterize the DCM phenotype and include LV dilatation and systolic dysfunction, LV diastolic dysfunction, and bi-atrial enlargement. Atrial standstill and an increased risk of embolic phenomena may also occur.[16] Marchel *et al*. demonstrated that up to 41% of EDMD patients (median age, 43 years) had LV dilation and 32% had an LVEF lower than 50%. Atrial enlargement is present in more than 2/3 of cases and predominates over ventricular dilation. Echocardiographic changes are similar in EDMD types 1 and 2 despite LMNA gene mutations being more frequently associated with DCM, heart failure and sudden cardiac death, regardless of the presence of peripheral skeletal muscle involvement.[24]

The frequency of echocardiographic assessment is not well established, but in our clinical practice, we recommend ECG, 24-hour Holter monitoring, and transthoracic echocardiography at diagnosis and annually thereafter. The

literature is scarce on the use of new echocardiographic techniques such as myocardial strain in EDMD. Due to the high risk of conduction disorders, ventricular arrhythmias, and sudden cardiac death associated with EDMD, cardiac screening of first-degree relatives and asymptomatic carriers should be performed routinely. For the same reason, an implantable cardioverter-defibrillator should be considered for primary prevention in EDMD type 2.[17]

Authors' contributions

Manuscript writing and critical review: Cirino RHD and Ducci RD.

Conflict of interest

The authors have declared that they have no conflict of interest.

References

Hermans MC, Pinto YM, Merkies IS, Die-Smulders CE, Crijns HJ, Faber CG. Hereditary muscular dystrophies and the heart. Neuromuscul Disord. 2010;20(8):479-92. doi: https://doi.org/10.1016/j.nmd.2010.04.008

Badila E, Lungu II; Grumezescu AM; Udriste AS. Diagnosis of cardiac abnormalities in muscular dystrophies. Medicina (Kaunas). 2021;57(5)488. doi: https://doi.org/10.3390/medicina57050488

Cirino RH, Scola RH, Ducci RD, Camarozano AC, Kay CS, Lorenzoni PJ, et al. Predictors of early left ventricular systolic dysfunction in duchenne muscular dystrophy patients. Muscle Nerve. 2018 Feb 14. doi: https://doi.org/10.1002/mus.26102

Power LC, O'Grady GL, Hornung TS, Jefferies C, Gusso S, Hofman PL. Imaging the heart to detect cardiomyopathy in Duchenne muscular dystrophy: A review. Neuromuscul Disord. 2018;28(9):717-730. doi: https://doi.org/10.1016/j.nmd.2018.05.011

Kamdar F, Garry DJ. Dystrophin-deficient cardiomyopathy. J Am Coll Cardiol. 2016;67(21):2533-46. doi: https://doi.org/10.1016/j.jacc.2016.02.081.

Soslow JH, Xu M, Slaughter JC, Stanley M, Crum K, Markham LW, et al. Evaluation of echocardiographic measures of left ventricular function in patients with Duchenne muscular dystrophy: assessment of reproducibility and comparison to cardiac magnetic resonance imaging. J Am Soc Echocardiogr. 2016;29(10):983-991. 10.1016/j.echo.2016.07.001

Amedro P, Vincenti M, Villeon GD, Lavastre K, Barrea C, Guillaumont S, et al. Speckle-tracking echocardiography in children with Duchenne muscular dystrophy: a prospective multicenter controlled cross-sectional study. J Am Soc Echocardiogr. 2019;32(3):412-422. doi: https://doi.org/10.1016/j.echo.2018.10.017

Cirino RH, Scola RH, Ducci RD, Camarozano AC; Kay CS, Lorenzoni PJ, et al. Evaluation of left-sided heart chambers with novel echocardiographic techniques in men With Duchenne or Becker muscular dystrophy. Am J Cardiol. 2019;123(6):972-978. 10.1016/j.amjcard.2018.12.011

Spurney CF, McCaffrey FM, Cnaan A, Morgenroth LP, Ghelani SJ, Gordish-Dressman H, et al. Feasibility and reproducibility of echocardiographic measures in children with muscular dystrophies. J Am Soc Echocardiogr. 2015;28(8):999-1008. doi: https://doi.org/10.1016/j.echo.2015.03.003

Taqatqa A, Bokowski J, Al-Kubaisi M, Khalil A, Miranda C, Alaksham H, et al. The use of speckle tracking echocardiography for early detection of myocardial dysfunction in patients with Duchenne muscular dystrophy. Pediatr Cardiol. 2016;37(8):1422-1428. doi: https://doi.org/10.1007/s00246-016-1451-2

Cho M, Lee J, Lee J, Shin YB. Evaluation of early left ventricular dysfunction in patients with Duchenne muscular dystrophy using two-dimensional speckle tracking echocardiography and tissue Doppler imaging. Pediatr Cardiol. 2018;39(8):1614-1619. doi: https://doi.org/10.1007/s00246-018-1938-0

Yu H, Xia B, Liu X, Han C, Chen W, Li Z. Initial application of three-dimensional speckle-tracking echocardiography to detect subclinical left ventricular dysfunction and stratify cardiomyopathy associated with Duchenne muscular dystrophy in children. Int J Cardiovasc Imaging. 2019;35(1):67-76. doi: https://doi.org/10.1007/s10554-018-1436-8

Song G, Zhang J, Wang X, Zhang X, Sun F, Yu X. Usefulness of speckle-tracking echocardiography for early detection in children with Duchenne muscular dystrophy: a meta-analysis and trial sequential analysis. Cardiovasc Ultrasound. 2020;18(1):26. doi: https://doi.org/10.1186/s12947-020-00209-y

Lau JK, Sy RW, Corbett A, Kritharides L. Myotonic dystrophy and the heart: A systematic review of evaluation and management. Int J Cardiol. 2015;184:600-608. doi: https://doi.org/10.1016/j.ijcard.2015.03.069

Peric S, Bjelica B, Aleksic K, Kovacevic M, Cvitan E, Stojmenovic GM, et al. Heart involvement in patients with myotonic dystrophy type 2. Acta Neurol Belg. 2019;119(1):77-82. doi: https://doi.org/10.1007/s13760-018-1052-3

Arbustini E, Di Toro A, Giuliani L, Favalli V, Narula N, Grasso M. Cardiac phenotypes in hereditary muscle disorders. J Am Coll Cardiol. 2018;72(20):2485-2506. doi: https://doi.org/10.1016/j.jacc.2018.08.2182

Feingold B, Mahle WT, Auerbach S, Clemens P, Domenighetti AA, Jefferies JL, et al. Management of cardiac involvement associated with neuromuscular diseases: a scientific statement from the American Heart Association. Circulation. 2017;136(13):e200-e231. doi: https://doi.org/10.1161/CIR.0000000000000526

Russo V, Sperlongano S, Gallinoro E, Rago A, Papa AA, Golino P, et al. Prevalence of left ventricular systolic dysfunction in myotonic dystrophy type 1: a systematic review. J Card Fail. 2020;26(10):849-856. doi: https://doi.org/10.1016/j.cardfail.2019.07.548

Garcia R, Labarre Q, Degand B, Ingrand P, Gal FL, Bonnet B, et al. Apical left ventricular myocardial dysfunction is an early feature of cardiac involvement in myotonic dystrophy type 1. Echocardiography. 2017;34(2):184-190. doi: https://doi.org/10.1111/echo.13426

Van Westrum SM, Dekker LR, Voogt WG, Wilde AA, Ginjaar IB, Visser M, et al. Cardiac involvement in Dutch patients with sarcoglycanopathy: a cross-sectional cohort and follow-up study. Muscle Nerve. 2014;50(6):909-13. 10.1002/mus.24233

Petri H, Sveen ML, Thune JJ, Vissing C, Dahlqvist JR, Witting N, et al. Progression of cardiac involvement in patients with limb-girdle type 2 and Becker muscular dystrophies: a 9-year follow-up study. Int J Cardiol. 2015. Mar 1;182:403-11. doi: https://doi.org/10.1016/j.ijcard.2014.12.090

Fayssoil A, Nardi O, Annane D, Orlikowski D. Left ventricular function in alpha-sarcoglycanopathy and gamma-sarcoglycanopathy. Acta Neurol Belg. 2014;114(4):257-9. doi: https://doi.org/10.1007/s13760-013-0276-5

Libell EM, Richardson JA, Lutz KL, Ng BY, Mockler SR, Laubscher KM, et al. Cardiomyopathy in limb girdle muscular dystrophy R9, FKRP related. Muscle Nerve. 2020;62(5):626-632. doi: https://doi.org/10.1002/mus.27052

Marchel M, Madej-Pilarczyk A, Tyminska A, Steckiewicz R, Kochanowski J,

Wysinska J, et al. Echocardiographic features of cardiomyopathy in Emery-Dreifuss muscular dystrophy. Cardiol Res Pract. 2021;2021:8812044. doi: https://doi.org/10.1155/2021/8812044

Wang S, Daoquan P. Cardiac involvement in Emery-Dreifuss muscular dystrophy and related management strategies. Int Heart J. 2019;60(1):12-18. doi: https://doi.org/10.1536/ihj.17-604

Tricuspid Annular Plane Systolic Excursion and Mitral Annular Systolic Excursion: Correlation with Left Ventricular Diastolic Function

Excursão Sistólica do Anel Tricúspide e do Anel Mitral: Correlação com Função Diastólica Ventricular Esquerda

André Américo Bedenko Martins[1], Leonardo Yoshida Osaku[1], Ana Cristina Camarozano[1], Cintia Rocha Fortes de Sá[1], Daniela de Castro Carmo[1], Jerônimo Antonio Fortunato[1], Rubens Zenóbio Darwich[1], Liz Andréa Villela Baroncini[1]

[1]Red Cross Hospital, Curitiba, Paraná, Brazil.

Abstract

Introduction: Tricuspid annular plane systolic excursion and mitral annular systolic excursion are parameters used to assess the systolic function of the right ventricle and left ventricle, respectively. Little is known about its relationship with left ventricular diastolic function.

Objective: To assess whether the values of mitral annular systolic excursion and tricuspid annular plane systolic excursion correlate with parameters used in the evaluation of left ventricular diastolic function.

Method: Observational cross-sectional study. Two hundred nine individuals were selected, 116 women, with both ventricles normal systolic function. The analyzes were performed for men and women, through Pearson correlation coefficient and Sperman correlation coefficient. Tricuspid annular plane systolic excursion, mitral annular systolic excursion, atrial volumes and left ventricular diastolic function parameters on transthoracic echocardiogram were obtained.

Results: In women, mitral annular systolic excursion was positively correlated with lateral e '(Sperman correlation coefficient of 0.22; p=0.016) and tricuspid annular plane systolic excursion was positively correlated with E / A ratio (Sperman correlation coefficient of 0.23; p=0.037), lateral e' (Sperman correlation coefficient of 0.28; p=0.012), and septal e' (Sperman correlation coefficient of 0.28; p=0.012), and negatively with the E/e' ratio (Pearson correlation coefficient of -0.27; p=0.018), and A wave (Pearson correlation coefficient of -0.29; p=0.009). In men, only mitral annular systolic excursion correlated positively with E wave (Pearson correlation coefficient of 0.21; p=0.037), lateral e' (Sperman correlation coefficient of 0.34; p <0.001) and the septal e' (Sperman correlation coefficient of 0.26; p=0.008). There was no correlation between mitral annular systolic excursion and tricuspid annular plane systolic excursion and atrial volumes. Hypertension and diabetes mellitus influenced tricuspid annular plane systolic excursion and mitral annular systolic excursion values correlated to E and A waves, E/A ratio, septal and lateral e' waves, and E/e' ratio.

Conclusion: In the present study, mitral annular systolic excursion and tricuspid annular plane systolic excursion values showed a significant correlation with some parameters of left ventricular diastolic function, with stronger evidence on female sex.

Keywords: Cardiac function; Cardiovascular disease; COVID-19; Echocardiography; SARS-CoV-2

Resumo

Introdução: *A excursão sistólica do anel tricúspide e a do anel mitral são parâmetros utilizados para se avaliar a função contrátil do ventrículo direito e do ventrículo esquerdo, respectivamente. Pouco se conhece sobre sua relação com a função diastólica ventricular esquerda.*

Objetivo: *Avaliar se os valores de excursão sistólica do anel tricúspide e do anel mitral se correlacionam com parâmetros utilizados na avaliação da função diastólica ventricular esquerda.*

Métodos: *Estudo observacional transversal. Foram selecionados 219 indivíduos, sendo 116 mulheres, com função sistólica preservada de ambos os ventrículos. As análises foram feitas separadamente para os sexos masculino e feminino, por meio dos coeficientes de correlação de Pearson e de Sperman. Foram obtidos: excursão sistólica do anel tricúspide, excursão sistólica do anel mitral, volumes atriais e medidas relacionadas à avaliação da função diastólica do ventrículo esquerdo ao ecocardiograma transtorácico.*

Resultados: *No sexo feminino, a excursão sistólica do anel mitral se correlacionou positivamente com o e' lateral (coeficiente de correlação de*

Mailing Address: Liz Andréa Villela Baroncini •

E-mail: lizandreabaroncini@hotmail.com
Manuscript received 8/22/2021; revised 11/9/2021; accepted 2/22/2022

DOI: 10.47593/2675-312X/20223501eabc245

Sperman de 0,22; p=0,016) e a excursão sistólica do anel tricúspide se correlacionou positivamente com a relação E/A (coeficiente de correlação de Sperman de 0,23, p=0,037), com o e' lateral (coeficiente de correlação de Sperman de 0,28; p=0,012), com o e' septal (coeficiente de correlação de Sperman de 0,28; p=0,012) e negativamente com a relação E/e' (coeficiente de correlação de Pearson de -0,27; p=0,018) e onda A (coeficiente de correlação de Pearson de -0,29; p= 0,009). No sexo masculino, apenas a excursão sistólica do anel mitral se correlacionou positivamente com a onda E (coeficiente de correlação de Pearson de 0,21; p=0,037), e' lateral (coeficiente de correlação de Sperman de 0,34; p <0,001) e e' septal (coeficiente de correlação de Sperman de 0,26; p=0,008). Não houve correlação entre excursão sistólica do anel mitral e do anel tricúspide e volumes atriais. A presença de hipertensão arterial sistêmica e diabetes melito influenciou nos valores de excursão sistólica do anel tricúspide e do anel mitral correlacionados a ondas E e A, relação E/A, ondas e' septal e lateral e relação E/e'.

Conclusão: *No presente estudo, os valores da excursão sistólica do anel mitral e do anel tricúspide apresentaram correlação significativa com algumas variáveis da função diastólica ventricular esquerda com maior evidência no sexo feminino.*

Palavras-chave: *Ecocardiografia; Ventrículos do coração; Função ventricular.*

Introduction

The cardiac cycle encompasses several phases and corresponds to interdependent movements between several cardiac structures that determine its efficiency. A quick and accurate analysis is not possible.[1] Therefore, cardiac assessment by transthoracic echocardiography (TTE) is based on the acquisition of static and dynamic images associated with measurements and comparisons predetermined in uni- and multicentric studies and arranged in tables to define normality.[1,2]

In particular, two measurements stand out due to their correlation with and dependence on cardiac structures, the tricuspid annular plane systolic excursion (TAPSE) and the mitral annular plane systolic excursion (MAPSE), which are used to assess right ventricular (RV) and left ventricular (LV) contractile function, respectively.[3,4] Both TAPSE and MAPSE are evaluated in the apical four-chamber window by placing the M-mode on the lateral tricuspid or mitral annulus, respectively, and measuring the distance from the "lowest" to the "highest" point it reaches (Figure 1).[5] Thus, the M-mode angulation with other adjacent cardiac structures, especially the left and right atria, may interfere with these two measurements.[6,7]

Myocardial performance is directly related to ventricular architecture. Circumferential and longitudinal myocardial fibers, in addition to improving systole and diastole through shortening/widening, help displace the mitral and tricuspid annuli in the cardiac cycle.[8,9] Thus, any systolic or diastolic dysfunction would theoretically change these movements, which could be quantitatively assessed by MAPSE and TAPSE measurements. Previous studies confirmed the relationship between MAPSE and LV systolic function[5] even with sensitivity similar to the longitudinal strain[8]; however, little is known about its relationship with left ventricular diastolic function (LVDF). The same happens with TAPSE.[3,4]

Therefore, the present study aimed to assess whether MAPSE and TAPSE correlate with parameters used to assess LVDF and whether the behaviors of these variables differ between the sexes.[10-12]

Methods

Study population

This observational cross-sectional study enrolled a total of 219 patients (116 women [53%], 103 men [47%]) regardless of ethnicity who were referred by the assistant physician for TTE for any clinical indication from the cardiology outpatient clinic of the Red Cross Hospital of Curitiba, PR, Brazil. The patients were selected by convenience without statistical criteria

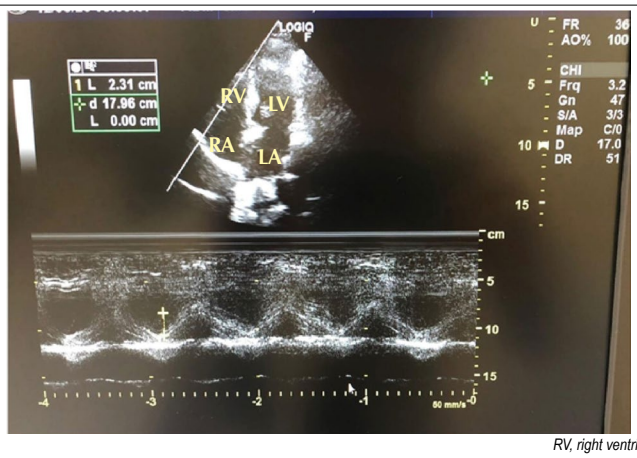

RV, right ventricle; LV, left ventricle; RA, right atrium; LA, left atrium.

Figure 1 – *Tricuspid annular plane systolic excursion image.*

according to each subject's availability to participate in the research. A protocol form with clinical and echocardiographic parameters was completed for each patient. The clinical data collected included age, sex, weight, height, body mass index (BMI), and the presence of systemic arterial hypertension (SAH), diabetes mellitus (DM), coronary artery disease (CAD), smoking (current or previous), and dyslipidemia. Information on SAH, DM, dyslipidemia, and smoking were collected from the patients' medical records and/or reported by them (referred information). CAD was confirmed by the medical record and the patient through a reported history of non-fatal myocardial infarction and surgical or percutaneous myocardial revascularization. Regularly used medications were also recorded.

The exclusion criteria were a) significant valvular disease (moderate and severe); b) valve prostheses; c) segmental LV contraction changes due to ischemic heart disease or other cardiomyopathies; d) declared pulmonary emphysema or chronic obstructive pulmonary disease;,,,,, e) moderate to severe pulmonary arterial hypertension (pulmonary artery systolic pressure [PASP] > 50 mmHg); f) LV contractile dysfunction (ejection fraction < 52% for men and < 54% for women); g) infiltrative and pericardial diseases; h) congenital heart disease with increased pulmonary blood flow with or without surgical correction; i) pacemakers or atrial fibrillation; and j) advanced-degree (II and III) LV diastolic dysfunction. Patients with any of the conditions described above were automatically excluded from the study. Only patients who met the selection criteria were invited to participate.

The patients underwent a complete two-dimensional TTE using Phillips IE 33, Envisor, or General Electric Vivid E echocardiography equipment. All acoustic windows and all standard echocardiographic measurements and analyses were performed on each patient. Sonographic measurements were performed by two experienced echocardiographers qualified in echocardiography by the Department of Cardiovascular Imaging of the Brazilian Society of Cardiology.

All patients signed an informed consent form. The study was approved by the institution's research ethics committee.

Main echocardiographic parameters analyzed in this study

The analyzed parameters included: RA indexed volume (normal up to 27 mL/m² in women, up to 32 mL/m² in men) measured in the apical four-chamber window; TAPSE measured in the apical four-chamber window (normal, ≥17 mm) (Figure 1); LA indexed volume (normal up to 34 mL/m² for women and men) measured in the apical four-chamber window; MAPSE measured in the apical four-chamber window (normal, ≥12 mm) on the lateral wall of the valve annulus. Measurements of the anterior, posterior, and septal walls of the annulus were excluded due to a greater possibility of errors and changes caused by pressure overload, ischemia, necrosis, and ventricular interdependence through the interventricular septum (Figure 2)[3]; E wave velocity, A wave velocity, and E/A ratio on transmitral spectral Doppler; e' septal wave velocity, e' lateral wave velocity, mean e' septal and e' lateral velocity, E/e' ratio (E wave velocity/mean e' septal and e' lateral velocity) on tissue Doppler of the mitral annulus; and PASP (mmHg) through the maximum tricuspid regurgitation velocity (m/s), when present, on continuous spectral wave Doppler, and inferior vena cava diameter (mm).

All quantifications and values considered in the present study were based on American Society of Echocardiography and the European Society of Cardiovascular Imaging guidelines.[13,16]

Statistical analysis

The results of this study are described as means, medians, minimum and maximum values, and standard deviations (quantitative variables) or as frequencies and percentages (categorical variables). The association between two quantitative variables was estimated by the Pearson (PCC) or Spearman (SCC) correlation coefficient. Quantitative variables were compared between two groups using the Student's t-test for independent samples or the non-parametric Mann-Whitney test. More than two groups were compared using one-way analysis of variance and the least significant difference test for multiple comparisons or the non-parametric Kruskal-Wallis test. The association between MAPSE (or TAPSE) and

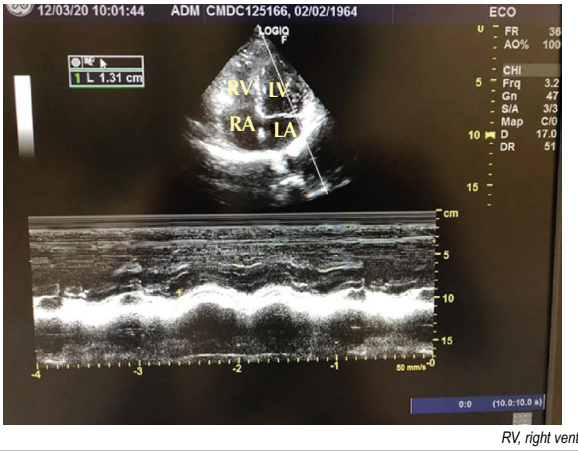

RV, right ventricle; LV, left ventricle; RA, right atrium; LA, left atrium.

Figure 2 – *Mitral annular plane systolic excursion image.*

diastolic function variables was assessed thought three linear regression models adjusted for MAPSE (or TAPSE) regardless of SAH, DM, BMI, and DSLP. The first included SAH and the diastolic function variable, the second included DM and the diastolic function variable, and the third included SAH, DM, BMI, DSLP, and the diastolic function variable. The normality of the variables was evaluated by the Kolmogorov-Smirnov test. P values < 0.05 were considered statistically significant.

The data were analyzed using SPSS Statistics software v.20.0 (IBM Corp., Armonk, NY, USA)

Results

A total of 140 patients were excluded from the final analysis for not meeting the inclusion criteria. Table 1 shows the clinical characteristics of the studied 116 women (62.8 ± 13.4 years; BMI, 28.8 ± 5.4 kg/m²) and 101 men (60.9 ± 16.5 years; BMI, 27.4 ± 5.5 kg/m²). The prevalence of cardiovascular comorbidities was similar between the sexes, with a predominance of SAH and grade I diastolic dysfunction (75% of women vs 70% of men) over the other studied comorbidities, with women having a higher incidence of SAH. Table 2 shows the baseline echocardiographic parameters of the studied population by sex.

In women (Table 3), MAPSE was positively correlated with lateral e' (SCC, 0.22; p = 0.016), while TAPSE was positively correlated with E/A ratio (SCC, 0.23; p = 0.037), lateral e' (SCC, 0.28; p = 0.012), and septal e' (SCC, 0.28; p = 0.012) and negatively correlated with E/e' ratio (PCC, -0.27; p = 0.018) and A wave (PCC, -0.29; p = 0.009). In men (Table 3), only MAPSE was positively correlated with E wave (PCC, 0.21; p = 0.037), lateral e' wave (SCC, 0.34; p < 0.001), and septal e' wave (SCC, 0.26; p = 0.008). TAPSE did not correlate with any variables in men. There was no correlation between MAPSE and TAPSE and atrial volumes in either sex (Table 3). There was no significant difference in TAPSE and/or MAPSE values by classification of grade I diastolic dysfunction and preserved LVDF (considered a categorical variable) (data not shown). Age showed a negative correlation with A wave, E/A ratio, septal e', and lateral e' wave and a positive correlation with A wave, E wave deceleration, and left atrial volume (LAV) in both sexes (Table 4). There was no correlation between age and TAPSE or MAPSE for either sex (Table 4). In women with SAH, MAPSE was positively and significantly correlated with E/A ratio, septal e' wave, and lateral e' wave when analyzed alone or with the other categorical variables. Likewise, in women, TAPSE was positively correlated with E/A ratio, septal e' wave, and lateral e' wave and negatively correlated with A wave and E/e' ratio. In women with DM, MAPSE was positively correlated with the septal and lateral e' waves, while TAPSE was negatively correlated with A wave and E/e' ratio and positively correlated with the septal and lateral e' waves (Tables 5 and 6).

In men with SAH and/or DM, MAPSE was positively correlated with E wave, septal e' wave, and lateral e' wave (Table 7). However, TAPSE values were not influenced by the presence of SAH and/or DM (data not shown). The presence of dyslipidemia, CAD, smoking, and BMI did not influence TAPSE or MAPSE values for either sex (data not shown).

Table 1 – Clinical characteristics of the study population.

Variable	Classification	Women		Men	
		n	%	n	%
Systemic arterial hypertension	No	31	26.7%	43	42.6%
	Yes	85	73.3%	58	57.4%
Diabetes mellitus	No	89	76.7%	73	72.3%
	Yes	27	23.3%	28	27.7%
Dyslipidemia	No	70	60.3%	68	67.3%
	Yes	46	39.7%	33	32.7%
Smoking	No	28	71.8%	27	79.4%
	Yes	11	28.2%	7	20.6%
Coronary artery disease	No	101	87.1%	70	69.3%
	Yes	15	12.9%	31	30.7%
Degree of diastolic dysfunction	No	9	24.3%	10	29.4%
	Grade I	28	75.7%	24	70.6%

Table 2 – Baseline echocardiographic parameters of the studied population.

	n	Women Mean ± SD	n	Men Mean ± SD
E wave (m/s)	116	0.69 ± 0.18	103	0.65 ± 0.21
A wave (m/s)	116	0.79 ± 0.20	103	0.77 ± 0.19
E/A ratio	116	0.94 ± 0.40	103	0.90 ± 0.41
Septal e' (m/s)	116	0.08 ± 0.03	102	0.08 ± 0.03
Lateral e' (m/s)	116	0.10 ± 0.04	102	0.10 ± 0.04
E/e' ratio	116	8.58 ± 2.74	102	7.6 ± 2.2
PASP (mmHg)	77	28.2 ± 6.7	46	26.8 ± 5.8
Left atrial volume (mL/m²)	116	30.9 ± 10.7	102	31.2 ± 9.2
MAPSE (mm)	116	15.6 ± 2.5	103	16.3 ± 2.8
Tricuspid velocity (m/s)	77	2.34 ± 0.41	45	2.3 ± 0.3
TAPSE (mm)	79	23.8 ± 3.0	70	23.5 ± 3.0
Right atrial volume (mL/m²)	79	21.2 ± 7.0	69	21.4 ± 7.6

MAPSE, mitral annular plane systolic excursion; PASP, pulmonary artery systolic pressure; TAPSE, tricuspid annular plane systolic excursion NOTE: p non-significant for all variables.

Discussion

In the present study, a significant correlation was found between TAPSE and MAPSE and some of the main LVDF parameters. Women presented a greater correlation, especially in the TAPSE assessment. Modin D et al.[17] demonstrated that TAPSE has an inverse correlation with age, hypertension, and E/e' ratio and that lower TAPSE values are associated with higher cardiovascular mortality regardless of sex. The studied population demonstrated a higher prevalence of SAH in women (73%) than in men (57%), and the E/e' ratio (corroborating the study findings of Modin D et al.[17]) and A wave increased as TAPSE decreased. Concomitantly, the E/A ratio and lateral and septal e' waves showed a positive correlation with TAPSE, with

Table 3 – Correlation between MAPSE and TAPSE and LV diastolic function indices.

Variable	Women			Men		
	n	r	p	n	r	p
MAPSE × LA volume	116	0.04	0.686	102	0.09	0.378
MAPSE × RA volume	79	-0.05	0.684	69	0.13	0.293
TAPSE × LA volume	79	-0.06	0.621	70	0.18	0.130
TAPSE × RA volume	79	0.10	0.383	69	0.06	0.608
MAPSE × E wave (m/s)	116	0.16	0.086	103	0.21	0.037
MAPSE × A wave (m/s)	116	-0.04	0.671	103	0.15	0.131
MAPSE × E/A ratio	116	0.13	0.164	103	0.10	0.303
MAPSE × septal e' (m/s)	116	0.10	0.310	102	0.26	0.008
MPASE × lateral e' (m/s)	116	0.22	0.016	102	0.34	<0.001
MAPSE × E/e'	116	-0.07	0.475	102	-0.11	0.257
TAPSE × E wave (m/s)	79	0.10	0.395	70	0.04	0.738
TAPSE × A wave (m/s)	79	-0.29	0.009	70	0.09	0.455
TAPSE × E/A ratio	79	0.23	0.037	70	-0.04	0.743
TAPSE × septal e' (m/s)	79	0.28	0.012	69	0.01	0.957
TAPSE × lateral e' (m/s)	79	0.28	0.012	69	-0.13	0.291
TAPSE × E/e'	79	-0.27	0.018	69	0.17	0.161

LA, left atrium; LV, left ventricle; MAPSE, mitral annular plane systolic excursion; RA, right atrium; TAPSE, tricuspid annular plane systolic excursion.

Table 4 – Correlation between age (years) and echocardiographic variables.

Variable	Women			Men		
	n	r	p	n	r	p
Age × E wave (m/s)	116	-0,39	<0,001	101	-0,49	<0,001
Age × A wave (m/s)	116	0,56	<0,001	101	0,45	<0,001
Age × E/A ratio	116	-0,63	<0,001	101	-0,51	<0,001
Age × septal e' (m/s)	116	-0,33	<0,001	101	-0,37	<0,001
Age × lateral e' (m/s)	116	-0,46	<0,001	101	-0,52	<0,001
Age × E/e'	116	0,17	0,070	101	0,18	0,069
Age × E decel T (s)	116	0,23	0,012	100	0,28	0,005
Age × PASP (mmHg)	77	0,34	0,003	45	-0,01	0,970
Age × LA volume (mL/m2)	116	0,28	0,002	100	0,33	0,001
Age × MAPSE (mm)	116	-0,15	0,102	101	-0,05	0,608
Age × Tric R vel (m/s)	77	0,28	0,015	45	0,10	0,533
Age × TAPSE	79	-0,15	0,194	68	0,06	0,630
Age × RA volume	79	0,19	0,101	67	0,23	0,064
Age × RV baseline s'	79	-0,11	0,314	67	-0,21	0,081

r, Pearson correlation coefficient (E wave, A wave, E/e', E accel T, E decel T, PASP, LA volume, MAPSE, Tric R Vel, IVC, TAPSE, RA volume, RA area); Spearman correlation coefficient (E/A ratio, septal e', lateral e', RV lateral s', RV baseline s'). E decel T, E wave deceleration time; IVC, inferior vena cava; LA, left atrium; MAPSE, mitral annular plane systolic excursion; PASP, pulmonary arterial systolic pressure; RA, right atrium; RV, right ventricle; TAPSE, tricuspid annular plane systolic excursion; Tric R vel, tricuspid regurgitation velocity.

lower TAPSE values corresponding to lower E/A ratio, lateral e', and septal e' values. These findings indicate progressive or worsened LVDF associated with a lower TAPSE value, i.e., RV systolic dysfunction is associated with progressive LV diastolic dysfunction, especially in women. However, previous studies[10-12] demonstrated a more pronounced effect and higher prevalence of SAH in women. In addition, the data presented here show more evident independent correlations between SAH, TAPSE, MAPSE, and diastolic variables in women, with only MAPSE being influenced by SAH in men. Therefore, we cannot rule out that the higher prevalence of SAH in the female population studied here influenced the results. As for DM, a correlation was also observed between MAPSE and septal and lateral e' waves in both sexes and with E wave in men only. DM was correlated with preclinical LV diastolic dysfunction, which significantly worsens over the years regardless of the presence of SAH or CAD.

Other studies[18-20] demonstrated significant ventricular structural and functional differences between men and women, which are mainly related to the RV and have greater impact on the prognosis of cardiovascular morbidity and mortality in women. In addition, women have a higher prevalence of heart failure (HF) with preserved LV ejection fraction (HFpEF) than men, indicating diastolic dysfunction as the predominant cause of HF in women.[21-22] Lundorff et al.[20] identified higher E/e' ratios in women and lower lateral and septal e' waves on tissue Doppler of the mitral annulus in a population of patients with HF with reduced LV ejection

Table 5 – Association between categorical variables and MAPSE in women.

	Independent variable (n=116)	Estimated coefficient	95% CI	p*
Model 1	SAH	0.80	-0.26; 1.87	0.140
	E/A ratio	1.39	0.20; 2.58	0.024
Model 2	DM	-0.32	-1.39; 0.76	0.565
	E/A ratio	1.01	-0.14; 2.16	0.087
Model 3	DM	-0.48	-1.60; 0.64	0.404
	SAH	0.84	-0.28; 1.96	0.144
	E/A ratio	1.34	0.11; 2.58	0.035
Model 1	SAH	0.48	-0.52; 1.48	0.347
	Septal e' (m/s)	20.53	4.39; 36.7	0.014
Model 2	DM	-0.29	-1.35; 0.77	0.595
	Septal e' (m/s)	19.15	2.78; 35.5	0.024
Model 3	DM	-0.42	-1.54; 0.70	0.460
	SAH	0.54	-0.53; 1.60	0.325
	Septal e' (m/s)	20.60	3.54; 37.6	0.020
Model 1	SAH	0.86	-0.17; 1.88	0.104
	Lateral e' (m/s)	20.03	7.42; 32.6	0.002
Model 2	DM	-0.14	-1.22; 0.93	0.793
	Lateral e' (m/s)	16.52	3.90; 29.1	0.012
Model 3	DM	-0.33	-1.44; 0.78	0.560
	SAH	0.84	-0.24; 1.91	0.130
	Lateral e' (m/s)	20.02	6.69; 33.3	0.004

*CI, confidence interval; DM, diabetes mellitus; MAPSE, mitral annular plane systolic excursion; SAH, systemic arterial hypertension. *Linear regression model, p < 0.05.*

Table 6 – Association between categorical variables and TAPSE in women.

	Independent variable (n=79)	Estimated coefficient	95% CI	p*
Model 1	SAH	0.35	-1.13; 1.84	0.641
	A wave (m/s)	-4.91	-8.5; -1.33	0.009
Model 2	DM	-0.14	-1.78; 1.49	0.864
	A wave (m/s)	-4.66	-8.25; -1.07	0.013
	DM	-0.14	-1.89; 1.62	0.879
Model 3	SAH	0.42	-1.15; 1.99	0.599
	A wave (m/s)	-4.43	-8.43; -0.43	0.033
Model 1	SAH	0.35	-1.19; 1.89	0.657
	E/A ratio	1.80	0.05; 3.54	0.047
Model 2	DM	-0.28	-1.94; 1.39	0.746
	E/A ratio	1.63	-0.09; 3.35	0.067
	DM	-0.24	-2.01; 1.53	0.791
Model 3	SAH	0.42	-1.19; 2.03	0.611
	Rel. E/A	1.56	-0.31; 3.42	0.107
Model 1	SAH	-0.07	-1.5; 1.37	0.929
	Septal e' (m/s)	34.79	11.87; 57.7	0.004
Model 2	DM	-0.18	-1.79; 1.42	0.826
	Septal e' (m/s)	34.32	11.0; 57.6	0.005
	DM	-0.13	-1.85; 1.60	0.886
Model 3	SAH	0.06	-1.46; 1.58	0.942
	Septal e' (m/s)	34.02	8.94; 59.1	0.010
Model 1	SAH	0.41	-1.08; 1.91	0.590
	Lateral e' (m/s)	26.50	6.87; 46.1	0.010
Model 2	DM	-0.05	-1.71; 1.61	0.952
	Lateral e' (m/s)	25.01	5.23; 44.8	0.015
	DM	-0.05	-1.80; 1.70	0.955
Model 3	SAH	0.48	-1.08; 2.05	0.547
	Lateral e' (m/s)	25.76	4.55; 47.0	0.020
Model 1	SAH	0.08	-1.39; 1.55	0.916
	E/e'	-0.27	-0.49; -0.05	0.018
Model 2	DM	-0.30	-1.93; 1.33	0.720
	E/e'	-0.26	-0.48; -0.04	0.023
	DM	-0.24	-1.99; 1.50	0.784
Model 3	SAH	0.18	-1.37; 1.73	0.820
	E/e'	-0.25	-0.48; -0.02	0.038

*CI, confidence interval; DM, diabetes mellitus; SAH, systemic arterial hypertension; TAPSE, tricuspid annular plane systolic excursion. *Linear regression model, p < 0.05.*

Table 7 – Association between categorical variables and MAPSE in men.

	Independent variable (n=101)	Estimated coefficient	95% CI	p*
Model 1	SAH	0.28	-0.84; 1.41	0.625
	E wave (m/s)	2.85	0.23; 5.46	0.036
Model 2	DM	1.01	-0.20; 2.23	0.105
	E wave (m/s)	2.91	0.35; 5.47	0.028
	DM	0.12	-1.28; 1.51	0.872
Model 3	SAH	-0.63	-1.89; 0.62	0.324
	E wave (m/s)	2.82	0.28; 5.36	0.032
Model 1	SAH	0.37	-0.77; 1.51	0.526
	Septal e' (m/s)	21.57	1.85; 41.3	0.034
Model 2	DM	1.12	-0.11; 2.34	0.076
	Septal e' (m/s)	22.65	3.55; 41.8	0.022
	DM	0.13	-1.25; 1.50	0.855
Model 3	SAH	-0.58	-1.82; 0.66	0.361
	Septal e' (m/s)	26.26	7.19; 45.33	0.008
Model 1	SAH	0.42	-0.72; 1.56	0.472
	Lateral e' (m/s)	16.42	3.00; 29.8	0.018
Model 2	DM	1.13	-0.09; 2.34	0.072
	Lateral e' (m/s)	16.91	3.95; 29.9	0.012
	DM	0.20	-1.17; 1.58	0.772
Model 3	SAH	-0.48	-1.73; 0.77	0.451
	Lateral e' (m/s)	18.34	5.33; 31.3	0.007

*CI, confidence interval; DM, diabetes mellitus; MAPSE, mitral annular plane systolic excursion; SAH, systemic arterial hypertension. *Linear regression model, p < 0.05.*

fraction (HFrEF), with TAPSE and LV isovolumetric relaxation time (IVRT) indicating a worse cardiovascular prognosis. Therefore, the findings of this study corroborate those in the current literature, which identifies a strong correlation between RV systolic function, assessed mainly through TAPSE, and LVDF in women. Corroborating these findings, uni- and multivariate analyses identified that the presence of SAH influenced TAPSE in women only.

The MAPSE analysis evidenced a positive correlation with lateral e' values in both sexes and a positive correlation with septal e' and E wave in men. MAPSE values correlate with better LVDF. However, atrioventricular annulus plane motion has a well-known correlation with LV systolic function. Lower MAPSE values are associated with adverse events in several cardiovascular diseases.[23] However, no studies significantly and definitively correlating MAPSE values with LVDF indices were found in the current literature. On the contrary, the few existing studies failed to find such an association,[24,25] unanimously identifying the need for further studies in this area.

Another relevant finding presented here was the association between LVDF parameters with age, with TAPSE and MAPSE values not being influenced by age. The prevalence of LV diastolic dysfunction increases with age, especially in hypertensive women,[26-28] indicating progressive LV relaxation worsening. However, no study has consistently correlated TAPSE and MAPSE values with advancing age. Once again, the findings of the present study corroborate those of the current literature.

Some limitations should be mentioned. First, the relatively small number of participants and the higher prevalence of SAH in women may have influenced the results. The small number of participants may also have corroborated the fact that no significant differences were found in TAPSE and MAPSE when the diastolic function was classified as a categorical variable. Finally, the exclusion criteria were strict, excluding patients with advanced degrees (II and III) of diastolic and LV systolic dysfunction, making it impossible to assess the behaviors of the MAPSE and TAPSE values in these cases.

Conclusions

In the present study, MAPSE and TAPSE values showed a significant correlation with some LVDF variables, especially in women. More studies are needed in this area to validate our findings.

Authors' contributions

Data collection: Baroncini LAV, Martins AAB, Osaku LY, Camarozano AC, Carmo DC, Sá CRF, Fortunato JA, Darwich RZ; Data analysis: Baroncini LAV, Martins AAB, Osaku LY, Camarozano AC, Carmo DC; Data design: Baroncini LAV, Martins AAB, Osaku LY, Camarozano AC; Manuscript writing: Baroncini LAV, Martins AAB, Osaku LY, Camarozano AC, Carmo DC, Sá CRF, Fortunato JA, Darwich RZ; Critical review of the manuscript for important intellectual content: Baroncini LAV, Martins AAB, Osaku LY, Camarozano AC.

Conflict of interest

The authors have declared that they have no conflict of interest.

References

Lossnitzer D., Buss S., Steen H. Reference values of mitral and tricuspid annular plane systolic excursion for the evaluation of left and right ventricular performance. Journal of Cardiovascular Magnetic Resonance. 2012.

Baron T., Flachskampf F.A., Johansson K., Hedin E., Christersson. C. Usefulness of traditional echocardiographic parameters in assessment of left ventricular function in patients with normal ejection fraction early after acute myocardial infarction: results from a large consecutive cohort. Eur Heart J Cardiovasc Imaging. 2016.

Hu K., Liu D., Herrmann S., Niemann M., Gaudron P.D., Voelker W., et al. Implication of mitral annular plane systolic excursion for patients with cardiovascular disease, European Heart Journal - Cardiovascular Imaging, Volume 14, Issue 3, 1 March 2013.

Bytyçi I., Haliti E., Berisha G., Tishukaj A., Shatri F., Bajraktari G., et al. Left ventricular longitudinal systolic dysfunction is associated with right atrial dyssynchrony in heart failure with preserved ejection fraction, Port Cardiol, 2016.

Matos J, Kronzon I, Panagopoulos G, Perk G. Mitral annular plane systolic excursion as a surrogate for left ventricular ejection fraction. J Am Soc Echocardiogr. 2012 Sep;25(9):969-74.

DiLorenzo M., Bhatt S., & Mercer-Rosa. How best to assess right ventricular function by echocardiography. Cardiology in the Young. 2015.

Bruhl S. R., Chahal M., Khouri S. J. A Novel Approach to Standard Techniques in the Assessment and Quantification of the Interventricular Systolic Relationship. Cardiovasc Ultrasound. 2011

Amado J, Islas F, Isla IL, Diego JJ, Augustin A, et al. M-mode apical systolic excursion: A new and simple method to evaluate global left ventricular longitudinal strain. Rev Port Cardiol. 2015; 34(9):551–554.

Nagueh SF, Smiseth OA, Appleton CP, Byrd BF 3rd, Dokainish H, Edvardsen T, Flachskampf FA, Gillebert TC, Klein AL, Lancellotti P, Marino P, Oh JK, Popescu BA, Waggoner AD. Recommendations for the Evaluation of Left Ventricular Diastolic Function by Echocardiography: An Update from the American Society of Echocardiography and the European Association of Cardiovascular Imaging. J Am Soc Echocardiogr. 2016 Apr;29(4):277-314.

Sandberg K, Ji H. Sex differences in primary hypertension. Biol Sex Differ 2012;3:7.

Zabalgoitia M, Rahman SN, Haley WE, Mercado R, Yunis C, Lucas C, Yarows S, Krause L, Amarena J. Comparison in systemic hypertension of left ventricular mass and geometry with systolic and diastolic function in patients <65 to >65 years of age. Am J Cardiol 1998;82:604-608.

Sant'Anna MP, Mello RJ, Montenegro LT, Araújo MM. Left and right ventricular hypertrophy at autopsy of hypertensive individuals. Rev Assoc Med Bras 2012;58:41-47.

Norbert F. Voelkel, Robert A. Quaife, Leslie A. Leinwand, Robyn J. Barst, Michael D. McGoon, Daniel R. Meldrum, Jocelyn Dupuis, Carlin S. Long, Lewis J. Rubin, Frank W. Smart, Yuichiro J. Suzuki, Mark Gladwin, Elizabeth M. Denholm and Dorothy B. Gail Right Ventricular Function and Failure: Report of a National Heart, Lung, and Blood Institute Working Group on Cellular and Molecular Mechanisms of Right Heart Failure. Circulation. 2006;114:1883-1891.

Lang RM, Badano LP, Mor-Avi V, Afilalo J, Armstrong A, Ernande L, Flachskampf FA, Foster E, Goldstein AS, Kuznetsova T, Lancellotti P, Muraru D, Picard MH, Rietzschel ER, Rudski L, Spencer KT, Tsang W, Voigt JU. Recommendations for cardiac chamber quantification by echocardiography in adults: an update from the American Society of Echocardiography and the European Association of Cardiovascular Imaging. J Am Soc Echocardiogr 2015;28:1-39 e14.

Grünig E, Biskupek J, D'Andrea A, Ehlken N, Egenlauf B, Weidenhammer J, Marra AM, Cittadini A, Fischer C, Bossone E. Reference ranges for and determinants of right ventricular area in healthy adults by two-dimensional echocardiography. Respiration. 2015;89(4):284-93.

Bulluck H., Ngamkasem H., Sado D., Treibel T.A., Fontana M., at al. A simple technique to measure TAPSE and MAPSE on CMR and normal values. Journal of Cardiovascular Magnetic Resonance. 2014.

Modin D, Møgelvang R, Andersen DM, Biering-Sørensen T. Right ventricular function evaluated by tricuspid annular plane systolic excursion predicts cardiovascular death in the general population. J Am Heart Assoc 2019;8e:012197.

Merkus D. Right ventricular function in dilated cardiomyophathy: women are the stronger sex. Neth Heart J 2015;23:576-577.

Kawut SM, Lima JAC, Barr G, Chahal H, Jain A, Tandri H, Praestgaard A, Bagiella E, Kizer JR, Johnson C, Kronmal RA, Bluemke DA. Sex and race differences in right ventricular structure and function. Circulation 2011;123:2542-2551.

Lundorff IJ, Sengeløv M, Jørgensen PG, Pedersen S, Modin D, Bruun NE, Fritz-Hansen T, Jensen JS, Biering-Sørensen T. Echocardiographic predictors of mortality in women with heart failure with reduced ejection fraction. Circ Cardiovasc Imaging 2018;11:e008031.

Tanai E, Frantz S. Pathophysiology of heart failure. Compr Physiol. 2016; 6:187–214.

Gotsman I, Zwas D, Lotan C, Keren A. Heart failure and preserved left ventricular function: Long term clinical outcome. PLoS One. 2012;7(7): e41022.

Mayr A, Pamminger M, Reindl M, Greulich S, Reinstadler SJ, Tiller C, Holzknecht M, Nalbach T, Plappert D, Kranewitter C, Klug G, Metzler B. Mitral annular plane systolic excursion by cardiac MR is an easy tool for optimized prognosis assessment in ST-elevation myocardial infarction. European Radiology 2020;30:620-629.

Hernandez-Suarez DF, Lopez-Menendez F, Roche-Lima A, Lopez-Candales A. Assessment of mitral annular plane systolic excursion in patients with left ventricular diastolic dysfunction. Cardiol Res 2019;10:83-88.

Burgos PMH, López-Candales A. Changes in mitral annular ascent with worsening echocardiographic parameters of left ventricular diastolic

function. Scientifica 2016;1-4.

Pyszko J, Václavík J, Václavík T, Kociánová E, Kamasová M, Lazárová M, Táborský M. Effects of age on left ventricular diastolic function. Cor et Vasa 2018; https://doi.org/ 10.1016/j.crvasa.2018.10.003.

Hoshida S, Shinoda Y, Ikeoka K, Fukuoka H, Inui H, Watanabe T. Age- and sex-related differences in diastolic function and cardiac dimensions ina hypertensive population. ESC Heart Failure 2016;3:270-277.

Bruhl SR, Chahal M, Khouri SJ. A novel approach to standard techniques in the assessment and quantification of the interventricular systolic relationship. Cardiovascular Ultrasound 2011;9-42.

Factors Associated With Abnormalities On Myocardial Perfusion Scintigraphy In Diabetic Patients

Fatores Associados a Anormalidades na Cintilografia de Perfusão Miocárdica de Pacientes Diabéticos

Alfredo Lírio da Cruz1; Álisson Carvalho de Freitas[1]; Bianca Naomi Sada Watanabe[1]; Helena Bigarella Nascimento[1]; Heloisa Porath[2]; Luiz Antonio Fruet Bettini[1,3]; Luciane Moreira[1,4,5]; Marcos Germano Dopheide[1]

[1]Positivo University, Curitiba, Paraná, Brazil. [2]Faculdade Evangélica do Paraná, Curitiba, Paraná, Brazil. [3]Universidade Federal do Paraná, Curitiba, Paraná, Brazil. [4]Hospital Universitário Evangélico de Curitiba, Curitiba, Paraná, Brazil. [5]Universidade Federal de São Paulo, São Paulo, Brazil.

Abstract

Diabetes mellitus (DM) is the greatest risk factor for coronary artery disease. In addition to a long duration of diabetes, the presence of peripheral arterial disease and smoking are strong predictors of abnormalities on myocardial perfusion scintigraphy (MPS). This study aimed to assess the impact of risk factors in diabetic patients on MPS results and compare them with those of non-diabetic patients in a nuclear medicine clinic. A retrospective cross-sectional study was performed through the analysis of the medical records of patients who underwent MPS in 2010–2019. A total of 34,736 medical records were evaluated. Analyzing the stress phase of MPS, DM patients required two-fold more pharmacological stimulation than non-diabetic patients for MPS. Factors that negatively impact the MPS results were also evaluated, and DM (33.6%), insulin therapy (18.1%), systemic arterial hypertension (69.9%), dyslipidemia (53%), sedentary lifestyle (83.1%), use of pharmacological stress (50.6%), typical chest pain (8.5%), and limiting angina during the test (1.7%) were significantly associated ($p < 0.001$) with test abnormalities.

Keywords: Diabetes Mellitus; Ventilation-Perfusion Scan; Pharmacological Stress.

Resumo

O diabetes melito é o maior fator de risco para doença arterial coronariana. Além da longa duração de diabetes, outros fatores, como presença de doença arterial periférica e tabagismo são fortes preditores para anormalidades na cintilografia de perfusão do miocárdio. O objetivo deste estudo foi avaliar o impacto dos fatores de risco de pacientes diabéticos nos resultados da cintilografia de perfusão do miocárdio e comparar com os resultados de pacientes não diabéticos em uma clínica de medicina nuclear. Foi realizado um estudo transversal retrospectivo por meio da análise de prontuários de pacientes que realizaram cintilografia miocárdica no período de 2010 a 2019. Foram avaliados 34.736 prontuários. Analisando a fase de estresse da cintilografia de perfusão do miocárdio, os portadores de diabetes melito precisaram receber estímulo farmacológico duas vezes mais que os não diabéticos para sua realização. Também foram avaliados fatores que tivessem impacto negativo no resultado da cintilografia de perfusão do miocárdio, e foi visto que o diabetes melito (33,6%), a insulinoterapia (18,1%), a hipertensão arterial sistêmica (69,9%), a dislipidemia (53%), o sedentarismo (83,1%), o uso de estresse farmacológico (50,6%), a dor torácica típica (8,5%) e a angina limitante durante o teste (1,7%) estiveram associados significativamente (p<0,001) a anormalidades neste exame.

Palavras-chave: *Diabetes mellitus; Cintilografia de ventilação/perfusão; Fatores de risco.*

Introduction

Diabetes mellitus (DM) has become a disease of high prevalence, morbidity, and mortality worldwide, causing serious public health problems, especially in underdeveloped or developing countries.[1] An estimated 382 million people currently live with DM, a figure that is projected to grow to 592 million people by 2035, with around 11 million cases in Brazil.[2] About 5.1 million people died from DM complications in 2013.[3,4] This increased incidence is mainly due to population aging and new eating habits, obesity, and sedentary lifestyles, which have become common in today's society.[1,3]

DM is a major disease that has both early and late complications, all of which have poor prognosis if left untreated.[5,6]

Mailing Address: Heloisa Porath •
Rua Padre Anchieta, 2.933 – Bigorrilho. CEP 80730-000 – Curitiba, PR, Brazil.
E-mail: heloisa_porath@hotmail.com
Manuscript received 11/23/2021; revised 2/26/2022; accepted 3/2/2022

DOI: 10.47593/2675-312X/20223501eabc274

The Framingham study pointed out that DM patients have a two- to four-fold greater risk of developing coronary heart disease than individuals without DM.[7] This happens because the atherosclerotic process progresses earlier and more rapidly in DM patients than in the general population.[2,8]

The main causes of death in patients with DM are acute myocardial infarction (AMI) and stroke, but they do not always show clinical signs and symptoms compatible with these acute arterial events, which greatly delays the start of cardiovascular treatment.[3,5] Haffner et al. estimated that patients with coronary artery disease (CAD) and DM have a greater than 70% higher risk of death within 10 years and reported that the mortality rate from cardiovascular diseases in DM patients without a history of AMI was similar to that of patients without type 2 DM and a history of AMI. In addition, the association of DM and CAD is already seen in the early stages of glucose intolerance and abnormal fasting glucose levels.[6,9]

Thus, the early diagnosis of these patients is relevant to avoiding negative outcomes. In addition to investigating traditional risk factors, cardiovascular disease screening in DM patients should also be complemented by other tests, such as electrocardiography (ECG), echocardiography, exercise stress testing, myocardial perfusion scintigraphy (MPS), and magnetic resonance imaging.[10]

The American Diabetes Association recommends that DM patients with typical or atypical symptoms of CAD or a resting ECG showing changes suggestive of AMI should undergo echocardiography or MPS under physical or pharmacological stress. The exercise test is the most indicated for asymptomatic patients aged over 35 years who are sedentary and planning to start physical activity or patients with arteriopathy (peripheral, carotid) or at least two risk factors (systemic arterial hypertension [SAH], dyslipidemia, smoking, family history of AMI, and albuminuria).[11]

MPS presents a specificity of 74% and sensitivity of 88% in CAD assessments . Nevertheless, the 2020 Brazilian Nuclear Cardiology Guideline highlights that patients at intermediate risk of ischemic heart disease benefit more from MPS than patients at low risk.[12,13]

The Basel Asymptomatic High-Risk Diabetics' Outcome Trial multicenter study of 400 DM patients without CAD history or symptoms revealed that male sex, long-term DM, peripheral arterial disease, smoking, and high systolic blood pressure were strong predictors of MPS abnormalities. When more than three factors were present, 47% of patients had abnormal scan findings. The study also showed that 22% of evaluated patients had silent CAD.[6]

In contrast, the Detection of Ischemia in Asymptomatic Diabetics clinical trial questioned the usefulness of MPS as a screening test. The study assessed 1,123 patients with type 2 DM without symptoms of coronary heart disease and previously recognized coronary disease, reporting a small rate of cardiac events not significantly reduced by myocardial ischemia screening with adenosine perfusion scintigraphy during a follow-up of 4.8 years.[7]

Thus, this study aimed to compare the impact of cardiovascular risk factors on MPS results between diabetic and non-diabetic patients.

Methods

This clinical, retrospective, cross-sectional, and observational study analyzed the medical records of patients undergoing MPS between February 2010 and May 2019 in a private nuclear medicine service in the city of Curitiba, Paraná, Brazil.

In this interval, 44,584 patients underwent MPS. Of them, 9,848 were removed for meeting the exclusion criteria (history of previous CAD, congenital heart disease, being younger than 18 years, and unknown DM status). The final sample consisted of 34,736 patients, who were divided into two groups: 7,968 (22.9%) were diabetic and 26,768 (77.1%) were non-diabetic.

The collected and analyzed variables included imaging test results (fibrosis and ischemia), age, body mass index (BMI), presence of SAH (previous documentation of blood pressure > 140/90 mmHg in two or more occasions and/or history of antihypertensive drug use), DM (previous documentation of fasting blood glucose > 126 mg/dL, blood glucose > 200 mg/dL after oral glucose tolerance test, glycated hemoglobin higher than 6.5%, and/or history of hypoglycemic drug use), dyslipidemia (low-density lipoprotein cholesterol > 100 mg/dL, triglycerides > 150 mg/dL, and/or high-density lipoprotein cholesterol < 45 mg/dL), smoking, sedentary lifestyle (aerobic physical activity for less than 30 min three times a week), chest pain (typical or atypical), positive family history of CAD, use of insulin, need for pharmacological stimulation in the stress phase of the test, and presence of angina (according to the angina index, which assesses the presence of angina during exercise testing and its test limitations).

MPS was performed by single photon emission computed tomography, in which three-dimensional and tomographic images of the heart were obtained (in the long horizontal, long vertical, and short axis views) after isotonic exercise on a treadmill or pharmacological stress in cases of patients who were unable to perform exercise; and at rest, 60 min after intravenous administration of the 99mTc-SESTAMIBI radiotracer. Transient or persistent perfusion defects were considered criteria for the diagnosis of myocardial ischemic disease, and the presence of these defects categorized the MPS findings as positive.

The data were stored in a database and subsequently analyzed using Stata software. The qualitative variables are expressed as absolute (n) and relative (%) frequencies, while quantitative variables are expressed as mean and standard deviation. Differences between quantitative variables were calculated using Student's t-test. Differences between qualitative variables were calculated using the chi-square or Fisher's exact test when indicated. The significance level was set at $p < 0.05$ (5%).

This study was authorized by the Research Ethics Committee of Positivo University (Plataforma Brasil: 4316693), which waived the need for informed consent because of its retrospective nature of data collection from medical records, lack of patient risk, and lack of directly or indirectly interfering with treatment.

Results

Of the 34,736 evaluated patients, 7,968 (22.9%) had DM; of those, 2,602 (32.6%) showed MPS changes (fibrosis and/or ischemia). As for the 26,768 (77.1%) non-diabetic evaluated patients, 19.2% underwent MPS (Table 1).

Mean age and BMI were significantly higher in patients with DM ($p < 0.001$). DM patients had a higher prevalence of SAH, dyslipidemia, and sedentary lifestyle ($p < 0.001$) and needed pharmacologically induced stress during the test. In addition, smokers ($p < 0.001$) and male subjects ($p = 0.047$) showed a higher prevalence of non-DM (Table 2).

Most participants were asymptomatic, and atypical chest pain was more prevalent than typical chest pain in both groups (Table 3). Among our population, 33,328 (95.9%) patients experienced no pain during cardiovascular stress testing (95.8% of non-diabetic versus 96% of diabetic participants). In both groups, 0.5% of the patients had angina with test limitations and just over 3% had angina without test limitations ($p = 0.88$).

The group of patients with changes on MPS had a higher rate of DM and insulin dependency, older age, higher BMI, SAH, dyslipidemia, sedentary lifestyle, use of pharmacological stress testing, chest pain, and angina during exercise testing (Table 4; $p < 0.001$). Male patients were more prevalent in the group without changes on MPS ($p < 0.001$), while smoking and a family history of CAD showed no statistically significant intergroup differences.

Table 1 – Myocardial perfusion scintigraphy results by study group.

Results	Changed		Unchanged		p value
	Diabetic	Non-diabetic	Diabetic	Non-diabetic	
	2,602 (32.7%)	5,144 (19.2%)	3,089 (67.3%)	21,624 (80.8%)	
Changes					**p<0.001**
Fibrosis + ischemia	97 (1.2%)	203 (0.8%)	---	---	
Fibrosis	129 (1.6%)	331 (1.2%)	---	---	
Ischemia	2,376 (29.8%)	4,610 (17.2%)	---	---	

Table 2 – Profiles of diabetic versus non-diabetic patients undergoing myocardial perfusion scintigraphy.

Variable	Non-diabetic (n = 26,798 [77.1%])	Diabetic (n = 7,968 [22.9%])	Valor p
Age (years)	60.03±12.91	64.92±10.58	<0.001
Men (Overall: 16,564 [47.68%])	12,842 (48.0%)	3,722 (46.7%)	0.047
Body mass index	27.62 ± 4.82	29.60 ± 5.28	<0.001
Systemic arterial hypertension	14,368 (53.7%)	6,296 (79.0%)	<0.001
Dyslipidemia	12,277 (45.9%)	5,000 (62.8%)	<0.001
Family history of CAD	4,769 (17.8%)	1,370 (17.2%)	0.2
Sedentary lifestyle	20,315 (75.9%)	6,385 (80.1%)	<0.001
Current smoking	2,663 (9.9%)	681 (8.5%)	<0.001
Pharmacological stress	7,202 (26.9%)	3,089 (38.8%)	<0.001
Insulin therapy	---	1,125 (14,1%)	---

CAD, coronary artery disease.

Discussion

DM and its effect on the cardiovascular system are associated with risk factors, with atherosclerosis being ascribed a central role in the etiology of cardiac ischemic events. The hypothesis for the initial atherosclerotic lesion is based on endothelial dysfunction, which presents as an early marker of cardiovascular disease.[14]

Traditional cardiovascular risk factors include those disrupting or attacking the oxidative metabolism of this tissue, which

Table 3 – Symptoms of diabetic versus non-diabetic patients undergoing myocardial perfusion scintigraphy.

Variable	Non-diabetic (n = 26,798 [77.1%])	Diabetic (n = 7,968 [22.9%])	P value
Chest pain			**0.002**
Absent	18.221 (68.3%)	5.511 (69.5%)	
Atypical	7.011 (26.3%)	1.947 (24.5%)	
Typical	1.439 (5.4%)	474 (6.0%)	
Angina index			**0.88**
Absence of pain	25.654 (95.8%)	7.647 (96.0%)	
Non-limiting angina	969 (3.6%)	280 (3.5%)	
Limiting angina	144 (0.5%)	41 (0.5%)	

Table 4 – Myocardial perfusion scintigraphy results by risk factors.

Variables (n; %)	Myocardial perfusion scintigraphy result		P value
	Changed (N = 7,746 [22.2%])	Unchanged (N = 26,990 [77.7%])	
Diabetes	2.602 (33.6%)	5.366 (19.9%)	<0.001
Insulin therapy	471 (18.1%)	654 (12.2%)	<0.001
Age	66.21 ± 11.92	59.70 ± 12.39	<0.001
Men	3.251 (42.0%)	13.313 (49.3%)	<0.001
Body mass index	28.50 ± 5.17	27.95 ± 4.94	<0.001
Systemic arterial hypertension	5.414 (69.9%)	15.250 (56.5%)	<0.001
Dyslipidemia	4.109 (53.0%)	13.168 (48.8%)	<0.001
Family history of coronary artery disease	1.354 (17.5%)	4.785 (17.7%)	0.61
Sedentary lifestyle	6.438 (83.1%)	20.262 (75.1%)	<0.001
Smoking	776 (10.0%)	2.568 (9.5%)	0.19
Pharmacological stress	3.907 (50.6%)	6.384 (23.7%)	<0.001
Chest pain			**<0.001**
Absent	4.960 (64.5%)	18.772 (69.8%)	
Atypical	2.080 (27.0%)	6.878 (25.6%)	
Typical	654 (8.5%)	1.259 (4.7%)	
Angina index			**<0.001**
Absence of pain	7.077 (91.4%)	26.224 (97.2%)	
Non-limiting angina	536 (6.9%)	713 (2.6%)	
Limiting angina	133 (1.7%)	52 (0.2%)	

were also seen in this study: age, male sex, SAH, dyslipidemia, hyperglycemia, sedentary lifestyle, and overweight.[14,15]

Although smoking and a family history of CAD are established risk factors in the literature, they were not statistically significant in this study. The lack of information on smoking history and on diseases affecting family members interfered with the research results.

Endothelial dysfunction has been documented in patients with DM, insulin resistance, or a high risk for the development of type 2 DM. Such patients require multidisciplinary follow-up to stop the progression of DM complications and assess the prognosis.[14]

Our sample demonstrated that DM is such an important risk factor that it stands out compared to others. Of all variables analyzed, DM is an alarming risk factor, alone or in combination.

During examination, patients are subjected to exercise stress testing or pharmacological stress testing to assess the cardiac response to exertion. DM patients may be unable to complete a symptom-limited exercise test due to obesity, peripheral vascular disease, or peripheral neuropathy, thus requiring pharmacological stress testing. In this study, the use of pharmacological stress and the presence of chest pain were higher in DM patients, being linked to more MPS changes than in non-diabetic patients.[7]

Studies by Caobelli F et al and Bourque JM et al also discussed the relationship between these factors. Both stated that a greater need for pharmacological stress is related to the presence of more comorbidities and physical limitations, consequently leading to a worse prognosis. Caobelli reinforced that diabetic patients tend to have worse health conditions (presence of peripheral arterial disease, lower aerobic capacity, reduced strength compared to healthy patients, and others). The author also emphasized that the longer the DM duration, the greater the limitations and risk of complications.[16,17]

The present study has some biases that limit its objectivity. The first is its sample, since the participants undergoing MPS had clinical indications and were not randomly selected from the general population. Another challenge was the scarcity of data on continuous-use medications, time of DM progression, smoking history, complete lipid profile, and adequate comorbidity and symptom control related to the MPS results. We emphasize that the patient profiles involved healthcare bias due to the presence of multiple comorbidities and the need for increased health care. DM patients more commonly require frequent medical appointments and greater attention to their health, which could have caused statistically significant changes.

Conclusion

Diabetic patients had a higher prevalence of risk factors and abnormal MPS results than non-diabetic patients. Thus, DM, physical inactivity, arterial hypertension, dyslipidemia, typical chest pain, limiting angina during pharmacological stress, need for pharmacological stress testing, and insulin therapy significantly influenced the test results. In addition, DM patients have a greater need for pharmacological stimulation to undergo MPS testing than non-diabetic patients.

Authors' contributions

Research conception and design: LAF Bettini, MG Dopheide; Data collection: AC Freitas, LAF Bettini; Data analysis and interpretation: MG Dopheide, H Porath; Statistical analysis: AL Cruz, BS Watanabe; Manuscript writing: BS Jaya, AC Freitas; Critical review of the manuscript for important intellectual content: H Bigarella, H Porath, L Moreira.

Conflict of interest

The authors have declared that they have no conflict of interest.

References

Guariguata L, Whiting DR, Hambleton I, Beagley J, Linnenkamp U, Shaw JE. Global estimates of diabetes prevalence for 2013 and projections for 2035. Diabetes Res Clin Pract. 2014;103(2):137-49. doi: 10.1016/j.diabres.2013.11.002

Wild S, Roglic G, Green A, Sicree R, King H. Global prevalence of diabetes: estimates for the year 2000 and projections for 2030. Diabetes Care. 2004;27(5):1047-53. doi: 10.2337/diacare.27.5.1047.

International Diabetes Federation (IDF). Diabetes atlas. 6th ed. Bruxelas, Bélgica: IDF; 2013.

Shaw JE, Sicree RA, Zimmet PZ. Global estimates of the prevalence of diabetes for 2010 and 2030. Diabetes Res Clin Pract. 2010;87(1):4-14. doi: 10.1016/j.diabres.2009.10.007.

Wackers FJ, Young LH, Inzucchi SE, Chyun DA, Davey JA, Barrett EJ, et al.; Detection of Ischemia in Asymptomatic Diabetics Investigators. Detection of silent myocardial ischemia in asymptomatic diabetic subjects: the DIAD study. Diabetes Care. 2004;27(8):1954-61. doi: 10.2337/diacare.27.8.1954. Erratum in: Diabetes Care. 2005;28(2):504.

Zellweger MJ, Maraun M, Osterhues HH, Keller U, Müller-Brand J, Jeger R, et al. Progression to overt or silent CAD in asymptomatic patients with diabetes mellitus at high coronary risk: main findings of the prospective multicenter BARDOT trial with a pilot randomized treatment substudy. JACC Cardiovasc Imaging. 2014;7(10):1001-10. doi: 10.1016/j.jcmg.2014.07.010

Young LH, Wackers FJ, Chyun DA, Davey JA, Barrett EJ, Taillefer R, et al.; DIAD Investigators. Cardiac outcomes after screening for asymptomatic coronary artery disease in patients with type 2 diabetes: the DIAD study: a randomized controlled trial. JAMA. 2009;301(15):1547-55. doi: 10.1001/jama.2009.476.

Emerging Risk Factors Collaboration, Sarwar N, Gao P, Seshasai SR, Gobin R, Kaptoge S, Di Angelantonio E, Ingelsson E, et al. Diabetes mellitus, fasting blood glucose concentration, and risk of vascular disease: a collaborative meta-analysis of 102 prospective studies. Lancet. 2010;375(9733):2215-22. doi: 10.1016/S0140-6736(10)60484-9. Erratum in: Lancet. 2010;376(9745):958. Hillage, H L [corrected to Hillege, H L].

Haffner SM, Lehto S, Rönnemaa T, Pyörälä K, Laakso M. Mortality from coronary heart disease in subjects with type 2 diabetes and in nondiabetic subjects with and without prior myocardial infarction. N Engl J Med. 1998;339(4):229-34. doi: 10.1056/NEJM199807233390404

Falludi AA, Izar CO, Saraiva JF, Bianco HT, Chacra AP, Bertoluci MC, et al. Diretriz brasileira baseada em evidências sobre prevenção de doenças

cardiovasculares em pacientes com diabetes: posicionamento da Sociedade Brasileira de Diabetes (SBD), da Sociedade Brasileira de Cardiologia (SBC) e da Sociedade Brasileira de Endocrinologia e Metabologia (SBEM). Arg Bras Cardiol. 2017;109(6). doi: https://doi.org/10.5935/abc.20170188

ADA – American Diabetes Association. Lifestyle Management: Standards of Medical Care in Diabetes – 2019. Diabetes Care 2019;42(Suppl. 1):S46–S60. Doi:10.2337/dc19-S005. http://care.diabetesjournals.org/content/42/Supplement_1/S46.full-text.pdf

Grossman GB. O papel da cintilografia miocárdica na avaliação da cardiopatia isquêmica. Revista da Sociedade de Cardiologia do Rio Grande Do Sul. 2009 [citado 2022 Mar 17];XVII(16). Disponível em: http://sociedades.cardiol.br/sbc-rs/revista/2009/16/pdf/O_Papel_da_cintilografia_miocardica.pdf

Mastrocola LE, Amorim BJ, Vitola JV, Brandão SC, Grossman GB, Lima RS, et al. Update of the Brazilian Guideline on Nuclear Cardiology - 2020. Arq Bras Cardiol. 2020 [citado 2022 Mar 17];114(2):325-429. Disponível em: https://www.scielo.br/j/abc/a/fz9qLY36jNTQQVgwNQqzTNx/?lang=en&format=pdf

Wajchenberg BL. Disfunção Endotelial no Diabetes do Tipo 2. Arq Bras Endocrinol Metab. 2002;46(5):514-9. doi: https://doi.org/10.1590/S0004-27302002000500004

Monteiro Júnior FC, Cunha FS, Salgado Filho N, Barbosa JB, Furtado JR, Ferreira PA, et al. Prevalência de fatores de risco coronarianos e alterações da perfusão miocárdica à cintilografia em pacientes diabéticos assintomáticos ambulatoriais. Arq Bras Cardiol. 2007;89(5):306-11. https://doi.org/10.1590/S0066-782X2007001700005

Caobelli F, Haaf P, Chronis J, Haenny G, Brinkert M, Pfisterer ME, et al. Basel Asymptomatic High-Risk Diabetics' Outcome Trial (BARDOT) Investigators. Prognostic Usefulness of Cardiac Stress Test Modalities in Patients With Type 2 Diabetes Mellitus Who Underwent Myocardial Perfusion Scintigraphy (from the Basel Asymptomatic High-Risk Diabetics' Outcome Trial). Am J Cardiol. 2017;120(7):1098-103. doi: doi: 10.1007/s00259-021-05349-5

Bourque JM, Patel CA, Ali MM, Perez M, Watson DD, Beller GA. Prevalence and predictors of ischemia and outcomes in outpatients with diabetes mellitus referred for single-photon emission computed tomography myocardial perfusion imaging. Circ Cardiovasc Imaging. 2013;6(3):466-77. doi: 10.1161/CIRCIMAGING.112.000259.

Right Ventricular Outflow Tract Acceleration Time: Correlation with Left Ventricular Diastolic Function, Sex, And Age

Tempo de Aceleração na Via de Saída do Ventrículo Direito: Correlação com a Função Diastólica do Ventrículo Esquerdo, Sexo e Idade

Renan Macedo Coimbra[1], Ana Cristina Camarozano[1], Cintia Rocha Fortes de Sá[1], Daniela de Castro Carmo[1], Jerônimo Antonio Fortunato[1], Rubens Zenóbio Darwich[1], Liz Andréa Villela Baroncini[1]

[1]Red Cross Hospital – Brazilian Red Cross, Curitiba, Paraná, Brazil.

Abstract

Background: Pulmonary artery acceleration time (PAAT) can be used as a parameter in the evaluation of pulmonary hypertension and aids left ventricular diastolic function (LVDF) analyses.

Objective: To assess whether there is a correlation between PAAT and LVDF parameters in individuals with a preserved left ventricular systolic function and by sex, age, and cardiovascular risk factors.

Method: Observational cross-sectional study. One hundred nineteen patients were selected (59 women [49.6%]). The subjects underwent transthoracic echocardiography including measurements of PAAT, E and A waves and E/A ratio, e' septal and e' lateral waves and E/e' ratio, pulmonary artery systolic pressure (PASP), and left atrial volume.

Results: In female patients, a positive correlation (Spearman's correlation coefficient – Spearman correlation coefficient [SCC]) was found between the PAAT value and the lateral e' (SCC, 0.47; p = 0.002), with the E/A ratio (SCC, 0.32; p = 0.04), and with septal e' (SCC, 0.36; p = 0.023), and a negative correlation between PAAT and PASP (SCC, -0.43; p = 0.034). In men, no correlation was found between PAAT and any parameters. Lower PAAT values were found in women with systemic arterial hypertension (hypertension) than in women without hypertension (0.13 ± 0.03 s versus 0.16 ± 0.03 s; p = 0.015).

Conclusion: The present study showed a significant correlation between PAAT and some LVDF parameters in female patients only. Hypertension was correlated with lower PAAT values in women.

Keywords: Cardiac function; Cardiovascular disease; COVID-19; Echocardiography; SARS-CoV-2

Resumo

Fundamento: *O tempo de aceleração na artéria pulmonar (TAP) pode ser utilizado para avaliação da hipertensão pulmonar na análise da função diastólica do ventrículo esquerdo.*

Objetivo: *Avaliar se existe correlação entre o valor do tempo de aceleração na artéria pulmonar e parâmetros da função diastólica do ventrículo esquerdo em indivíduos com função sistólica do ventrículo esquerdo preservada e de acordo com sexo, idade e fatores de risco cardiovasculares.*

Métodos: *Estudo observacional, transversal. Foram selecionados 119 pacientes (59 mulheres; 49,6%). Os indivíduos foram submetidos ao ecocardiograma transtorácico incluindo os valores de tempo de aceleração na artéria pulmonar; ondas E e A e relação E/A ao Doppler espectral do influxo mitral; ondas e' septal, e' lateral e relação E/e' ao Doppler tecidual do anel mitral; pressão sistólica na artéria pulmonar e volume atrial esquerdo.*

Resultados: *No sexo feminino, foi encontrada correlação positiva (coeficiente de correlação de Spearman) entre o valor do tempo de aceleração na artéria pulmonar e e' lateral (coeficiente de correlação de Spearman de 0,47; p=0,002), relação E/A (coeficiente de correlação de Spearman de 0,32; p=0,04) e e' septal (coeficiente de correlação de Spearman de 0,36; p=0,023) e uma correlação negativa entre o valor do tempo de aceleração na artéria pulmonar e pressão sistólica na artéria pulmonar (coeficiente de correlação de Spearman de -0,43; p=0,034). No sexo masculino, não foi encontrada correlação significativa. Foram encontrados menores valores de tempo de aceleração na artéria pulmonar em mulheres com hipertensão arterial sistêmica quando comparadas a mulheres sem hipertensão arterial sistêmica (0,13±0,03 segundos versus 0,16±0,03 segundos; p = 0,015).*

Conclusão: O presente estudo mostrou correlação significativa dos valores do TAP com alguns parâmetros da função diastólica do ventrículo esquerdo apenas no sexo feminino, sendo que mulheres hipertensas apresentaram menores valores de TAP.

Palavras-chave: Artéria pulmonar; Hipertensão pulmonar; Ecocardiografia.

Mailing Address: Renan Macedo Coimbra •
E-mail: renancoimbra@hotmail.com
Manuscript received 22/8/2021; revised 9/11/2021; accepted 22/2/2022

DOI: 10.47593/2675-312X/20223501eabc242

Introduction

Transthoracic echocardiography (TTE) is an important tool in the investigation of several pathologies affecting the heart that analyzes the interdependence between various cardiac structures with noninvasive precision, particularly the correlation between the systolic function of the left (LV) and right ventricles (RV).[1] However, the blood flow to the lungs and its correlation with the parameters that determine LV diastolic function (LVDF) have been poorly investigated.

The RV outflow tract acceleration time, also called pulmonary artery acceleration time (PAAT), corresponds to the time the flow through the pulmonary valve takes to reach its maximum peak velocity estimated by spectral pulsed-wave Doppler in the RV outflow tract. This value is considered normal when >120 ms and abnormal when <105 ms,[2–4] suggesting the presence but not severity of pulmonary hypertension (PH). Although it is not as reliable as tricuspid regurgitation velocity, which more accurately estimates pulmonary artery systolic pressure (PASP), PAAT can also be used in this assessment.[5]

Assessing left ventricular diastolic dysfunction is a complex task based on several echocardiographic measurements and parameters, including PASP. This value cannot be estimated without adequate tricuspid regurgitation.[6–7] Therefore, the present study aimed to assess whether there is a correlation between PAAT and LVDF parameters in subjects with preserved LV systolic function in the absence of advanced LV diastolic dysfunction and by sex, age, and cardiovascular risk factors.

Methods

Study population

This was an observational cross-sectional study. A total of 119 patients aged over 18 years, including 59 women (49.6%), were selected regardless of ethnicity from the cardiology outpatient clinic of the Red Cross Hospital of Curitiba after being referred for TTE by the assistant physician for any clinical indication.

The patients were selected by convenience, without statistical criteria, according to their availability to participate in the research. A protocol form with clinical and echocardiographic parameters was completed for each patient. The clinical data collected were age, sex, weight, height, body mass index (BMI), and presence of systemic arterial hypertension (SAH), diabetes mellitus (DM), coronary artery disease (CAD), smoking (current or previous), and dyslipidemia. SAH, DM, dyslipidemia, and smoking were listed in the patients' medical records and/or reported by them. CAD was confirmed by the medical record review and the patient through a reported history of non-fatal myocardial infarction and surgical or percutaneous myocardial revascularization. Regularly used medications were also recorded.

The exclusion criteria were a) significant valvular disease (moderate or severe); b) valve prostheses; c) segmental LV contraction changes due to ischemic heart disease or other cardiomyopathies; d) pulmonary emphysema or chronic obstructive pulmonary disease; e) moderate to severe pulmonary arterial hypertension (PASP > 50 mmHg); f) left ventricular contractile dysfunction (ejection fraction < 52% for men and < 54% for women); g) infiltrative and pericardial diseases; h) congenital heart disease with increased pulmonary blood flow with or without surgical correction; i) pacemaker; j) atrial fibrillation; and k) advanced (II and III) LV diastolic dysfunction.

The patients underwent complete two-dimensional TTE using Phillips IE 33, Envisor or General Electric Vivid E echocardiography equipment. All acoustic windows and all standard echocardiographic measurements and analyses were performed for each patient. Sonographic measurements were performed by two experienced echocardiographers qualified in echocardiography by the Department of Cardiovascular Imaging of the Brazilian Society of Cardiology.

All patients signed an informed consent form. The study was approved by the institution's research ethics committee.

Main echocardiographic parameters analyzed in this study

The following parameters were examined: E and A waves and E/A ratio on spectral pulsed-wave Doppler of the mitral inflow; Septal and lateral e' waves and E/e' ratio (E wave/average between septal and lateral e' velocities) on pulsed tissue Doppler of the mitral annulus; PASP (mmHg) through the maximum tricuspid regurgitation velocity (m/s), when present, on continuous spectral wave Doppler of tricuspid regurgitation, and inferior vena cava diameter (mm); PAAT measured immediately above the pulmonary valve leaflets on spectral pulsed-wave Doppler of the RV outflow tract (Figures 1 and 2); Indexed left atrial volume (normal up to 34 mL/m^2 for women and men) measured using the modified biplane Simpson's method in four- and two-chamber orthogonal projections.

All quantifications and values considered in the present study were based on American Society of Echocardiography and European Society of Cardiovascular Imaging guidelines.[8–10]

Statistical analysis

The women and men were analyzed separately. The study results are described as mean, median, minimum and maximum value, and standard deviation for quantitative variables or as frequency and percentage for categorical variables. The association between two quantitative variables was estimated by the Pearson or Spearman correlation coefficient (PCC and SCC, respectively). Quantitative variables were compared using Student's t-test for independent samples or the non-parametric Mann-Whitney test. More than two groups were compared using one-way analysis of variance and the least significant difference test for multiple comparisons or the non-parametric Kruskal-Wallis test. The normality of the variables was evaluated by the Kolmogorov-Smirnov test. P values < 0.05 were considered statistically significant.

The data were analyzed using SPSS Statistics software v.20.0 (IBM Corp., Armonk, NY, USA).

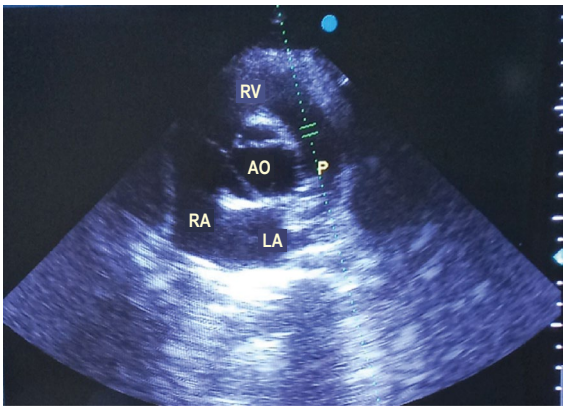

AO, aortic valve; LA, left atrium; P, pulmonary artery; PAAT, pulmonary artery acceleration time; RA, right atrium; RV, right ventricle

Figure 1 – *Parasternal cross-sectional view at the level of the base vessels. The figure shows the pulsed-wave Doppler cursor positioned on the right ventricular outflow tract used to obtain the PAAT.*

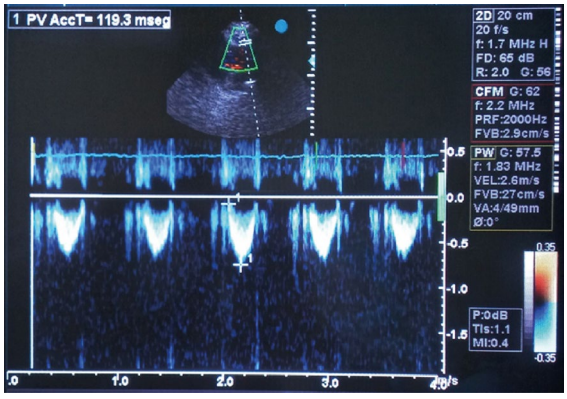

Figure 2 – *Pulsed-wave Doppler PAAT scan.*

Results

The final analysis included 119 subjects, 59 (49.6%) women (62.6 ± 16.5 years) and 60 (50.4%) men (65.1 ± 11.2 years). The clinical and epidemiological characteristics of the studied population are shown in Table 1. The baseline echocardiographic parameters of the studied population agreed with the literature.[8–10]

Women showed a positive and significant correlation between PAAT and lateral e' (SCC, 0.47; p = 0.002), E/A ratio (SCC, 0.32; p = 0.04), and septal e' (SCC, 0.36; p = 0.023); and a negative correlation between PAAT and PASP (SCC -0.43; p = 0.034), (Figures 3 and 4). The other variables were not correlated with PAAT, and the male participants showed no significant correlation with the analyzed parameters (Table 3).

PAAT was not influenced by sex, BMI, DM, dyslipidemia, CAD, or smoking (data not shown). However, lower PAAT values were found in women with versus without SAH (0.13 ± 0.03 versus 0.16 ± 0.03 s, respectively; p = 0.015).

Age was not significantly correlated with PAAT in either sex (SCC, -0.27, p = 0.068 for women; SCC, -0.31, p = 0.065 for men).

Discussion

The present study found a significant positive correlation between PAAT and LVDF parameters (septal and lateral e' waves and E/A ratio) in women only, in whom the presence of SAH was associated with a lower PAAT. However, the general analysis of the studied population showed no significant PAAT differences in sex, age, or BMI.

PASP is currently the most commonly used PH data in LVDF assessments. PH degree is usually assessed by PASP estimated by tricuspid valve regurgitation. PAAT has a negative correlation with PASP (data also found in the present study). According to Granstam et al.,[11] tricuspid regurgitation may not be present or be unreliable for the correct estimation of PASP during TTE examinations. Considering this, they estimated pulmonary vascular resistance invasively, correlating it with PAAT values as a possible alternative for identifying PH. Therefore, considering those findings, it is important to have more than one method available to estimate PH in an LVDF study, especially when it is not possible to reliably estimate tricuspid regurgitation or in early cases of diastolic dysfunction that lack a significantly increased pulmonary pressure. In cases of preserved LV systolic

function, the differentiation between normal and abnormal diastolic function becomes complicated due to overlapped indices obtained by Doppler. Although age structurally changes the heart and the vessels, the analysis of healthy older people by Doppler showed similar values to those of younger age groups (40–60 years of age).[12] Considering the mean age of the studied population (relatively young subjects) and that all had preserved LV systolic function, no significant differences were expected in the parameters evaluated by Doppler. However, we expected that the inclusion of PAAT values could differentiate between early stages of diastolic dysfunction when PASP is not extremely high.

A study by Baroncini et al.[13] of 87 participants also showed a negative correlation between PAAT and age and a positive correlation between PAAT and E/A ratio with no significance between other variables or the sexes. This study demonstrated that PAAT values < 0.135 s were associated with grade I diastolic dysfunction, while those > 0.135 s were associated with normal diastole. These studies suggest that PAAT correlates with parameters used to assess LVDF, even in the early stages when there are no signs of significant pulmonary arterial hypertension. At this stage,

Table 1 - Basic characteristics of the study population.

Variable	n	Women	n	Men
Age, years	59	62.6 ± 16.5	60	65.1 ± 11.2
BMI				
<30	41	72	41	68
≥30	16	28	19	32
SAH				
Yes	37	68	39	70
No	17	32	17	30
Dyslipidemia				
Yes	24	44	15	27
No	30	56	41	73
DM				
Yes	20	37	16	29
No	34	63	40	71
CAD				
Yes	11	20	21	37
No	43	80	35	62

BMI, body mass index; CAD, coronary artery disease; DM, diabetes mellitus; SAH, systemic arterial hypertension; SD, standard deviation.

Table 2 – Echocardiographic and hemodynamic parameters of the study population.

Variable	n	Mean	SD	p*
E wave				
Female	45	0.75	0.27	0.070
Male	43	0.65	0.27	
A wave				
Female	41	0.80	0.20	0.484
Male	39	0.77	0.24	
E/A ratio				
Female	41	0.97	0.44	0.234
Male	39	0.92	0.65	
Lateral e' wave				
Female	43	0.10	0.04	0.835
Male	42	0.09	0.03	
Septal e' wave				
Female	43	0.08	0.03	0.509
Male	42	0.07	0.03	
E/e' ratio				
Female	43	10.0	4.7	0.150
Male	41	8.6	2.7	
PASP				
Female	31	28.8	11.7	0.346
Male	29	29.7	9.0	
AE volume				
Female	35	36.7	19.3	0.772
Male	42	35.1	14.0	
PAAT				
Female	45	0.15	0.04	0.404
Male	37	0,14	0,03	

**Student's t-test for independent samples or non-parametric Mann-Whitney test, p < 0.05. LA, left atrium; PAAT, pulmonary artery acceleration time; PASP, pulmonary artery systolic pressure; SD, standard deviation.*

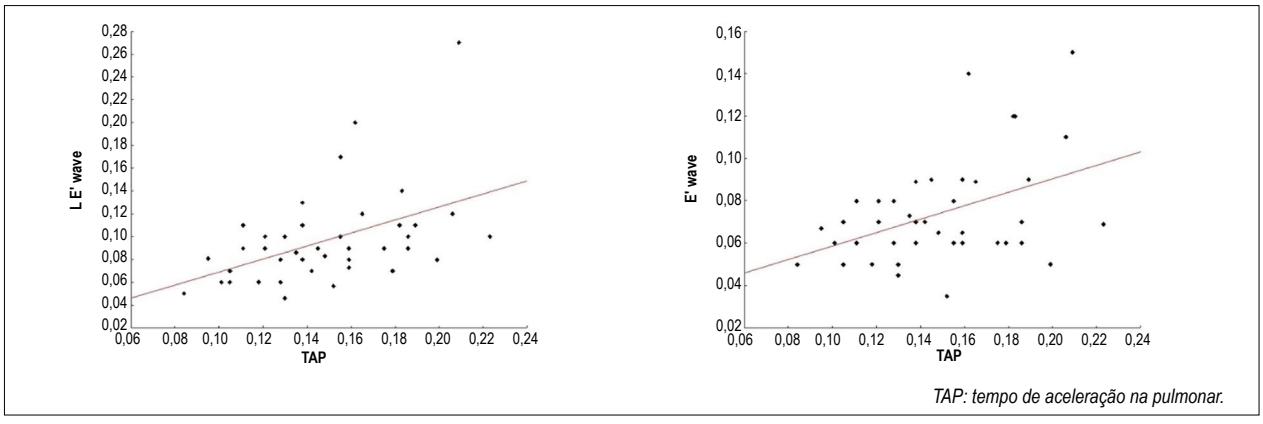

Figure 3 – *Correlation between pulmonary artery acceleration time (PAAT) and lateral E' and medial e' waves in women.*

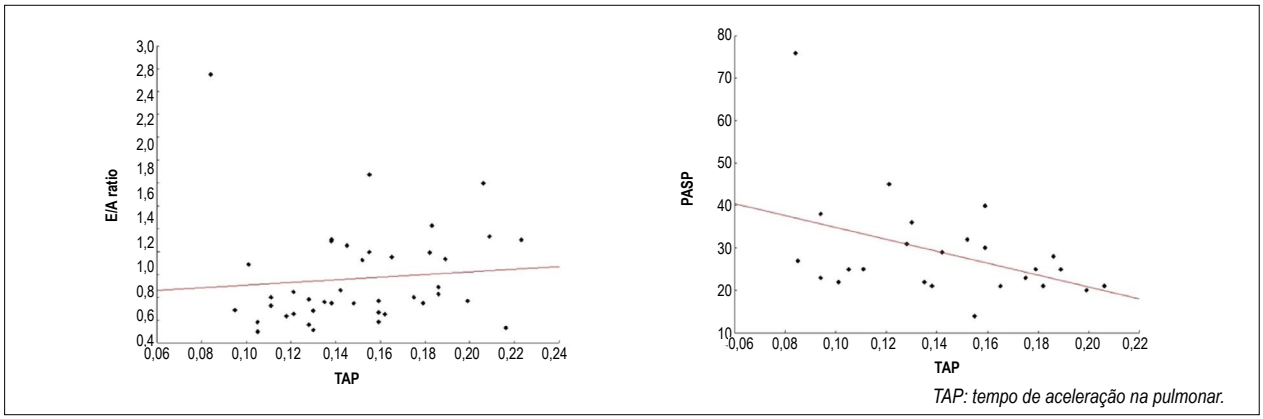

Figure 4 – *Correlation between pulmonary artery acceleration time (PAAT), E/A ratio, and pulmonary artery systolic pressure (PASP).*

Table 3 – Correlation between PAAT and diastolic function parameters.

Variable	n	r	p
PAAT × E/A ratio			
Female	41	0.32	0.040
Male	35	0.32	0.061
PAAT × septal e' wave			
Female	40	0.36	0.023
Male	35	0.30	0.081
PAAT × E/e' ratio			
Female	40	-0.13	0.436
Male	35	-0.04	0.822
PAAT × PASP			
Female	25	-0.43	0.034
Male	19	-0.21	0.380
PAAT × LAV			
Female	28	-0.08	0.701
Male	29	-0.11	0.577

the E/e' ratio is still low and the PAAT values are within the normal range (>120 ms).[14,15]

In a study of a larger number of participants, Marra et al.[16] analyzed 1,029 healthy subjects and reported no differences in PAAT values between men and women. However, they noticed a small reduction in this parameter with advancing age, increasing BMI, and higher systolic and diastolic systemic blood pressure. Similar to our findings, they also found a positive correlation between PAAT and E/A ratio; however, they did not discuss this last finding, suggesting the need for further studies in the area.

A study by Zabalgoitia et al.[17] prospectively analyzed LV mass, relative wall thickness, and systolic and diastolic interaction in 508 hypertensive patients aged 50–80 years according to age and sex. In men, most measures were similarly distributed. Nevertheless, women aged 65 years and older presented smaller LV systolic dimensions, greater ventricular thicknesses, greater fractional shortening, and less end-systolic wall stress, i.e., structural and functional changes were more pronounced in women.

In the present study, statistically significant findings, particularly in women, correlated with the findings by Zabalgoitia et al.,[17] indicating the importance of further studies on systolic ventricular function, diastolic function, possible hormonal influence, and SAH behavior in the female heart. Previous studies already reported hormonal influence in pre- and postmenopausal women and a higher incidence of heart failure with preserved ejection fraction in women.[18,19] Likewise, SAH causes different structural changes in ventricular geometric patterns in men and women, with possible deleterious effects that are more pronounced in women.[20]

A study by Alecrin et al.[21] with postmenopausal hypertensive women showed that hormone replacement therapy with oral estradiol for 12 weeks significantly improved LVDF on TTE. Mohamed et al.[22] correlated diastolic dysfunction with age and arterial hypertension and concluded that arterial hypertension duration, systolic and diastolic arterial hypertension level, and age are important prognostic indicators for predicting the development of diastolic dysfunction in hypertensive patients. A better understanding of these particularities may improve the treatment of hypertension and congestive heart failure.

Liebson et al.[23] evaluated a large population of men (n=511) and women (n=333) with mild primary hypertension and found a substantial percentage of participants with left ventricular hypertrophy diagnosed on echocardiography. In that study, left ventricular mass indices were positively correlated with systolic blood pressure, BMI, urinary sodium excretion, and smoking, with no significant difference between the sexes. Also, similar to findings presented here, they found a positive correlation between the PAAT and E/A ratio, without, however, discussing the later finding, suggesting further studies in this area.

The main limitation of the present study is the small number of participants (N=119), especially compared to other studies, thus increasing the chances of outliers that may have influenced the final results presented here. Another relevant factor was the exclusion of patients with more advanced degrees of diastolic dysfunction (DD), hindering the assessment of PAAT behavior in these situations. However, the main objective was to evaluate PAAT behavior in the initial stages of left ventricular

DD. Echocardiographic measurement intra- and inter-observer variability is also possible,[24] but this analysis was not performed in the parameters evaluated here. However, none of the studies cited in the discussion presented this PAAT analysis. Likewise, heart rate and blood pressure were also not measured concomitantly. According to Marra et al.,[16] who analyzed eight previous studies with 1,029 healthy subjects, PAAT values were weakly influenced by both heart rate and blood pressure.

Conclusions

The present study correlated PAAT with signs of early left ventricular DD in women only. Among the cardiovascular risk factors, the presence of SAH influenced PAAT in women only.

Authors' contributions

Data collection: Coimbra RM, Baroncini LAV, Camarozano AC, Carmo DC, Sá CRF, Fortunato JA, Darwich RZ; Data analysis: Coimbra RM, Baroncini LAV, Camarozano AC, Carmo DC; Data design: Coimbra RM, Baroncini LAV, Camarozano AC; Manuscript writing: Coimbra RM, Baroncini LAV, Camarozano AC, Carmo DC, Sá CRF, Fortunato JA, Darwich RZ; Critical review of the manuscript for important intellectual content: Coimbra RM, Baroncini LAV, Camarozano AC.

Conflict of interest

The authors have declared that they have no conflict of interest.

References

Bruhl SR, Chahal M, Khouri SJ. A novel approach to standard techniques in the assessment and quantification of the interventricular systolic relationship. Cardiovasc Ultrasound. 2011;9:42. doi: https://doi.org/10.1186/1476-7120-9-42.

Yared K, Noseworthy P, Weyman AE, McCabe E, Picard MH, Baggish AL. Pulmonary artery acceleration time provides an accurate estimate of systolic pulmonary arterial pressure during transthoracic echocardiography. J Am Soc Echocardiogr. 2011;24(6):687-92. doi: https://doi.org/10.1016/j.echo.2011.03.008.

Lopez-Candales A, Eleswarapu A, Shaver J, Edelman K, Gulyasy B, et al. Right ventricular outflow tract spectral signal: a useful marker of right ventricular systolic performance and pulmonary hypertension severity. Eur J Echocardiogr. 2010 Jul;11(6):509-15. doi: https://doi.org/1010.1093/ejechocard/jeq009

Grapsa J, Tzemos N. Echocardiography in pulmonar hypertension: current evidence and future perspectives. Continuing Cardiology Education. 2018;3:4. doi: https://doi.org/10.1002/cce2.67

Sbano JC, Tsutsui JM, Terra-Filho M, Mathias Junior W. Papel da ecodopplercardiografia na avaliação da hipertensão arterial pulmonar. J Bras Pneumol. 2004;30(1):78-86. doi: https://doi.org/10.1590/S1806-37132004000100014

Little WC, Downes TR. Clinical evaluation of left ventricular diastolic performance. Prog Cardiovasc Dis. 1990;32(4):273-90. doi: https://doi.org/1010.1016/0033-0620(90)90017-v

Mirsky I, Pasipoularides A. Clinical assessment of diastolic function. Prog Cardiovasc Dis. 1990;32(4):291-318. doi: https://doi.org/1010.1016/0033-0620(90)90018-w

Lang RM, Badano LP, Mor-Avi V, Afilalo J, Armstrong A, Ernande L, et al. Recommendations for cardiac chamber quantification by echocardiography in adults: an update from the American Society of Echocardiography and the European Association of Cardiovascular Imaging. J Am Soc Echocardiogr. 2015;28(1):1-39.e14. doi: https://doi.org/1010.1016/j.echo.2014.10.003

DiLorenzo MP, Bhatt SM, Mercer-Rosa L. How best to assess right ventricular function by echocardiography. Cardiol Young. 2015;25(8):1473-81. doi: https://doi.org/1010.1017/S1047951115002255

Rudski LG, Lai WW, Afilalo J, Hua L, Handschumacher MD, Chandrasekaran K, et al. Guidelines for the echocardiographic assessment of the right heart in adults: a report from the American Society of Echocardiography endorsed by the European Association of Echocardiography, a registered branch of the European Society of Cardiology, and the Canadian Society of Echocardiography. J Am Soc Echocardiogr. 2010;23(7):685-713; quiz 786-8. doi: https://doi.org/1010.1016/j.echo.2010.05.010

Granstam SO, Björklund E, Wikström G, Roos MW. Use of echocardiographic pulmonary acceleration time and estimated vascular resistance for the evaluation of possible pulmonary hypertension. Cardiovasc Ultrasound. 2013;11:7. doi: https://doi.org/1010.1186/1476-7120-11-7

Nagueh SF, Smiseth OA, Appleton CP, Byrd BF 3rd, Dokainish H, Edvardsen T, et al. Recommendations for the Evaluation of Left Ventricular Diastolic Function by Echocardiography: An Update from the American Society of Echocardiography and the European Association of Cardiovascular Imaging. J Am Soc Echocardiogr. 2016;29(4):277-314. doi: https://doi.org/1010.1016/j.echo.2016.01.011

Baroncini LA, Urnau K, Camarozano AC, Carmo DC, Fortunato JA, Darwich RZ. Rigth ventricle Outflow Tract Acceleration Time: Correlation with Left Ventricular Diastolic Function. J Clinical Imaging and Intervencional Radiology. 2020;2(1):1-5.

Kadappu KK, Thomas L. Tissue Doppler imaging in echocardiography: value and limitations. Heart Lung Circ. 2015;24(3):224-33. doi: https://doi.org/1010.1016/j.hlc.2014.10.003

Zhang W, Kovács SJ. The age dependence of left ventricular filling efficiency. Ultrasound Med Biol. 2009;35(7):1076-85. doi: https://doi.org/1010.1016/j.ultrasmedbio.2009.01.009

Marra AM, Benjamin N, Ferrara F, Vriz O, D'Alto M, D'Andrea A, et al. Reference ranges and determinants of right ventricle outflow tract acceleration time in healthy adults by two-dimensional echocardiography. Int J Cardiovasc Imaging. 2017;33(2):219-26. doi: https://doi.org/1010.1007/s10554-016-0991-0

Zabalgoitia M, Rahman SN, Haley WE, Mercado R, Yunis C, Lucas C, et al. Comparison in systemic hypertension of left ventricular mass and geometry with systolic and diastolic function in patients <65 to > or = 65 years of age. Am J Cardiol. 1998;82(5):604-8. doi: https://doi.org/1010.1016/s0002-9149(98)00404-4

Hirokawa M, Daimon M, Lee SL, Nakao T, Kawata T, Kimura K, et al. Early menopause does not influence left ventricular diastolic dysfunction: A clinical observational study in healthy subjects. J Cardiol. 2016;68(6):548-553. doi: https://doi.org/1010.1016/j.jjcc.2015.11.014

Zhao Z, Wang H, Jessup JA, Lindsey SH, Chappell MC, Groban L. Role of estrogen in diastolic dysfunction. Am J Physiol Heart Circ Physiol. 2014;306(5):H628-40. doi: https://doi.org/1010.1152/ajpheart.00859.2013

Argemiro AJ, Camarozano AC, Carmo DC, Fortunato JA, Darwich RZ, Baroncini LA. Hipertensão arterial sistêmica e ventrículo direito: dados ecocardiográficos preliminares. Arq Bras Cardiol: Imagem Cardiovasc. 2018;31:268-76.

Alecrin IN, Aldrighi JM, Caldas MA, Gebara OC, Lopes NH, Ramires JA. Acute and chronic effects of oestradiol on left ventricular diastolic function in hypertensive postmenopausal women with left ventricular diastolic dysfunction. Heart. 2004;90(7):777-81. doi: https://doi.org/1010.1136/

hrt.2003.016493

Mohamed AL, Yong J, Masiyati J, Lim L, Tee SC. The prevalence of diastolic dysfunction in patients with hypertension referred for echocardiographic assessment of left ventricular function. Malays J Med Sci. 2004;11(1):66-74.

Liebson PR, Grandits G, Prineas R, Dianzumba S, Flack JM, Cutler JA, et al. Echocardiographic correlates of left ventricular structure among 844 mildly hypertensive men and women in the Treatment of Mild Hypertension Study (TOMHS). Circulation. 1993;87(2):476-86. doi: https://doi.org/1010.1161/01.cir.87.2.476

Ferrara F, Gargani L, Contaldi C, Agoston G, Argiento P, Armstrong WF, et al.; RIGHT Heart International NETwork (RIGHT-NET) Investigators. A multicentric quality-control study of exercise Doppler echocardiography of the right heart and the pulmonary circulation. The RIGHT Heart International NETwork (RIGHT-NET). Cardiovasc Ultrasound. 2021;19(1):9. doi: https://doi.org/1010.1186/s12947-021-00238-1

Review Article

Myocardial Involvement in Chagas Disease: From the Perspective of Cardiovascular Magnetic Ressonance Assessment

Acometimento Miocárdico na Doença de Chagas: Uma Perspectiva a partir da Avaliação pela Ressonância Magnética Cardiovascular

Henrique Turin Moreira[1], Gustavo Jardim Volpe[1], André Schmidt[1]
Hospital das Clínicas, School of Medicine of Ribeirão Preto[1], University of São Paulo, Ribeirão Preto, SP, Brazil.

Abstract

Chagas disease represents an important public health problem, especially in endemic countries in Latin America. Chronic cardiomyopathy is its most frequent clinical presentation. Myocardial involvement has a multifactorial pathogenesis and can lead to heart failure, thromboembolic events, arrhythmias, and sudden death. In this context, cardiovascular magnetic resonance imaging (CMR) is an excellent noninvasive method for investigating myocardial damage and understanding the mechanisms and consequences of these injuries. CMR has high spatial resolution and tissue characterization capacity, enabling a highly reliable morphofunctional analysis and the identification of risk markers for adverse events in patients with Chagas disease. This exam is very useful for the diagnosis and follow-up of these patients in the routine clinical setting.

Introduction

Despite efforts to reduce new cases of Chagas disease, especially by interrupting its transmission by domiciled triatomines and serological screening in blood banks, its prevalence remains high worldwide. A recent estimate by the World Health Organization points to 6–7 million people infected by the protozoa *Trypanosoma cruzi* worldwide, most of them residing in one of the 21 Latin American countries where Chagas disease is considered endemic, in addition to approximately 70 million people at risk of contracting it in this region.[1] An estimated 30–40% of infected individuals will develop clinical presentations in the chronic phase of the disease, with cardiomyopathy being the most frequent and severe presentation.[2] Cardiac impairment have a multifactorial pathogenesis and include silent myocarditis related to parasite persistence and autoimmune reactions after the infection, in addition to microvascular disorders and autonomic denervation, which lead to heterogeneous cases of dilated heart disease and changes in the cardiac electrical-conduction system.[3] After almost 30 years since the first clinical studies on chronic Chagas disease cardiomyopathy (CCDC) by cardiovascular magnetic resonance imaging (CMR), this method has helped increase our understanding of the pathology and improved staging and risk stratification in routine clinical practice.[4-6]

This study aimed to revisit myocardial involvement in patients with Chagas disease from the perspective of CMR findings. It focused on morphofunctional changes in the left and right ventricles, including the characterization of myocardial fibrosis and its relationship with functional changes and cardiac arrhythmias, also addressing the prognostic value of CMR findings in cardiovascular risk stratification in CCDC patients.

Regional changes, aneurysms, and thrombi in the left ventricle

CMR is a reference method for cardiac morphofunctional assessment. Its high spatial resolution provides high-quality heart images, enabling very reliable and reproducible measurements. Furthermore, the assessment of ventricular systolic performance by CMR, particularly the calculation of ejection fraction, is based on the measurement of cavity volumes without the need for geometric assumptions.[7] These properties improve the assessment of patients with Chagas disease, especially considering the peculiarities of this clinical condition.[8]

Regional left ventricular (LV) systolic function changes are relatively common in patients with Chagas disease, thus limiting volumetric estimates either from linear measurements or by endocardial measurements based on only two two-dimensional cardiac image projections. Clinical studies using CMR to assess LV wall motion show that the inferolateral and apical regions are the most frequently affected in patients with Chagas disease, corroborating the knowledge obtained over time using other diagnostic methods.[9,10] Although the reason for this segmentally distributed myocardial damage is not fully understood, evidences suggest that mechanisms related to microvascular ischemia caused by Chagas disease are involved in its pathogenesis.[11,12]

Another particularity of CCDC is the onset of ventricular aneurysms, more frequently in the apical region.[13] These changes can range from small aneurysms with a narrow neck, to large aneurysmal dilatations with a wide neck and dyskinetic walls. The noninvasive assessment of these abnormalities can be challenging using other imaging methods such as echocardiography. On the one hand, small lesions may not be easily perceived, especially in

Keywords

Chagas disease; Ventricular dysfunction; Magnetic resonance imaging.

Mailing Address: Henrique Turin Moreira •
Avenida Bandeirantes, 3.900, Vila Monte Alegre. CEP 14.048-900 – Ribeirão Preto, SP, Brasil.
E-mail: hturin@fmrp.usp.br
Manuscript received 1/24/2022; revised 1/25/2022; accepted 1/27/2022

DOI: 10.47593/2675-312X/20223501eabc285

conventional echocardiographic imaging planes, which often shorten the visualized apical region (Figure 1).

On the other hand, in cases of large lesions, it may not be possible to analyze the entire aneurysmal region in the same image plane due to the smaller extension of the echocardiographic near field. Such obstacles can be overcome by CMR, which routinely includes the acquisition of planes transverse to the long LV axis encompassing the entire apical region and the complete visualization of apical aneurysms (Figure 2).

In CCDC patients, the prevalence of LV apical aneurysms on CMR is 20–28%, with no sex-based difference.[14-16] Ventricular aneurysms are risk factors for intracavitary thrombosis, especially when located in the apical region in patients with a reduced LV ejection fraction.[17] Myocardial lesions associated with blood stasis resulting from reduced ventricular systolic function predispose an individual to thrombus formation, which can provoke thromboembolic phenomena in CCDC.[18] The presence of prominent apical myocardial trabeculae commonly causes differential diagnostic difficulties. The avascularity of the thrombi is easily noticeable on CMR images obtained by myocardial perfusion sequences with infusion of a paramagnetic gadolinium-based contrast agent. The images acquired by this technique show thrombi as low-intensity signal structures surrounded by areas of increased signal generated by intracavitary blood content and adjacent viable myocardium. Non-viable myocardium and sessile thrombi can be differentiated by delayed enhancement present in scar regions but absent in thrombotic structures. Despite these attributes, the use of CMR to investigate ventricular aneurysms and thrombi has not been the focus of clinical studies of patients with Chagas disease. In this context, the use of CMR is noteworthy for risk stratification of thromboembolic events, but its use in CCDC patients has not been well established.[19]

Right ventricle in Chagas disease

The cardiac form of Chagas disease can affect both ventricles. Experimental *T. cruzi* infection models demonstrated prominent right ventricular (RV) lesions with inflammatory infiltrate, edema, parasitism, and myocardial fiber degeneration

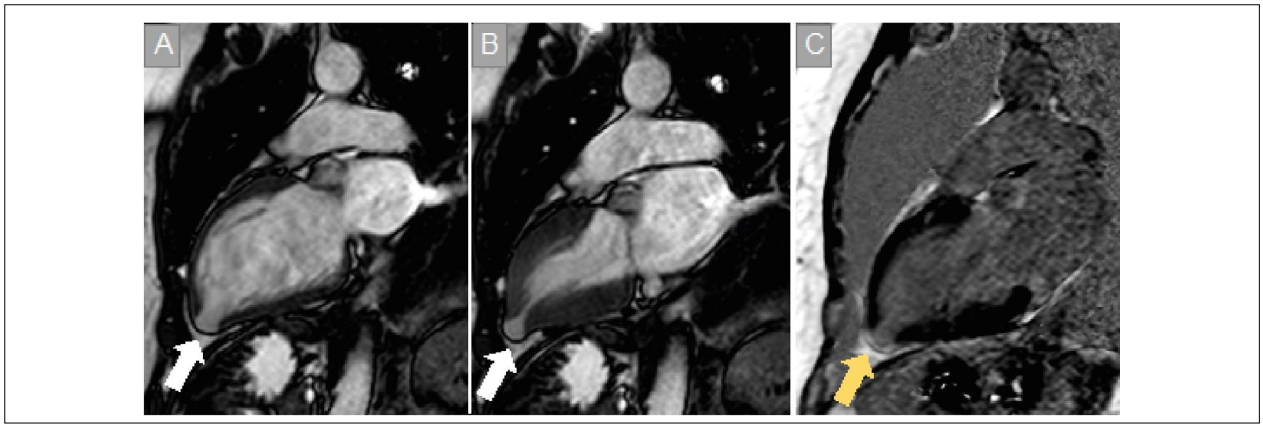

Figure 1 – *Narrow neck aneurysm at the apex of the left ventricle. Two-chamber tomographic sections obtained by cine-magnetic resonance imaging in ventricular diastole (A) and systole (B) showing a small apical aneurysm region. Myocardial scar evidenced by hypersignal intensity in the region of the aneurysm in a delayed gadolinium enhancement sequence (C).*

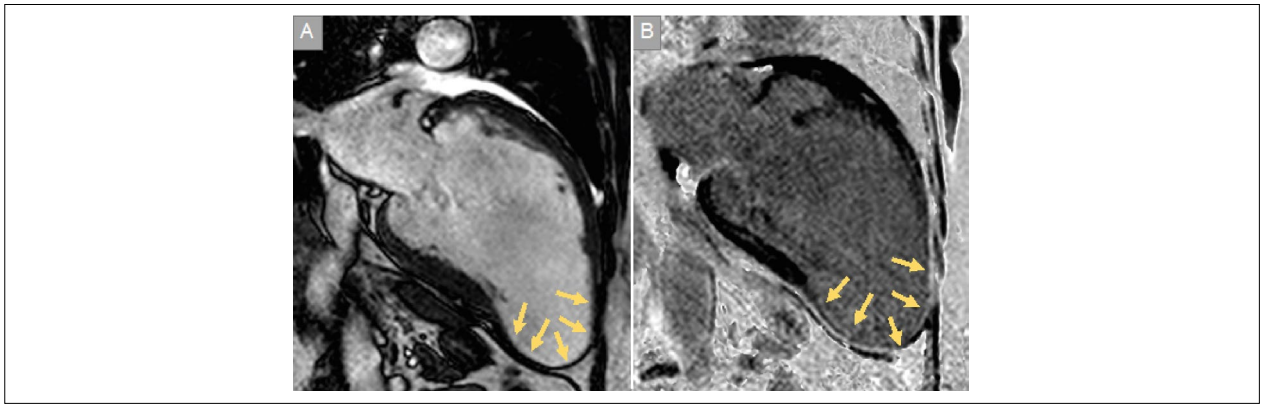

Figure 2 – *Wide neck aneurysm at the apex of the left ventricle. Two-chamber tomographic sections obtained in cine-magnetic resonance imaging in diastole showing parietal thinning and cavity enlargement in the apical region (A). Delayed gadolinium enhancement sequence showing an extensive hypersignal region compatible with transmural fibrosis in the aneurysmal area (C).*

in the acute phase in addition to RV dilatation progressively developing over the chronic phase.[20-22] RV dilatation and parietal thinning are common findings in necropsy studies of CCDC patients. On the other hand, histological analysis shows the replacement of RV muscle fibers by fibro-adipose tissue, more frequently in the apical region, that may show aneurysmal conformation.[23]

The first detailed descriptions of clinical presentations of CCDC were highlighted by a remarkable and predominant right heart failure with signs and symptoms of intense systemic congestion.[24] Seminal studies using radionuclide ventriculography supported the hypothesis of early and predominant RV involvement in CCDC.[25, 26] More recent studies associated RV systolic dysfunction with a worse prognosis in patients with heart failure due to Chagas disease, who are at a higher risk of death and require urgent heart transplantation.[27]

Thus, it is essential to examine the RV of patients with Chagas disease during clinical follow-up. However, the peculiar characteristics of this chamber, particularly its thin walls and complex geometry, may be obstacles to its analysis. Nevertheless, CMR presents a spatial resolution of the RV endocardial borders that is relatively superior to other imaging methods used in clinical routine, providing reliable and reproducible volumetric estimates.[28] In addition, RV ejection fraction calculation requires no geometric assumptions similarly to the analysis of this parameter in the LV.[29]

A clinical study using CMR to calculate RV ejection fraction in the chronic phase of Chagas disease reported RV systolic dysfunction in 37% of the 158 evaluated patients.[30] Most patients with right ventricular dysfunction in the investigation had a concomitantly reduced LV ejection fraction. However, RV systolic dysfunction was observed alone in approximately 4% of the studied population, including patients with the indeterminate form of the disease (Figure 3). Although the RV presents histopathological changes early after *T. cruzi* infection, the signs of its systolic dysfunction usually appear late in the disease course, when the LV ejection fraction is reduced with a subsequent pulmonary arterial pressure increase. In this condition, RV structural lesions prevent it from adapting to the increased afterload, ultimately leading to right heart failure.[31]

Myocardial fibrosis and LV systolic dysfunction

Chagas disease myocardial fibrosis results from a multifactorial pathogenic mechanism that includes myocarditis related to parasite persistence, an autoimmune reaction triggered by the parasitic infection, and microvascular ischemia.[3] Delayed gadolinium enhancement shows areas of myocardial necrosis and fibrosis usually at 10 min after the intravenous infusion. This technique has high sensitivity and specificity for myocardial scar investigation and is the current method of choice for this purpose.[7]

In the chronic phase of Chagas disease, delayed enhancement can identify scar areas early in the indeterminate form of the disease.[32] However, the prevalence of fibrosis identified by CMR at this disease stage is not well established since most populations studied to date are relatively small. The combined analysis of studies reporting delayed enhancement in patients with the indeterminate form shows the occurrence of myocardial scar in 19% of the pooled population (Table 1).[9,10, 32-39] Myocardial fibrosis progressively increases with disease progression, being considered a marker of CCDC severity.[9] The higher the proportion of delayed enhancement in relation to the LV mass, the lower the ejection fraction of this chamber and the worse the estimated functional class.[9, 10] However, the correlation between fibrosis extent and LV systolic function appears nonlinear. Small scar areas are seen in ventricles with normal systolic function, even when ventricular function is examined by more sensitive methods (Figure 4).[39] Patients with Chagas disease and a fibrotic mass on CMR greater than 10% present significantly lower LV systolic function than those with less extensive fibrosis.[36]

The most frequent areas of delayed myocardial enhancement in Chagas disease are the inferolateral and apical regions of the LV. Although there is an association between fibrosis and myocardial wall motion abnormalities,

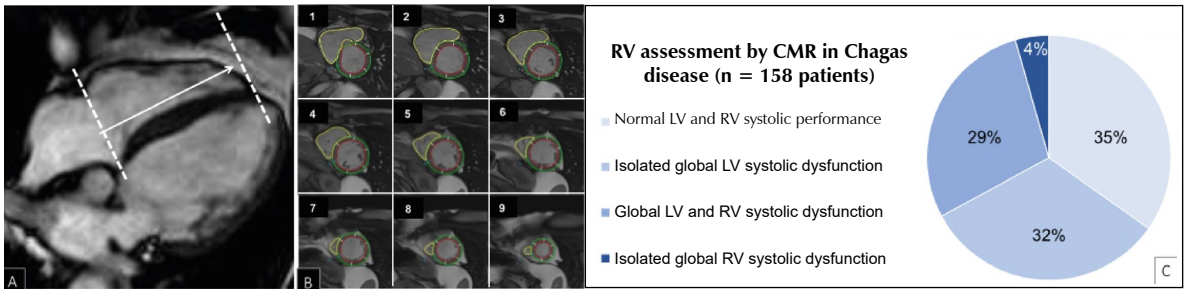

Adapted from: Moreira HT et al. Circ Cardiovasc Imaging (2017). 10:e005571 (30) under permission of Wolters Kluwer Health Inc. (license number 5235470656058).

Figure 3 – *Right ventricular assessment in patients with Chagas disease. RV scan limits shown in a four-chamber cine-magnetic resonance section (A). Short-axis sections from the basal to the apical region for RV endocardial border delineation (yellow lines), thus allowing the calculation of end-diastolic and systolic volumes and ejection fraction (B). A cohort of 158 patients with Chagas disease evaluated by magnetic resonance imaging showed global RV systolic dysfunction commonly associated with concomitant depressed LV systolic function, although isolated RV dysfunction has also been identified, even in cases of the indeterminate form of the disease.*

small areas of delayed enhancement may be seen in myocardial segments with normal mobility. However, more extensive scars, particularly those affecting at least 50% of the myocardial wall, are usually related to areas of LV hypokinesia and akinesia. The distribution of LV fibrosis in Chagas disease varies. Subendocardial and transmural patterns are the most common, being indistinguishable from sequelae of infarction caused by coronary artery disease. Mesocardial and subepicardial patterns are also common.[9, 10] While myocardial scars present a homogeneously and localized pattern in some individuals, diffuse fibrosis of varied patterns are seen in others. In both cases, the presence of speckled pattern scars can be an obstacle to their quantification (Figure 5).

Recently, a serial cardiac assessment of CCDC patients by CMR associated myocardial fibrosis with a decreased LV ejection fraction.[40] The percentage of LV mass with signs of delayed enhancement significantly increased from 13±8% to 18±14% in subjects evaluated over a mean 5-year follow-up. However, the prognostic value of this finding remains uncertain. Issues related to the reproducibility of delayed myocardial enhancement measurements represent a limitation in the interpretation of serial assessment results. In this context, investigating factors related to the onset of myocardial scars in patients not previously presenting this finding can improve our understanding of the progression of myocardial damage in Chagas disease.

Table 1 - Prevalence of delayed myocardial enhancement by CMR in patients with the indeterminate form of Chagas disease.

Authors	Patients with the indeterminate form evaluated by CMR	Presence of delayed myocardial enhancement
Rochitte et al.[9]	15	3 (20)
Regueiro et al.[10]	27	2 (7)
Noya-Rabelo et al.[32]	17	6 (35)
Tassi et al.[33]	26	5 (19)
Torreão et al.[34]	16	2 (13)
Lee-Felker et al.[35]	50	4 (8)
Uellendahl et al.[36]	11	3 (27)
Melendez-Ramirez et al.[37]	8	4 (50)
Pinheiro et al.[38]	16	7 (44)
Romano et al.[39]	19	2 (11)
Total	205	38 (19)

CMR, cardiac magnetic resonance.

Myocardial fibrosis and ventricular arrhythmias

CCDC is considered an arrhythmogenic cardiomyopathy due to frequent cardiac electrical conduction system abnormalities and arrhythmias.[41] Sudden cardiac death can occur at any stage of the disease, especially as a result of malignant ventricular arrhythmias such as sustained ventricular tachycardia.[42] Myocardial fibrosis foci are the main arrhythmogenic substrates in the chronic form of Chagas disease, although other mechanisms such as microvascular disorders and sympathetic denervation also play a role in the pathogenesis of ventricular arrhythmias in this clinical condition.[43, 44]

The high spatial resolution of CMR to detect, characterize, and quantify myocardial fibrosis is a major advantage for the noninvasive risk stratification of adverse events in patients with Chagas disease, including malignant ventricular arrhythmias. Cross-sectional and case-control studies showed that areas of delayed myocardial enhancement on CMR are highly prevalent findings in patients with Chagas disease and a clinical history of concomitant sustained ventricular tachycardia.[9, 45] Notably,

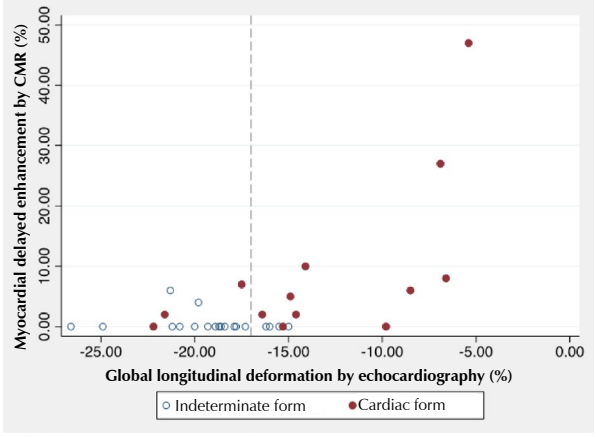

Adapted from: Romano MMD et al. PLoS Negl Trop Dis (2020). 14(11): e0008795 under permission from Creative Commons Attribution License (CC BY 4.0).

Figure 4 – *Correlation between extent of myocardial fibrosis assessed by delayed enhancement on magnetic resonance imaging and LV systolic function assessed by speckle tracking echocardiography is nonlinear in Chagas disease. Patients with small fibrotic areas (generally smaller than 10% of the myocardial mass) may have normal global LV systolic function (to the left of the dashed line, which represents the normal limit of global longitudinal myocardial deformation). A systolic global longitudinal strain lower than 15% (specific value for the software used for analysis) is usually associated with the presence of myocardial fibrosis. Additionally, the presence of myocardial scars is shown in two patients with the indeterminate form of the disease.*

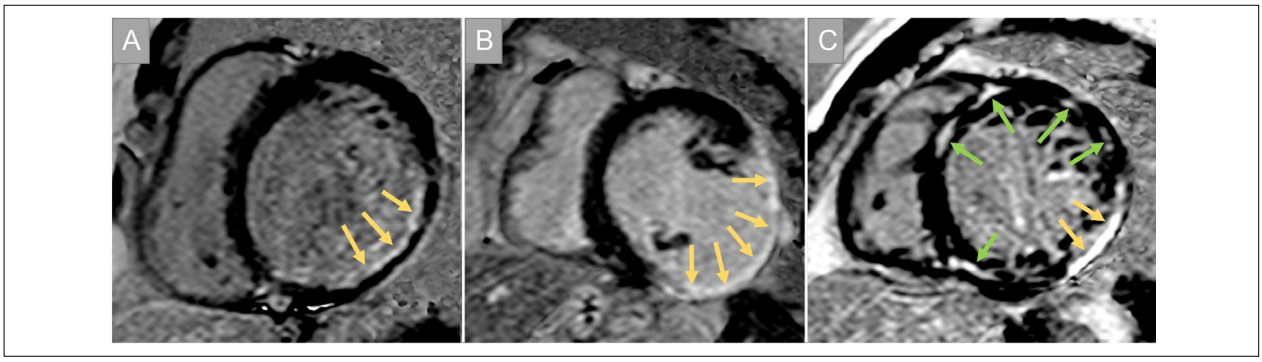

Figure 5 – *Myocardial LV scars evidenced in short-axis tomographic sections using the delayed gadolinium enhancement technique. Subendocardial fibrosis in the inferolateral region of the LV (A) and transmural fibrosis involving the anterolateral, inferolateral, and inferior LV regions (B). Diffuse and mixed myocardial fibrosis pattern with an area of transmural scar (yellow arrows) in the inferolateral region and the foci of diffuse mesocardial scars (green arrows) involving other LV regions (C).*

fibrosis identified by CMR may be the only myocardial abnormality found in Chagas patients presenting electrical instability, defined by frequent ventricular premature beats or episodes of sustained or non-sustained ventricular tachycardia.[33] In addition, myocardial scars identified by CMR are anatomically correlated with regions showing signs of autonomic denervation and ischemia assessed by myocardial perfusion scintigraphy, suggesting an inextricable participation of these factors in the pathogenesis of ventricular arrhythmias in CCDC.[46]

A transmural myocardial fibrosis pattern is more frequently noted on CMR in Chagas patients with sustained ventricular tachycardia than in those without this clinical sign. The presence of two or more continuous myocardial segments with transmural delayed enhancement is associated with a history of sustained ventricular tachycardia regardless of age, sex, LV ejection fraction, and the percentage of delayed enhancement.[45]

In addition, myocardial scar characterization by CMR can be an auxiliary tool in ventricular tachycardia ablation in patients with CCDC.[47] Scar patterns that are transmural or have subepicardial involvement, usually present in the inferolateral segments of the LV, often lead to predominantly epicardial reentrant circuits.[48] Under these conditions, combined endocardial and epicardial ablation is more effective at stopping malignant ventricular arrhythmias in CCDC patients in the short and long term.[49]

New CMR techniques seem promising for assessing interstitial fibrosis in patients with Chagas disease. A cross-sectional study of 47 Chagas patients demonstrated that higher interstitial fibrosis by its CMR-derived extracellular volume is associated with non-sustained ventricular tachycardia regardless of ejection fraction and delayed LV myocardial enhancement quantification.[38]

Prognostic value of myocardial fibrosis in chronic Chagas heart disease

In Chagas disease patients, prognostic assessments can identify individuals at greater risk of cardiovascular events throughout the disease course, thus helping decision-making regarding the need for specialized follow-up and therapeutic planning. LV systolic dysfunction is the most consistent predictor of death in patients with Chagas disease.[50] However, other factors, such as male sex, New York Heart Association functional class III/IV, low-voltage QRS complexes on an electrocardiogram, cardiomegaly on chest radiography, and non-sustained ventricular tachycardia identified on 24-hour electrocardiographic monitoring also indicate higher risk of adverse events and high mortality in this clinical setting. These predictors are gathered in the score proposed by Rassi et al. that was originally developed and validated for the risk stratification of death in patients with CCDC.[51] In a cross-sectional study, the greater extent of myocardial fibrosis assessed by CMR was positively correlated with Rassi score.[36]

Two recent longitudinal studies demonstrated the role of myocardial fibrosis identification and quantification by CMR in the risk stratification of this clinical condition.[14, 15] In a prospective cohort of 140 CCDC patients, myocardial scar was related with the occurrence of combined sustained ventricular tachycardia and cardiovascular death at a median 3-year follow-up period. A significant association was also reported between myocardial fibrosis and the combined outcome including hospital admission for heart failure. Also, the greater the extent of myocardial scar, the greater the risk of these combined events regardless of age and LV ejection fraction (Figure 6). [14] In another retrospective cohort of 130 CCDC patients, the presence and greater extent of delayed myocardial enhancement were related to a high incidence of the combined outcome of overall mortality, heart transplantation, appropriate implantable cardioverter-defibrillator therapy, and aborted sudden death in a median 5-year follow-up period. In that study, the presence of a fibrotic mass equal to or greater than 12.3 g was significantly and independently associated with the combined outcome studied. Additionally, a bivariate analysis including fibrotic mass and the Rassi risk score as predictive variables showed the association of both with the composite outcome.[15] Remarkably, the absence of fibrosis in these studies was an excellent marker of the non-occurrence of adverse events in patients with CCDC. However, the question remains about the

role of myocardial fibrosis in prognostic reclassification after use of the Rassi score, especially in individuals initially stratified by this classification system as being at low or intermediate risk.[52] Nevertheless, these recent studies demonstrated the potential benefits of myocardial scar assessment by CMR in the stratification of cardiovascular risk in Chagas patients, while the role of this evaluation in clinical decision-making may be demonstrated in future clinical trials.

Myocarditis assessment of Chagas patients

Myocarditis due to parasitic persistence is considered one of the main pathogenic mechanisms of myocardial injury by Chagas disease.[53] In the acute phase, severe myocarditis can lead to death, although this has been noted in only a small number of symptomatic patients. However, the prevalence of myocardial inflammation in the acute phase of the disease is probably underestimated due to diagnostic difficulty. In the chronic phase, low-intensity myocarditis is recognized as a key pathological mechanism in the genesis of myocardial lesions in Chagas disease. Exacerbations can occur in immunosuppressed patients, reactivating parasite replication and causing severe myocarditis, acute heart failure, and death.

Despite the outstanding role of CMR in the noninvasive assessment of myocarditis, its use in patients with Chagas disease has been scarcely reported in the scientific literature. A cross-sectional study of 54 patients with Chagas disease using conventional CMR techniques showed that myocardial hyperemia and edema, considered criteria for the noninvasive diagnosis of myocarditis, can occur in all phases of CCDC, even early in patients with preserved LV systolic function or with the indeterminate form.[34] As highlighted by the authors, these subclinical abnormalities show the risk of more severe conditions and can increase our understanding of the natural history of the disease.

In addition to traditional strategies for investigating suspected myocarditis, the CMR myocardial mapping technique provides a quantitative and more objective analysis of areas of myocardial edema. A case of Chagas myocarditis in an adult patient reported that this technique helped diagnose myocarditis in the acute phase and over the follow-up period, showing progressive regression of the edematous myocardial areas in serial CMR tests.[54] The use of myocardial mapping in the chronic phase of Chagas disease is promising, as it may reveal subclinical changes and identify individuals at high risk of progressing to more advanced CCDC stages.

Conclusions

CMR assesses myocardial involvement in Chagas disease with highly reliable and reproducible cardiac morphofunctional characterization, especially in the presence of regional LV systolic function changes and RV dysfunction. CMR has high sensitivity for detecting myocardial scars, proving a valuable tool for cardiovascular risk stratification in CCDC patients. The presence and greater extent of myocardial fibrosis areas on CMR are associated with LV systolic dysfunction and the occurrence of ventricular arrhythmias in these patients. In addition, clinical cohorts have recently demonstrated the prognostic value of delayed myocardial gadolinium enhancement areas with adverse cardiovascular events such as hospital admissions for heart failure, sustained ventricular tachycardia, and sudden cardiac death. More advanced CMR techniques, such as myocardial mapping for the assessment of myocardial edema and diffuse fibrosis, were recently used in the clinical evaluation of patients with Chagas disease with very promising preliminary results.

Authors' contribution

Manuscript concept and writing: Moreira HT; Critical review for important intellectual content: Volpe GJ, Schmidt A

Conflict of interest

The authors have declared that they have no conflict of interest.

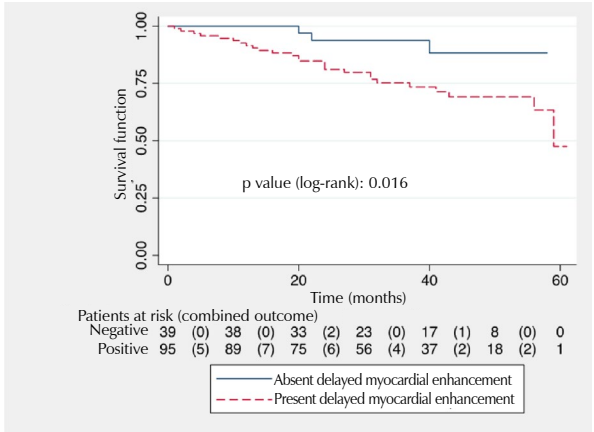

Adapted from: Volpe GJ et al. J Am Coll Cardiol (2018). 72:2567-76 (14) under permission from Elsevier (license number 5235480481082).

Figure 6 – *Association between myocardial fibrosis and the occurrence of the combined outcome of cardiovascular death, sustained ventricular tachycardia, or hospitalization for heart failure in patients with chronic Chagas heart disease. The presence of delayed myocardial enhancement by CMR is a risk predictor of the combined outcome compared with the absence of myocardial scar.*

References

1. World Health Organization (WHO). Integrating neglected tropical diseases into global health and development: fourth WHO report on neglected tropical diseases. Genève: WHO; 2017 [cited 2022 Feb 7]. Available from: https://apps.who.int/iris/handle/10665/255011

2. Rassi A Jr, Rassi A, Marin-Neto JA. Chagas disease. Lancet. 2010;375(9723):1388-402. doi: 10.1016/S0140-6736(10)60061-X

3. Marin-Neto JA, Cunha-Neto E, Maciel BC, Simões MV. Pathogenesis of chronic Chagas heart disease. Circulation. 2007;115(9):1109-23. doi: 10.1161/CIRCULATIONAHA.106.624296

4. Kalil R, Bocchi EA, Ferreira BM, de Lourdes Higuchi M, Lopes NH, Magalhães AC, et al. [Magnetic resonance imaging in chronic Chagas cardiopathy. Correlation with endomyocardial biopsy findings]. Arq Bras Cardiol. 1995;65(5):413-6. Portuguese. PMID: 8729858.

5. Bellotti G, Bocchi EA, de Moraes AV, Higuchi M L, Barbero-Marcial M, Sosa E, et al. In vivo detection of Trypanosoma cruzi antigens in hearts of patients with chronic Chagas' heart disease. Am Heart J. 1996;131(2):301-7. doi: 10.1016/s0002-8703(96)90358-0. Erratum in: Am Heart J. 1998;135(3):550

6. Bocchi EA, Kalil R, Bacal F, de Lourdes Higuchi M, Meneghetti C, Magalhães A, et al. Magnetic resonance imaging in chronic Chagas' disease: correlation with endomyocardial biopsy findings and gallium-67 cardiac uptake. Echocardiography. 1998;15(3):279-88. doi: 10.1111/j.1540-8175.1998.tb00608.x

7. Sara L, Szarf G, Tachibana A, Shiozaki AA, Villa AV, de Oliveira AC, et al. Sociedade Brasileira de Cardiologia; Colégio Brasileiro de Radiologia. II [II Guidelines on Cardiovascular Magnetic Resonance and Computed Tomography of the Brazilian Society of Cardiology and the Brazilian College of Radiology]. Arq Bras Cardiol. 2014;103(6 Suppl 3):1-86. Portuguese. doi: 10.5935/abc.2014S006

8. Nunes MC, Badano LP, Marin-Neto JA, Edvardsen T, Fernández-Golfín C, Bucciarelli-Ducci C, et al. Multimodality imaging evaluation of Chagas disease: an expert consensus of Brazilian Cardiovascular Imaging Department (DIC) and the European Association of Cardiovascular Imaging (EACVI). Eur Heart J Cardiovasc Imaging. 2018;19(4):459-60n. doi: 10.1093/ehjci/jex154

9. Rochitte CE, Oliveira PF, Andrade JM, Ianni BM, Parga JR, Avila LF, et al. Myocardial delayed enhancement by magnetic resonance imaging in patients with Chagas' disease: a marker of disease severity. J Am Coll Cardiol. 2005;46(8):1553-8. doi: 10.1016/j.jacc.2005.06.067

10. Regueiro A, García-Álvarez A, Sitges M, Ortiz-Pérez JT, De Caralt MT, Pinazo MJ, et al. Myocardial involvement in Chagas disease: insights from cardiac magnetic resonance. Int J Cardiol. 2013;165(1):107-12. doi: 10.1016/j.ijcard.2011.07.089

11. Campos FA, Magalhães ML, Moreira HT, Pavão RB, Lima Filho MO, Lago IM, et al. Chagas cardiomyopathy as the etiology of suspected coronary microvascular disease. a comparison study with suspected coronary microvascular disease of other etiologies. Arq Bras Cardiol. 2020;115(6):1094-101. doi: 10.36660/abc.20200381

12. Marin-Neto JA, Simões MV, Rassi Junior A. Pathogenesis of chronic Chagas cardiomyopathy: the role of coronary microvascular derangements. Rev Soc Bras Med Trop. 2013;46(5):536-41. doi: 10.1590/0037-8682-0028-2013

13. Oliveira JS, Mello De Oliveira JA, Frederigue U Jr, Lima Filho EC. Apical aneurysm of Chagas's heart disease. Br Heart J. 1981;46(4):432-7. doi: 10.1136/hrt.46.4.432

14. Volpe GJ, Moreira HT, Trad HS, Wu KC, Braggion-Santos MF, Santos MK, et al. Left ventricular scar and prognosis in chronic Chagas cardiomyopathy. J Am Coll Cardiol. 2018;72(21):2567-76. doi: 10.1016/j.jacc.2018.09.035

15. Senra T, Ianni BM, Costa AC, Mady C, Martinelli-Filho M, Kalil-Filho R, et al. Long-term prognostic value of myocardial fibrosis in patients With Chagas cardiomyopathy. J Am Coll Cardiol. 2018;72(21):2577-87. doi: 10.1016/j.jacc.2018.08.2195

16. Assuncao AN Jr., Jerosch-Herold M, Melo RL, Mauricio AV, Rocha L, Torreao JA, et al. Chagas' heart disease: gender differences in myocardial damage assessed by cardiovascular magnetic resonance. J Cardiovasc Magn Reson. 2016;18(1):88.

17. Dias Junior JO, da Costa Rocha MO, de Souza AC, Kreuser LJ, de Souza Dias LA, Tan TC, et al. Assessment of the source of ischemic cerebrovascular events in patients with Chagas disease. Int J Cardiol. 2014;176(3):1352-4.

18. Arteaga-Fernández E, Barretto AC, Ianni BM, Mady C, Lopes EA, Vianna Cde B, et al. Trombose cardíaca e embolia em pacientes falecidos de cardiopatia chagásica crônica [Cardiac thrombosis and embolism in patients having died of chronic Chagas cardiopathy]. Arq Bras Cardiol. 1989;52(4):189-92. Portuguese. PMID: 2604564.

19. Montanaro VV, da Silva CM, de Viana Santos CV, Lima MI, Negrão EM, de Freitas GR. Ischemic stroke classification and risk of embolism in patients with Chagas disease. J Neurol. 2016 Dec;263(12):2411-5. doi: 10.1007/s00415-016-8275-0

20. Kumar R, Kline IK, Abelmann WH. Experimental Trypanosoma cruzi myocarditis: relative effects upon the right and left ventricles. Am J Pathol. 1969;57(1):31-48. PMID: 4242332.

21. Andrade ZA, Andrade SG, Sadigursky M, Lima JA. [Experimental Chagas disease in dogs. Morphologic and electrocardiographic relations in the acute phase of the infection]. Arq Bras Cardiol. 1980;35(6):485-90. Portuguese. doi: https://doi.org/10.1590/0074-02760140208

22. Jelicks LA, Shirani J, Wittner M, Chandra M, Weiss LM, Factor SM, et al. Application of cardiac gated magnetic resonance imaging in murine Chagas' disease. Am J Trop Med Hyg. 1999;61(2):207-14. doi: 10.4269/ajtmh.1999.61.207

23. Rossi MA. Comparison of Chagas' heart disease to arrhythmogenic right ventricular cardiomyopathy. Am Heart J. 1995;129(3):626-9. doi: 10.1016/0002-8703(95)90297-x

24. Dias E, Laranja FS, Miranda A, Nobrega G. Chagas' disease; a clinical, epidemiologic, and pathologic study. Circulation. 1956;14(6):1035-60. doi: 10.1161/01.cir.14.6.1035

25. Marin-Neto JA, Marzullo P, Sousa AC, Marcassa C, Maciel BC, Iazigi N, et al. Radionuclide angiographic evidence for early predominant right ventricular involvement in patients with Chagas' disease. Can J Cardiol. 1988;4(5):231-6.

26. Marin-Neto JA, Bromberg-Marin G, Pazin-Filho A, Simões MV, Maciel BC. Cardiac autonomic impairment and early myocardial damage involving the right ventricle are independent phenomena in Chagas' disease. Int J Cardiol. 1998;65(3):261-9. doi: 10.1016/s0167-5273(98)00132-6

27. Issa VS, Ayub-Ferreira SM, Schroyens M, Chizzola PR, Soares PR, Lage SH, et al. The course of patients with Chagas heart disease during episodes of decompensated heart failure. ESC Heart Fail. 2021;8(2):1460-71. doi: 10.1002/ehf2.13232

28. Romano MM, Moreira HT, Schmidt A, Maciel BC, Marin-Neto JA. Imaging diagnosis of right ventricle involvement in Chagas cardiomyopathy. Biomed Res Int. 2017;2017:3820191. doi: 10.1155/2017/3820191

29. Surkova E, Muraru D, Iliceto S, Badano LP. The use of multimodality cardiovascular imaging to assess right ventricular size and function. Int J Cardiol. 2016;214:54-69. doi: 10.1016/j.ijcard.2016.03.074

30. Moreira HT, Volpe GJ, Marin-Neto JA, Ambale-Venkatesh B, Nwabuo CC, Trad HS, et al. Evaluation of right ventricular systolic function in Chagas disease using cardiac magnetic resonance imaging. Circ Cardiovasc Imaging. 2017;10(3):e005571. doi: 10.1161/CIRCIMAGING.116.005571

31. Marin-Neto JA, Andrade ZA. Por que é usualmente predominate a insuficiência cardíaca direita na doença de Chagas? [Why is there predominance of right heart failure in Chagas' disease?]. Arq Bras Cardiol. 1991;57(3):181-3. Portuguese. PMID: 1824192.

32. Noya-Rabelo MM, Macedo CT, Larocca T, Machado A, Pacheco T, Torreão J, et al. The presence and extension of myocardial fibrosis in the undetermined form of Chagas' disease: a study using magnetic resonance. Arq Bras Cardiol. 2018;110(2):124-31. doi: 10.5935/abc.20180016

33. Tassi EM, Continentino MA, Nascimento EM, Pereira Bde B, Pedrosa RC. Relationship between fibrosis and ventricular arrhythmias in Chagas heart disease without ventricular dysfunction. Arq Bras Cardiol. 2014;102(5):456-64. doi: 10.5935/abc.20140052

34. Torreão JA, Ianni BM, Mady C, Naia E, Rassi CH, Nomura C, et al. Myocardial tissue characterization in Chagas' heart disease by cardiovascular magnetic resonance. J Cardiovasc Magn Reson. 2015;17:97. doi: 10.1186/s12968-015-0200-7

35. Lee-Felker SA, Thomas M, Felker ER, Traina M, Salih M, Hernandez S, et al. Value of cardiac MRI for evaluation of chronic Chagas disease cardiomyopathy. Clin Radiol. 2016;71(6):618.e1-7. doi: 10.1016/j.crad.2016.02.015

36. Uellendahl M, Siqueira ME, Calado EB, Kalil-Filho R, Sobral D, Ribeiro C, et al. Cardiac magnetic resonance-verified myocardial fibrosis in Chagas disease: clinical correlates and risk stratification. Arq Bras Cardiol. 2016;107(5):460-6. doi: 10.5935/abc.20160168

37. Melendez-Ramirez G, Soto ME, Velasquez Alvarez LC, Meave A, Juarez-Orozco LE, Guarner-Lans V, et al. Comparison of the amount and patterns of late enhancement in Chagas disease according to the presence and type of ventricular tachycardia. J Cardiovasc Electrophysiol. 2019;30(9):1517-25. doi: 10.1111/jce.14015

38. Pinheiro MV, Moll-Bernardes RJ, Camargo GC, Siqueira FP, Azevedo CF, Holanda MT, et al. Associations between cardiac magnetic resonance T1 mapping parameters and ventricular arrhythmia in patients with Chagas disease. Am J Trop Med Hyg. 2020;103(2):745-51. doi: 10.4269/ajtmh.20-0122

39. Romano MM, Moreira HT, Marin-Neto JA, Baccelli PE, Alenezi F, Klem I, et al. Early impairment of myocardial deformation assessed by regional speckle-tracking echocardiography in the indeterminate form of Chagas disease without fibrosis detected by cardiac magnetic resonance. PLoS Negl Trop Dis. 2020;14(11):e0008795. doi: 10.1371/journal.pntd.0008795

40. Santos JB, Gottlieb I, Tassi EM, Camargo GC, Atié J, Xavier SS, et al. Cardiac fibrosis and changes in left ventricle function in patients with chronic chagas heart disease. Arq Bras Cardiol. 2021;117(6):1081-90. doi: 10.36660/abc.20200597

41. Nunes MC, Beaton A, Acquatella H, Bern C, Bolger AF, Echeverría LE, et al.; American Heart Association Rheumatic Fever, Endocarditis and Kawasaki Disease Committee of the Council on Cardiovascular Disease in the Young; Council on Cardiovascular and Stroke Nursing; and Stroke Council. Chagas cardiomyopathy: an update of current clinical knowledge and management: a scientific statement from the American Heart Association. Circulation. 2018;138(12):e169-e209. doi: 10.1161/CIR.0000000000000599

42. Sternick EB, Martinelli M, Sampaio R, Gerken LM, Teixeira RA, Scarpelli R, et al. Sudden cardiac death in patients with Chagas heart disease and preserved left ventricular function. J Cardiovasc Electrophysiol. 2006;17(1):113-6. doi: https://doi.org/10.1590/S0037-86822011005000020

43. Sarabanda AV, Sosa E, Simões MV, Figueiredo GL, Pintya AO, Marin-Neto JA. Ventricular tachycardia in Chagas' disease: a comparison of clinical, angiographic, electrophysiologic and myocardial perfusion disturbances between patients presenting with either sustained or nonsustained forms. Int J Cardiol. 2005;102(1):9-19. doi: 10.1016/j.ijcard.2004.03.087

44. Miranda CH, Figueiredo AB, Maciel BC, Marin-Neto JA, Simões MV. Sustained ventricular tachycardia is associated with regional myocardial sympathetic denervation assessed with 123I-metaiodobenzylguanidine in chronic Chagas cardiomyopathy. J Nucl Med. 2011;52(4):504-10. doi: 10.2967/jnumed.110.082032

45. Mello RP, Szarf G, Schvartzman PR, Nakano EM, Espinosa MM, Szejnfeld D, et al. Delayed enhancement cardiac magnetic resonance imaging can identify the risk for ventricular tachycardia in chronic Chagas' heart disease. Arq Bras Cardiol. 2012;98(5):421-30. English, Portuguese. doi: 10.1590/s0066-782x2012005000031

46. Barizon GC, Simões MV, Schmidt A, Gadioli LP, Murta Junior LO. Relationship between microvascular changes, autonomic denervation, and myocardial fibrosis in Chagas cardiomyopathy: Evaluation by MRI and SPECT imaging. J Nucl Cardiol. 2020;27(2):434-44. doi: 10.1007/s12350-018-1290-z

47. Romero J, Velasco A, Pisani CF, Alviz I, Briceno D, Díaz JC, et al. Advanced therapies for ventricular arrhythmias in patients with chagasic cardiomyopathy: JACC state-of-the-art review. J Am Coll Cardiol. 2021;77(9):1225-42. doi: 10.1016/j.jacc.2020.12.056

48. Sosa E, Scanavacca M, d'Avila A, Pilleggi F. A new technique to perform epicardial mapping in the electrophysiology laboratory. J Cardiovasc Electrophysiol. 1996;7(6):531-6. doi: 10.1111/j.1540-8167.1996.tb00559.x

49. Pisani CF, Romero J, Lara S, Hardy C, Chokr M, Sacilotto L, et al. Efficacy and safety of combined endocardial/epicardial catheter ablation for ventricular tachycardia in Chagas disease: A randomized controlled study. Heart Rhythm. 2020;17(9):1510-8. doi: 10.1016/j.hrthm.2020.02.009

50. Rassi A Jr, Rassi A, Rassi SG. Predictors of mortality in chronic Chagas disease: a systematic review of observational studies. Circulation. 2007;115(9):1101-8. doi: 10.1161/CIRCULATIONAHA.106.627265

51. Rassi A Jr, Rassi A, Little WC, Xavier SS, Rassi SG, Rassi AG, et al. Development and validation of a risk score for predicting death in Chagas' heart disease. N

Engl J Med. 2006;355(8):799-808. doi: 10.1056/NEJMoa053241

52. Rassi A Jr, Rassi A. Rassi Score: Another external validation with high performance in patients with Chagas cardiomyopathy. J Am Coll Cardiol. 2019;73(13):1734-5. doi: 10.1016/j.jacc.2018.12.079

53. Rassi A Jr, Marin JA Neto, Rassi A. Chronic Chagas cardiomyopathy: a review of the main pathogenic mechanisms and the efficacy of aetiological treatment following the benznidazole evaluation for interrupting Trypanosomiasis (BENEFIT) trial. Mem Inst Oswaldo Cruz. 2017;112(3):224-35. doi: 10.1590/0074-02760160334

54. Sousa AS, Derenne ME, Hasslocher-Moreno AM, Xavier SS, Gottlieb I. Myocardial edema without fibrosis by magnetic resonance T2 mapping in acute Chagas' myocarditis. Arq Bras Cardiol. 2017;109(4):378-9. doi: 10.5935/abc.20170113

Libman-Sacks endocarditis in a male patient with systemic lupus erythematosus

Endocardite de Libman-Sacks em Paciente Masculino com Lúpus Eritematoso Sistêmico

Álvaro Augusto Vedana Filho[1], Vivien Ritchie Bittencourt[1], Thaíssa Antunes Mattar Valente[1], Fernando Silva Botelho[1], Marco Stephan Lofrano Alves[1]

Hospital de Clinicas Complex of the Federal University of Paraná[1], Curitiba, Paraná, Brazil.

Introduction

Libman-Sacks endocarditis (LSE), also known as marantic or verrucous endocarditis, is a form of non-bacterial thrombotic endocarditis (NBTE) that involves the presence of sterile vegetations in the heart valves. These vegetations may be associated with malignancy, systemic lupus erythematosus (SLE), or antiphospholipid syndrome (APS), and although they are more commonly found in the mitral and aortic valves, other valves may be involved. Diagnosis requires high clinical suspicion when evaluating specific populations.[1]

Clinical case

A young 21-year-old illicit drug user diagnosed with SLE was admitted to the emergency unit with continuous non-traumatic epistaxis over the previous six hours. The patient reported episodes of melena and the onset of macular, erythematous, diffuse lesions on the soles of the feet over the previous two weeks (Figure 1). The patient denied fever or chills associated with the condition. Physical examination identified tachycardia (heart rate, 115 beats per minute) and cardiac auscultation with a regular rhythm, normal heart sounds, and a 3+/6+ systolic murmur in the mitral focus radiating to the axilla. Admission tests suggested active SLE and showed reduced complements C3 and C4; thrombocytopenia (2,000 U/μL); anti-double stranded DNA, 1:640; and hemoglobin, 8.8 mg/dL. Exams collected 10 months earlier showed negative lupus anticoagulant and positive anticardiolipin antibodies at low titers. Pulse therapy with methylprednisolone and intravenous human immunoglobulin was indicated and started by the rheumatology team. Transthoracic echocardiography was also

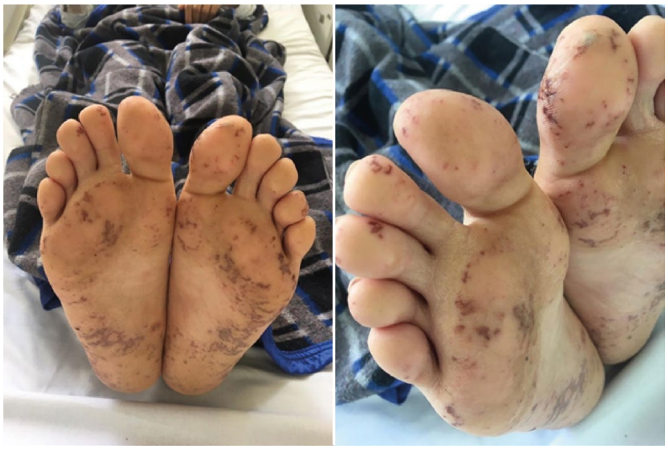

Figure 1 – *Macular, erythematous, and painless lesions with a two-week progression compatible with an embolic phenomenon. Description similar to Janeway lesions in infective endocarditis.*

Keywords

Endocarditis; Echocardiogram; Lupus Erythematosus, Systemic.

Mailing Address: Marco Stephan Lofrano Alves •
Rua General Carneiro, 181, Alto da Glória – CEP 80060-900 – Curitiba, PR, Brazil.
E-mail: mslalves@hc.ufpr.br; mslalves@hotmail.com
Manuscript received 5/4/2021; revised 11/10/2021; accepted 12/2/2021

DOI: 10.47593/2675-312X/20223501eabc224

requested to assess the cardiac involvement.

Transthoracic echocardiography showed an enlarged left ventricle with eccentric hypertrophy and a preserved ejection fraction. The mitral valve with diffusely thickened leaflets and amorphous isoechoic vegetation with irregular surface adhered to the ventricular face of the posterior leaflet (Video 1) measured 1.0 × 1.2 cm (Figure 2), restricting its mobility and causing important eccentric reflux (Video 2) directed to the posterior atrial wall. In addition, an enlarged left atrium was noted with a volume indexed by the body surface of 67 mL/m^2 and normal right chambers.

Due to the vegetation identified in the mitral valve, associated with the clinical context of the patient, the following were listed as possible differential diagnoses: 1) NBTE; and 2) infective endocarditis (IE). For better elucidation of the case, transesophageal echocardiography was requested and three blood cultures were collected. Empirical antibiotic therapy was not started due to a lack of evidence of infection.

Transesophageal echocardiography complemented the transthoracic examination by better delimiting the mitral valve lesions. Thickened leaflets were observed (Videos 3 and 4, Figure 3), with an echogenic sessile well-delimited image in the posterior portion of the valve annulus and ventricular face of the posterior leaflet (maximum thickness, 1.56 cm; Figure 4) encompassing all of their segments and part of the subvalvular apparatus, reducing the mobility of the posterior leaflet and causing moderate to severe reflux.

Blood cultures were negative after three days. Three other samples were collected that also showed negative bacterial growth results.

Considering complementary test findings, the patient's characteristics, and the absence of infectious evidence, the diagnosis of NBTE remained. The patient completed pulse therapy with methylprednisolone, underwent a course of intravenous immunoglobulin, and started therapy with cyclophosphamide.

Discussion

LSE is a rare condition, mostly found postmortem, with a prevalence of 0.9–1.6%. It commonly affects patients aged 40–80 years, but it can occur in any age group. NBTE is often

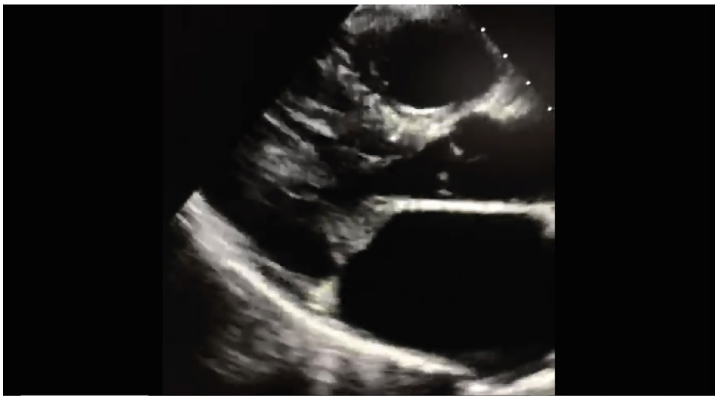

Video 1 – *Long-axis transthoracic echocardiography of the left parasternal window showing an amorphous image of the irregular surface on the ventricular surface of the posterior mitral valve leaflet without independent mobile echoes.*

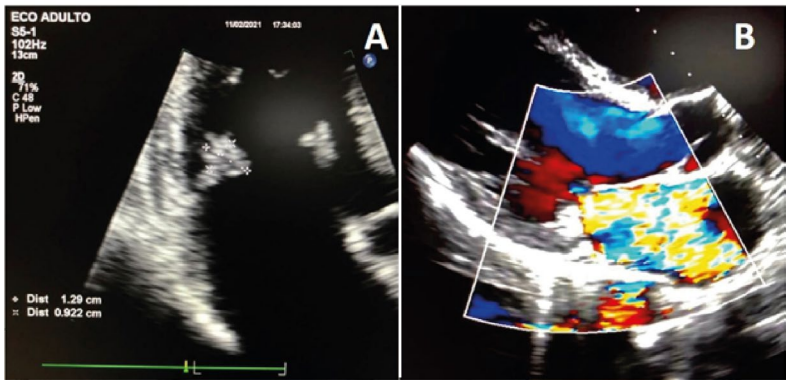

Figure 2 – *A: Apical window, three chambers showing amorphous image measuring 1.29 × 0.92 cm on the posterior mitral valve leaflet. B: Long-axis parasternal window showing important mitral regurgitation occupying almost the entire left atrium.*

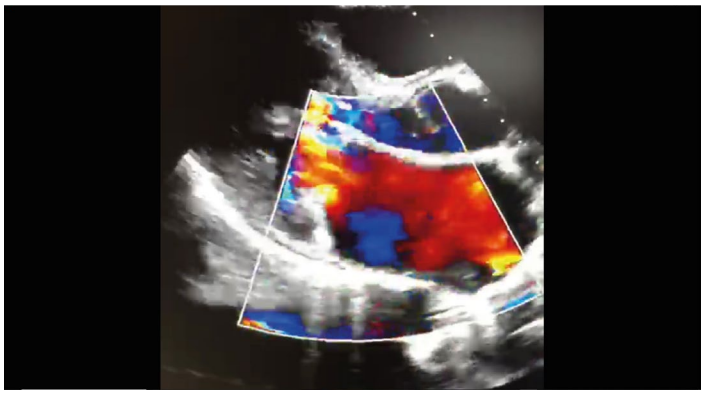

Video 2 – *Long-axis transthoracic echocardiography of the left parasternal window showing significant mitral valve reflux directed to the posterior wall of the left atrium.*

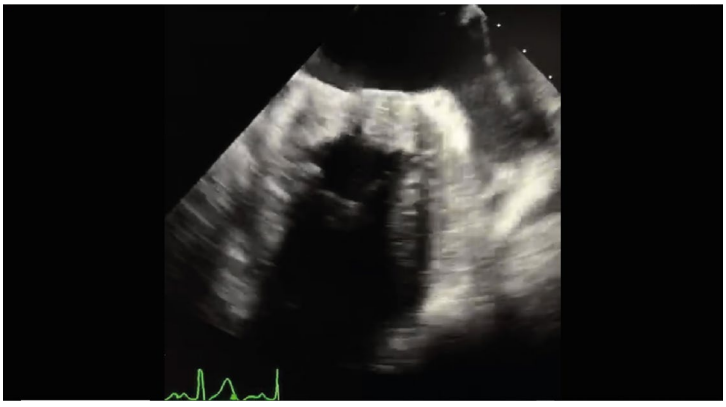

Video 3 – *Two-chamber transesophageal echocardiography (approximately 90º) demonstrating posterior mitral valve leaflet thickening.*

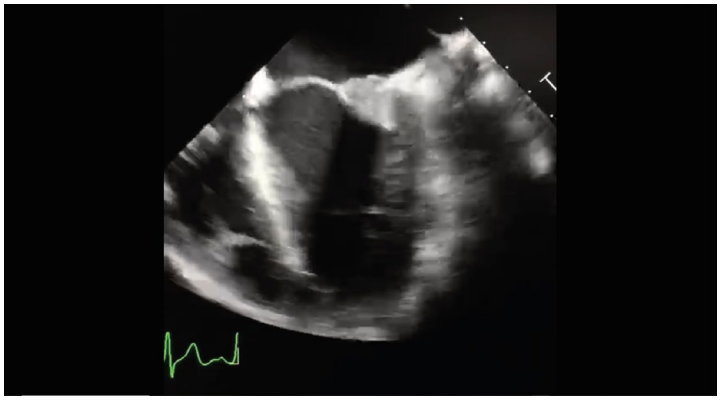

Video 4 – *Four-chamber transesophageal echocardiography (approximately 0º) showing a homogeneous echogenic, sessile, well-delimited image on the ventricular face of the posterior leaflet.*

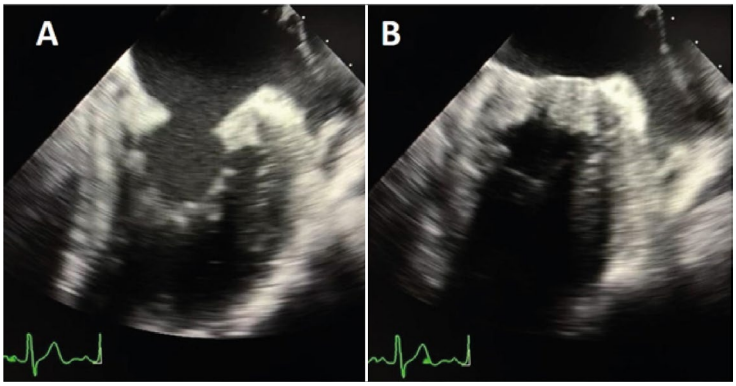

Figure 3 – *Two-chamber transesophageal echocardiography at 90º demonstrating diffuse thickening of mitral valve leaflets in diastole (A) and systole (B).*

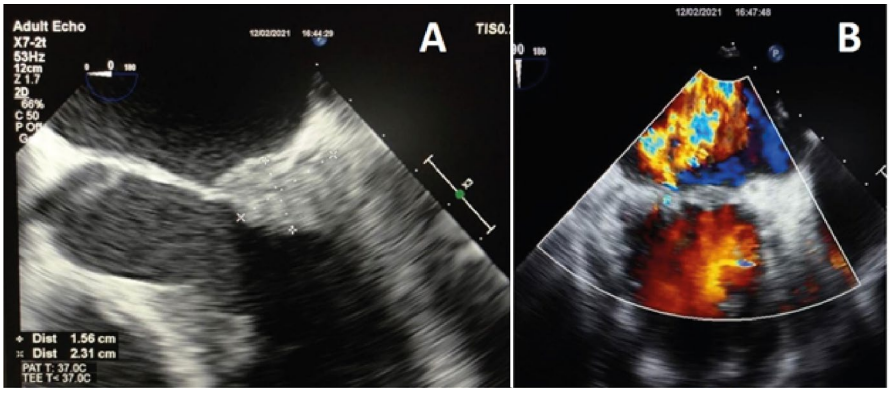

Figure 4 – *Transesophageal echocardiography A: four-chamber view at 0º showing a sessile image in the posterior mitral valve leaflet measuring 1.56 × 2.31 cm. B: two-chamber view at 90º demonstrating moderate to severe reflux toward the posterior wall of the left atrium.*

associated with hypercoagulable states such as malignant neoplasms, SLE, and APS. It is correlated with disease activity and duration and its prevalence increases in the overlap of these pathologies.[1] Studies do not show a sex predilection; however, SLE and APS, causes associated with LSE, occur five- to nine-fold more often in women of childbearing age than in men and are more prevalent in Black and Hispanic women.[2,3]

Patients are usually asymptomatic; findings are often incidental in the investigations of other cardiac conditions by imaging or on postmortem examination. The most common clinical presentations are secondary to valve embolism, such as stroke, transient ischemic attacks, or symptoms of peripheral embolization in the lower limbs. They also include symptoms related to the activity of underlying diseases, such as fever, malar rash, renal, hematological, or immunological changes, among others.[1]

High clinical suspicion is required for the diagnosis of NBTE. No laboratory tests can confirm this diagnosis. Patients with suspected NBTE should be screened for blood cell count, metabolic profile, and blood cultures for the differentiation from other etiologies such as IE. Hypercoagulability should be investigated, including lupus anticoagulant and antiphospholipid antibodies. Three blood culture samples should be tested before starting any empirical antibiotic therapy. The absence of typical or atypical endocarditis-causing agents may strengthen the NBTE suspicion.[1]

However, the primary screening test for LSE is echocardiography. Transesophageal echocardiography has greater sensitivity and specificity than transthoracic echocardiography. Irregular borders, heterogeneous echogenicity, and the absence of independent mobile echoes are characteristic of the masses (verrucous vegetation) found in the heart valves and endocardium. These are usually small sessile masses, but they can be larger than 10 mm. The basal and middle portion of the mitral and aortic valves are the most affected. Diffuse or focal thickening of the mitral and aortic valves may be seen. The involved valves may present regurgitation.[1] Vegetations are more frequent on the left side, with two thirds of cases involving the mitral valve, mainly on the ventricular face, and up to a quarter involving the aortic valve and less commonly both valves. Echocardiography cannot distinguish vegetations from thrombi but can provide

diagnostic clues for lesion characterization.[1]

NBTE treatment is based on expert positioning and small observational studies. Underlying disease control, anticoagulation in patients with major embolic phenomena, and serial echocardiograms are recommended for monitoring valve lesions. Surgical indications are the same as for IE (i.e., heart failure, acute valve rupture), but reports suggest that recurrent embolization prevention is the most common indication for surgery. In contrast to IE, which requires complete removal of the infected tissue, valve preservation may be possible in some NBTE cases.[1]

Authors' contributions

Research conception and design: Vedana Filho AA, Alves MSL; Data collection: Vedana Filho AA, Mattar TA; Manuscript writing: Vedana Filho AA, Bittencourt VR; Critical review of the manuscript: Alves MSL, Botelho FS.

Conflict of interest

The authors have declared that they have no conflict of interest.

References

1. Ibrahim AM, Siddique MS. Libman Sacks Endocarditis. 2021 Sep 8. In: StatPearls [Internet]. Treasure Island (FL): StatPearls Publishing; 2022 Jan–. PMID: 30422459.

2. Zuily S, Huttin O, Mohamed S, Marie PY, Selton-Suty C, Wahl D. Valvular heart disease in antiphospholipid syndrome. Curr Rheumatol Rep. 2013;15(4):320. doi: https://doi.org/10.1007/s11926-013-0320-8

3. Lenz CJ, Mankad R, Klarich K, Kurmann R, McBane RD. Antiphospholipid syndrome and the relationship between laboratory assay positivity and prevalence of non-bacterial thrombotic endocarditis: A retrospective cohort study. J Thromb Haemost. 2020;18(6):1408-14. doi: https://doi.org/10.1111/jth.14798.

Cardiac Fibroma: Long-Term Follow-up by Cardiac Magnetic Resonance

Fibroma Cardíaco: Seguimento a Longo Prazo por Ressonância Magnética Cardíaca

Fernanda Sayuri Oshiro[1], Raul Serra Valério[1], Alfredo Augusto Eyer Rodrigues[1], Gilberto Szarf[1], Marly Uellendahl[1], Maria Eduarda Menezes de Siqueira[1]

Federal University of São Paulo[1], São Paulo, Brazil

Abstract

Background: Primary cardiac neoplasms are rare, and a correct diagnosis is essential to planning the most appropriate treatment.

Objective: To demonstrate the role of cardiac magnetic resonance imaging (CMR) in the assessment, diagnosis, and follow-up of cardiac fibroma.

Case report: Female 21-year-old patient with a myocardial mass detected on echocardiogram. CMR confirmed a diagnosis of cardiac fibroma. The patient chose to be followed up, and her condition remained stable after six years.

Discussion: Cardiac fibromas are the second most common neoplasm in children and young people. On CMR, it is characterized by intense and homogeneous delayed enhancement. CMR plays an important role in the assessment of cardiac masses.

Introduction

Primary cardiac neoplasms are rare, with an estimated prevalence of 0.001–0.03% in autopsy studies, and may affect the endocardium, myocardium, and epicardium.[1] Secondary tumors are 20- to 40-fold more frequent than primary tumors. The diagnosis of cardiac tumors has increased in recent decades with complementary imaging methods in cardiology such as echocardiography, magnetic resonance, and tomography.[2]

More than 75% of primary tumors are benign[1]. Myxomas (about 50% of benign tumors), papillary fibroelastomas, and lipomas are the most common in adults, with rhabdomyoma and fibroma being the most common benign tumors in children.[2,3]

The clinical presentation varies and can mimic both cardiac and systemic diseases, which determines its inclusion as a differential diagnosis in different heart diseases. In general, the specific signs and symptoms of cardiac tumors are determined by their location in the heart rather than their histopathology.[2]

Keywords

Magnetic Resonance Imaging; Heart Neoplasms; Fibromas.

Mailing Address: Fernanda Sayuri Oshiro •
E-mail: fernanda_s_oshiro@hotmail.com
Manuscript received 10/14/2021; revised 11/16/2021; accepted 11/25/2021

DOI: 10.47593/2675-312X/20223501eabc263

Cardiac tumors are extremely rare; however, upon clinical suspicion, the correct diagnosis is essential to planning the most appropriate treatment and management. In this context, cardiac magnetic resonance imaging (CMR) plays an important role as a noninvasive test with high-resolution images of the heart that allows for tissue characterization of the tumor, size and location assessment, and correlation with other adjacent structures. Tissue characterization of cardiac masses is performed using T1 and T2[4] weighting techniques, fat suppression, perfusion, and delayed gadolinium enhancement, allowing the differentiation between malignant and benign tumors and sometimes indicating a suspected histological diagnosis.[1,3,5]

The objective of this report was to present the six-year follow-up of a patient referred to the Magnetic Resonance Service of the Federal University of São Paulo (*Universidade Federal de São Paulo*) for presenting a cardiac mass and demonstrate the role of CMR in its assessment, diagnosis, and follow-up.

Case report

A 21-year-old female student born in Macapá, AP, Brazil, and living in Diadema, SP, Brazil, sought medical care in 2013 for palpitations and dyspnea on great exertion for which cardiac investigations were initiated. Initial electrocardiography and 24-hour Holter monitoring showed no significant changes. Echocardiography showed the presence of a fixed mass affecting the inferolateral and anterolateral regions from the base to the apex of the left ventricle, with regular contours, hyperechoic, heterogeneous, with calcium spots inside measuring 5.5 × 4.4 cm in cross-section.

The patient was referred for CMR for better characterization of the mass: We noted the presence of an intramyocardial mass with regular contours affecting the lateral wall and part of the anterior and inferior walls of the left ventricle measuring 7.4 × 4.0 cm in four-chamber view, hypointense in steady-state free precession sequences and T2-weighted (Figure 1) and isointense on T1-weighted sequences (Figure 2). We also noted the absence of perfusion in the first gadolinium passage (Video 1) and the presence of intense and homogeneous delayed enhancement (Figure 3). No signs of compromised left ventricular global systolic function were noted on CMR (Video 2).

Cardiac fibroma was hypothesized. The patient was followed up for six years, with no clinical worsening and no signs of changes in the cardiac mass characteristics or dimensions or functional impairment of the left ventricle on CMR. Conservative treatment and follow-up were chosen due to the patient's stable condition.

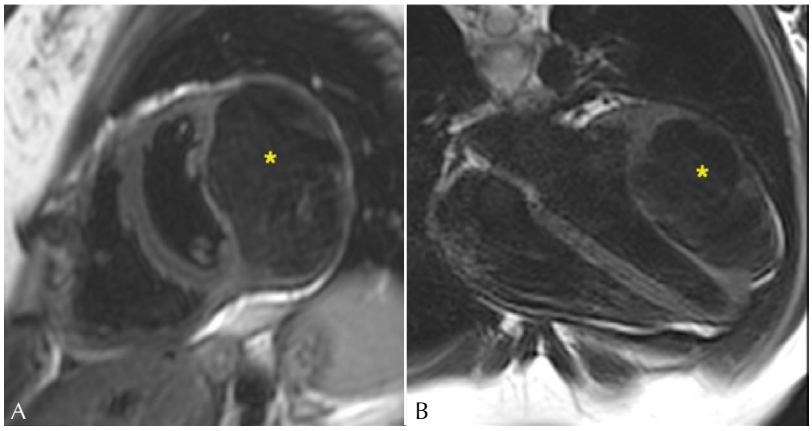

Figure 1 – *Short-axis (A) and four-chamber (B) section showing a hypointense intramyocardial mass (*) on T2-weighted cardiac magnetic resonance. Follow-up images from 2016 (A) and 2020 (B).*

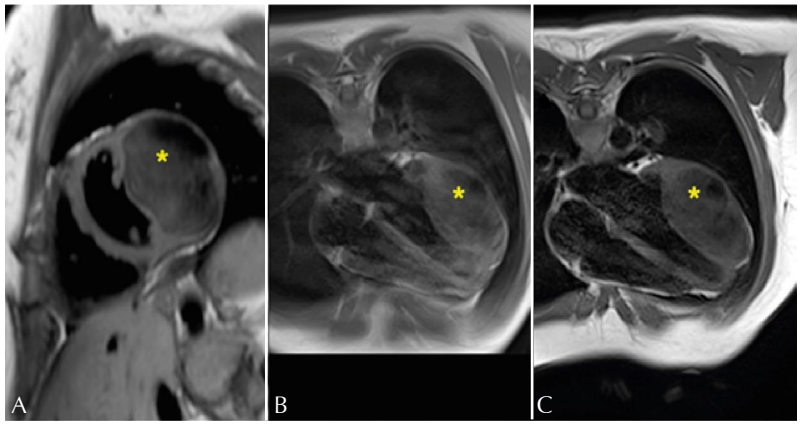

Figure 2 – *Short-axis (A) and four-chamber (B-C) section showing intramyocardial mass (*) isointensity on T1-weighted cardiac magnetic resonance. Follow-up images from 2016 (A), 2018 (B), and 2020 (C).*

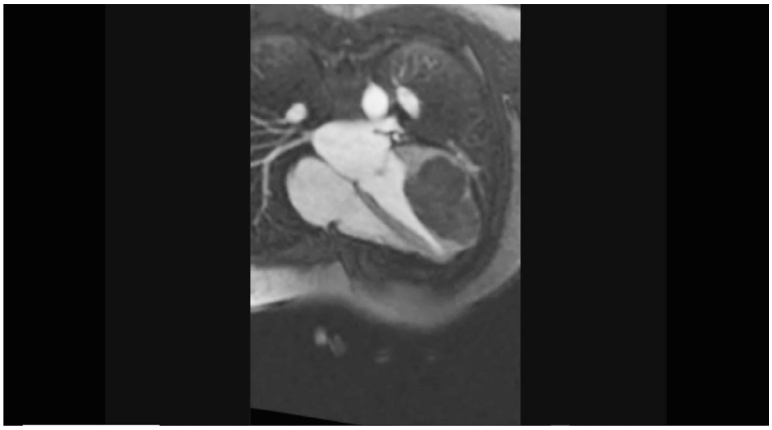

Video 1 – *Myocardial four-chamber perfusion confirming the absence of myocardial perfusion in the first gadolinium passage. Follow-up image from 2020.*

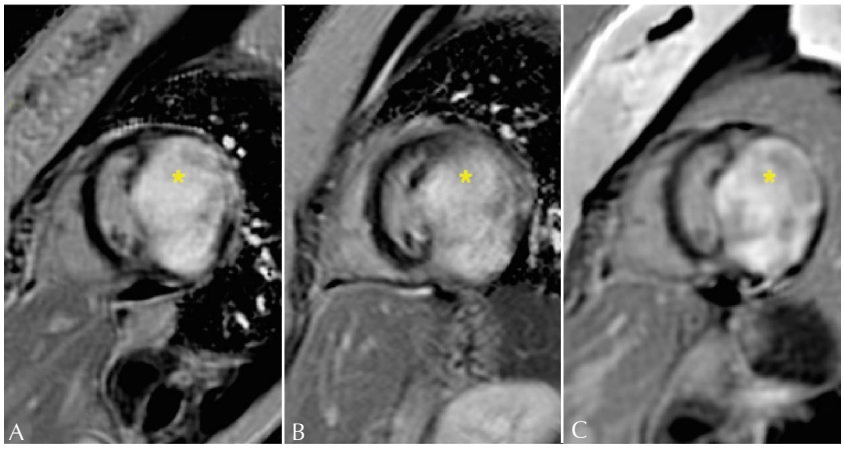

Figure 3 – *Short-axis section of the left ventricle showing an intramyocardial mass (*) with an intense and homogeneous pattern after delayed gadolinium enhancement. Follow-up images from 2014 (A), 2017 (B), and 2018 (C).*

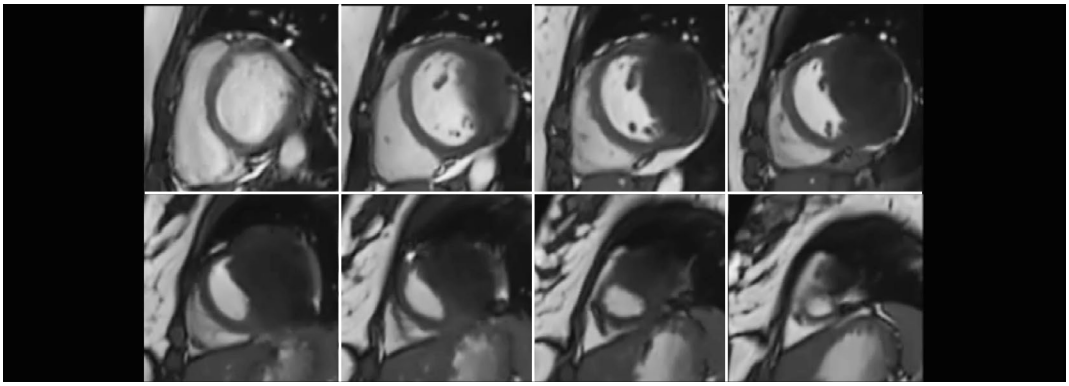

Video 2 – *Short-axis cine magnetic resonance imaging of the left ventricle showing an intramyocardial mass not compromising ventricular function (2020).*

Discussion

Primary cardiac neoplasms are extremely rare, have different clinical and histological presentations, and require a high index of clinical suspicion.[2]

Cardiac fibromas, the second most common neoplasm in children and young people, also affect adults. They originate in the myocardium and, more commonly, present as a single well-defined lesion that can become quite voluminous and does not regress spontaneously.[1] It occurs more frequently in the free wall of the left ventricle, interventricular septum, and the free wall of the right ventricle (in descending order).[6]

The described symptoms of left ventricular and interventricular septal tumors are dyspnea, fatigue, syncope, atypical chest pain, conduction disturbances, ventricular arrhythmias, and sudden death.[1]

On CMR, the lesion is characterized by isointensity or slight hyperintensity on T1-weighted sequences in relation to the myocardium and hypointensity on T2-weighted sequences. It presents no perfusion at rest as it is avascular; in delayed gadolinium enhancement sequences, fibromas present intense and homogeneous enhancement related to contrast medium extravasation and retention in the large extracellular space that permeates the fibrotic tissue of the tumor. The lesion may have a low-signal central component associated with calcifications.[1,6-8]

Symptomatic tumors must be completely resected. Very large tumors may require heart transplantation.[9,10]

In conclusion, CMR plays an important role in the assessment of cardiac masses, contributing to a more accurate noninvasive diagnosis and therapeutic planning and enabling safe clinical follow-up with good reproducibility.[1,5]

Authors' contribution

Data collection: Oshiro FS, Rodrigues AAE, Valério RS; Data analysis and interpretation: Oshiro FS, Rodrigues AAE,

Valério RS; Manuscript writing: Oshiro FS; Critical review of the manuscript for intellectual content: Szarf G, Uellendahl M, Siqueira MEM.

Conflict of interest

The authors have declared that they have no conflict of interest.

References

1. Braggion-Santos MF, Koenigkam-Santos M, Teixeira SR, Volpe GJ, Trad HS, Schmidt A. Avaliação por ressonância magnética de massas cardíacas. Arq Bras Cardiol. 2013;101(3):263-72. doi: https://doi.org/10.5935/abc.20130150
2. Fernandes F, Soufen HN, Ianni BM, Arteaga E, Ramires FJ, Mady C. Neoplasias primárias do coração. Apresentação Clínica e Histológica de 50 Casos. Arq Bras Cardiol. 2001;76(3):231-4.
3. Cordinhã C, Pereira A, Silva PV, Dionísio T, Martins P, Sousa G, et al. Tumor cardíaco em criança assintomática: um diagnóstico acidental. Revista Portuguesa de Cardiologia. 2011; 30(10):795-7. doi: https://doi.org/10.1016/S2174-2049(11)70028-9
4. Mousavi N, Cheezum MK, Aghayev A, Padera R, Vita T, Steigner M, et al. Assessment of Cardiac Masses by Cardiac Magnetic Resonance Imaging: Histological Correlation and Clinical Outcomes. J Am Heart Assoc. 2019; 8(1):e007829.
5. Sara L, Szarf G, Tachibana A, Shiozaki AA, Villa AV, Oliveira AC, et al. II Diretriz de Ressonância Magnética e Tomografia Computadorizada Cardiovascular da Sociedade Brasileira de Cardiologia e do Colégio Brasileiro de Radiologia. Arq Bras Cardiol. 2014;103(6):1-86. doi: https://doi.org/10.5935/abc.2014S006
6. Grunau GL, Leipsic JA, Sellers SL, Seidman MA. Cardiac fibroma in an adult airp best cases in radiologic-pathologic correlation. Radiographics. 2018;38(4):1022-2026. doi: https://doi.org/10.1148/rg.2018170205
7. Schuster A, Nagel E. Comprehensive assessment of myocardial fibroma by cardiovascular magnetic resonance imaging. Rev Esp Cardiol (Engl Ed). 2013;66(10):820. doi: https://doi.org/10.1016/j.rec.2012.01.001
8. Motwani M, Kidambi A, Herzog BA, Uddin A, Greenwood JP, Plein S. MR imaging of cardiac tumors and masses: a review of methods and clinical applications. Radiology. 2013;268(1):26-43. doi: https://doi.org/10.1148/radiol.13121239
9. Gaasch WH, Salm TJV. Cardiac Tumors. UpToDate. 2020 (acesso em 28/05/2020). Available from URL: https://www.uptodate.com/contents/cardiac-tumors?search=cardiac%20tumor&source=search_result&selectedTitle=1~150&usage_type=default&display_rank=1
10. Miana AA, Passos PH, Whitaker JF, Loures JB, Pimentel RC, Muniz AJ, et al. Tumores cardíacos: 10 anos de experiência. Rev Bras Cir Cardiovasc. 1997;12(1):46-51. doi: https://doi.org/10.1590/S0102-76381997000100008.

Case Report

Role of Transthoracic Echocardiography in the Diagnosis of Double Aortic Arch

Papel da Ecocardiografia Transtorácica no Diagnóstico de Duplo Arco Aórtico

Guilherme Gomes de Souza[1], Adriana Furletti Machado Guimarães[1], Ricardo Wang[1], Sandra Regina Tolentino Castilho[1], Henrique de Assis Fonseca Tonelli[1], Fátima Derlene da Rocha Araújo[1]

Hospital das Clínicas of the Federal University of Minas Gerais[1], Belo Horizonte, Minas Gerais, Brazil.

Introduction

Double aortic arch is the main cause of vascular ring in cardiovascular surgical case series records. This rare anomaly, caused by the non-involution of one of the embryonic aortic arches, is a challenge for the pediatric echocardiographer, often requiring other imaging methods such as computed tomography or cardiac magnetic resonance. This case report aimed to systematize echocardiographic findings to help diagnose double aortic arch.

Case report

A full-term newborn was born vaginally at 38 weeks' gestation with a birth weight of 3,390 g, and an APGAR 9/10. In the first hours of life, the patient presented respiratory discomfort associated with stridor, wheezing, and increased expiratory time requiring orotracheal intubation and high mechanical ventilation parameters. Chest X-ray showed signs of pulmonary hyperinflation.

The mother reported home contact with a confirmed case of severe acute respiratory syndrome coronavirus 2 approximately 15 days before delivery. A cardiac evaluation was requested due to the possibility of pediatric multisystem inflammatory syndrome, but this was not confirmed later. A cardiovascular system examination detected no changes.

Echocardiography showed coronary artery diameters within the upper limit of normal and an echogenic focus on the left coronary artery wall, preserved cardiac function, and no signs of significant pulmonary hypertension. An aortic arch to the left was visualized in longitudinal suprasternal section with the probe index pointed at 1 o'clock with the emergence of two vessels. Directing the probe index to 11 o'clock revealed another aortic arch of equal diameter with the emergence of two vessels. A double aortic arch forming a complete vascular ring was suggested.

Chest computed tomography angiography confirmed the presence of a tracheoesophageal vascular ring resulting from a balanced double aortic arch associated with tracheal stenosis.

Keywords

Vascular ring, Echocardiography, Heart Defects, Congenital.

Mailing Address: Guilherme Gomes de Souza •
Avenida Professor Alfredo Balena, 110, Santa Efigênia. CEP: 30130-100 – Belo Horizonte, MG, Brazil.
E-mail: gomesguilherme22@gmail.com
Manuscript received 11/1/2021; revised 11/19/2021; accepted 11/25/2021

DOI: 10.47593/2675-312X/20223501eabc267

The patient underwent surgical resection of the right aortic arch and release of tracheal compression that postoperatively progressed with extubation failure. Bronchoscopy showed 80% obstruction of the tracheal lumen during inspiration due to tracheomalacia for which a tracheostomy was indicated.

Discussion

Vascular rings represent less than 1% of all congenital heart diseases.[1-4] Double aortic arch, the most frequent type of vascular ring,[4-7] is caused by an embryogenic anomaly with persistent right and left fourth embryonic aortic arches.[4,8,9]

These two patent arches resulted in a bifurcated ascending aorta, whose branches encircle the trachea and esophagus and posteriorly join to form a single descending aorta, forming a ring around these structures that can cause compression.[1,2,4,8] The right arch is often dominant (75%), with only 5% of cases presenting both arches of equal size as in the case reported here.[2,4]

In most cases, double aortic arch occurs as an isolated lesion, although it may be associated with other malformations such as tetralogy of Fallot, truncus arteriosus, and transposition of the great arteries.[4,6] In cases of significant tracheal and esophageal compression, symptoms such as stridor, dyspnea, respiratory failure, and feeding difficulties may be observed soon after birth.[1,3,4,6,8,9]

On the other hand, if compression is minimal, the vascular ring will be accidentally diagnosed in asymptomatic adults.[3,6,8,9]

Treatment is reserved for symptomatic cases and consists of surgical resection of one of the aortic arches, preferably the smaller one.[2-4,6,9] However, after tracheal compression release, respiratory symptoms may persist in a significant number of children (54%) due to tracheomalacia, as in the case described in this report.[2,9]

Although computed tomography and cardiac magnetic resonance imaging are essential for confirming the diagnosis and surgical planning, an initial assessment with transthoracic echocardiography allows the identification of the double arch as in the case reported. Furthermore, it has the advantages of low cost and not requiring the use of contrast, sedation, or radiation.[1,3,4,6-9]

This report presents a systematic approach to diagnosing double aortic arch through transthoracic echocardiography, focusing on its presentation pattern in the different echocardiographic windows. A careful assessment of the aortic arch with determination of its laterality and the branching pattern of brachiocephalic vessels is essential for identifying a double aortic arch by echocardiographic examination.[3,4]

Longitudinal parasternal window

Standard section - probe index pointing at 1 o'clock

Visualization of the aortic arch to the left without the normal branching pattern and origination of two vessels - the left subclavian and common carotid arteries; however, it is impossible to demonstrate the origin of the brachiocephalic trunk[1,3,4,6,7] (Figure 1A); and

Counterclockwise rotation of the transducer - probe index pointing at 11 o'clock

Visualization of a similar image with an aortic arch to the right and origination of the two vessels - the right subclavian and common carotid arteries[1,4,6,7] (Figure 1B).

Cross-sectional parasternal window

Probe index pointing at 3 o'clock and with cephalic tilt

Identification of the ascending aorta bifurcating into the left and right aortic arches, with blood flow visualization by color Doppler in both arches[1,3,4,6-10] (Figure 2A); and

Most superior ultrasound beam tilt

Possible simultaneous identification of the four brachiocephalic vessels, two in each arch. This image is characteristic of the double aortic arch - the "four-vessel sign"[2,4,9,10] (Figure 2B).

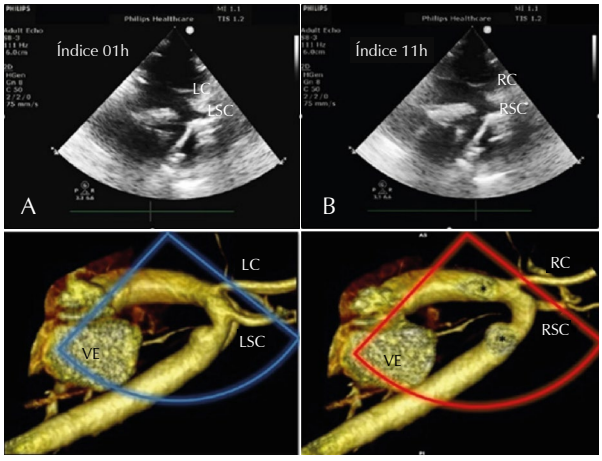

LC, left carotid; LSC, left subclavian; RC, right carotid; RSC, right subclavian.

Figure 1 – *Echocardiographic image in longitudinal suprasternal section with the probe index pointing at (A) 1 o'clock showing a left arch originating the left subclavian and common carotid arteries and at (B) 11 o'clock showing an aortic arch of the same caliber originating the right subclavian and common carotid arteries. Comparative image with CT angiography.*

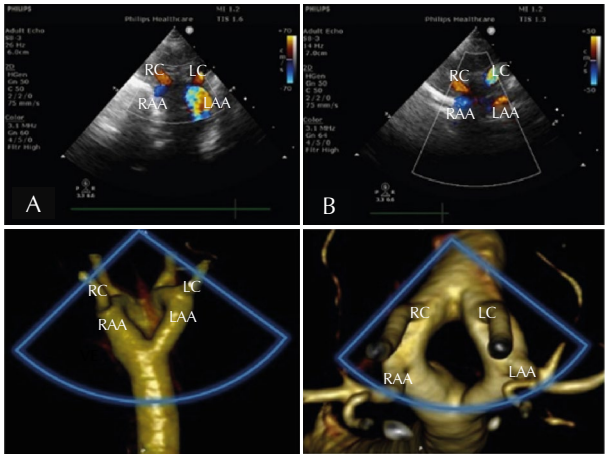

LAA, left aortic arch; LC, left carotid; LSC, left subclavian; RAA, right aortic arch; RC, right carotid; RSC, right subclavian.

Figure 2 – *Echocardiographic image in cross-sectional suprasternal section showing (A) the ascending aorta bifurcated into the right and left arches and (B) simultaneous identification of the four brachiocephalic vessels - the "four-vessel sign" characteristic of a double aortic arch. Comparative image on computed tomography angiography.*

Subcostal or five-chamber apical window

Visualization of a bifurcated ascending aorta similar to the pulmonary artery bifurcation

The aorta bifurcation into the double arch is seen at a significant distance from the aortic valve plane (about 4–4.5 cm) as opposed to the early bifurcation seen in the transposition of the great arteries, type I truncus, hemitruncus, and aortopulmonary window[5-7] (Figure 3).

Conclusion

Echocardiography is the ideal method of screening for double aortic arch due to being non-invasive, easily performed, and of low cost. The presence of an aortic arch on the right or left with a normal innominate artery branching pattern into the carotid and subclavian arteries or originating separately from the four cephalic vessels of the same arch excludes the presence of a double aortic arch. Cardiac magnetic resonance imaging and computed tomography should be reserved for diagnostic confirmation and preoperative planning.

Author's contributions

Research conception and design: Souza GG; Data collection: Wang R; Data analysis and interpretation: Guimarães AFM, Castilho SRT; Manuscript writing: Guimarães AFM, Souza GG; Critical review of the manuscript for intellectual content: Tonelli HAF, Araújo FDR.

Conflict of interest

The authors have declared that they have no conflict of interest.

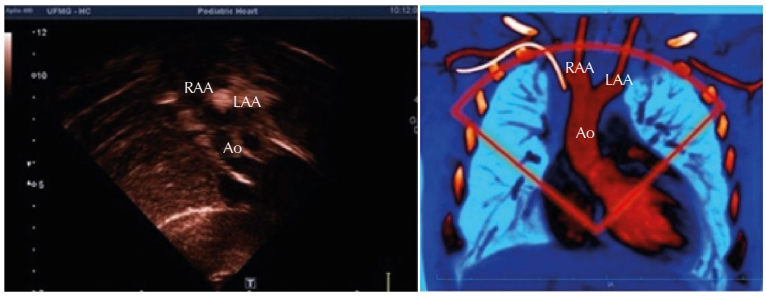

Ao, ascending aorta; LAA, left aortic arch; RAA, right aortic arch.

Figure 3 – *Subcostal echocardiographic image of the left ventricular outflow tract showing bifurcation of the ascending aorta into the right and left arches at a significant distance from the aortic valve plane. Comparative image on computed tomography angiography.*

References

1. Saito N, Kato S, Saito N, Nakachi T, Fukui K, Iwasawa T, et al. A case of complete double aortic arch visualized by transthoracic echocardiography. Echocardiography. 2017;34:1257–59. doi: https://doi.org/10.1111/echo.13568.
2. Mittal A, Chang C. Case of a septuagenarian with an asymptomatic double aortic arch. Chest. 2013;144(4):125A. doi: https://doi.org/10.2147/imcrj.s12009.
3. Parikh SR, Ensing GJ, Darragh RK, Caldwell RL. Rings, slings and such things: diagnosis and management with special emphasis on the role of echocardiography. J Am Soc Echocardiogr. 1993;6(1):1-11. doi: https://doi.org/10.1016/s0894-7317(14)80250-2
4. Blackwelder H, Madueme P, Dadlani G, Ivsic T. Multi-modality assessment of the aortic arch branching and vascular rings. Progress in Pediatric Cardiology. 2020;58:101268.
5. Sahn DJ, Valdes-Cruz LM, Ovitt TW, Pond G, Mammana R, Goldberg SJ, et al. Two dimensional echocardiography and intravenous digital video subtraction angiography for diagnosis and evaluation of double aortic arch. Am J Cardiol. 1982;50(2):342-6. doi: https://doi.org/10.1016/j.echo.2018.05.004.
6. Lee ML. Diagnosis of the double aortic arch and its differentiation from the conotruncal malformations. Yonsei Med J. 2007;48(5):818-26. doi: https://doi.org/10.3349/ymj.2007.48.5.818
7. Lillehei CW, Colan S. Echocardiography in the preoperative evaluation of vascular rings. J Pediatr Surg. 1992;27(8):1118-20; discussion 1120-1. doi: https://doi.org/10.1016/0022-3468(92)90571-n
8. Madry W, Zacharska-Kokot E, Karolczak MA. Methodology of echocardiographic analysis of morphological variations of the aortic arch and its branches in children - own experience. J Ultrason. 2019;19(76):24-42. doi: https://doi.org/10.15557/JoU.2019.0004
9. Poletto E, Mallon MG, Stevens RM, Avitabile CM. Imaging review of aortic vascular rings and pulmonary sling. J Am Osteopath Coll Radiol. 2017;6(2):5-14.
10. Murdison KA, Andrews BA, Chin AJ. Ultrasonographic display of complex vascular rings. J Am Coll Cardiol. 1990;15(7):1645-53. doi: https://doi.org/10.1016/0735-1097(90)92842-p.

Coronary Flow Velocity Reserve and Myocardial Contractility Under Stress in the Post-Infarction Ischemic Memory Dilemma

Reserva de Velocidade de Fluxo Coronariano e da Contratilidade Miocárdica sob Estresse no Dilema da Memória Isquêmica Pós-Infarto

Marilia Esther Benevides de Abreu[1], Tereza Cristina Diógenes Pinheiro[1], Antônio Augusto Lima Guimarães[2], José Sebastião de Abreu[1-3]

Clinicárdio Métodos Diagnósticos de Fortaleza[1], Fortaleza, CE, Brasil. Universidade Federal do Ceará[2], Fortaleza, CE, Brasil. Universidade Estadual do Ceará[3], Fortaleza, CE, Brasil.

Introduction

After acute myocardial infarction (AMI), some cases progress with deep T wave inversions on electrocardiogram (ECG). This electrocardiographic abnormality can continue for a prolonged period, even if a coronary intervention within a short time of AMI progression results in successful myocardial reperfusion. However, these deep T wave inversions can raise management questions when the patient is already being followed up in an outpatient clinic, particularly in the absence of relevant symptoms to support the resurgence of an ischemic process. In this context, a safe noninvasive assessment such as dobutamine stress echocardiography (DSE) associated with the analysis of coronary flow velocity reserve (CFVR) may be an option for this dilemma between myocardial ischemia and the possible post-infarction ischemic memory.[1-3]

Case report

A 59-year-old man with hypertension and dyslipidemia presented with intense oppression, retrosternal burning, and AMI. After approximately one hour of progression, he underwent a hemodynamic study that identified a proximal anterior descending coronary artery (ADA) occlusion (Figures 1A, 1B); the other coronary arteries were normal. The ADA became completely patent after stent implantation with *Thrombolysis in Myocardial Infarction* (TIMI) 3 without blushing (Figure 1C). Forty days after the AMI, the patient attended a cardiology appointment. He had been told about the ECG changes in a previous appointment and was unsure about to which restrictions he would be subjected. He reported mild nonspecific chest pain unrelated to exertion. A physical examination revealed good general condition, eupneic, normal pulmonary auscultation, regular rhythm in three heart beats by the fourth heart sound, and a blood

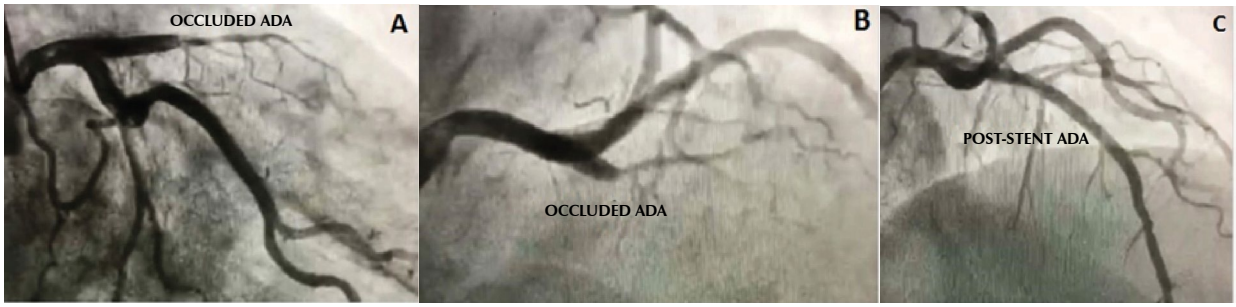

Figure 1 – *Coronary angiography showing ADA occlusion (A, B) and complete arterial patency after stent implantation (C). ADA, anterior descending coronary artery*

Keywords

Stress echocardiography; Dobutamine; Myocardial infarction.

Mailing Address: José Sebastião de Abreu •
Rua Dr. José Lourenço, 500, apto. 700, Meireles. CEP 60115280 – Fortaleza, CE, Brazil.
E-mail: jsabreu@cardiol.br/jsabreu10@yahoo.com.br
Manuscript received 5/28/2021; revised 12/15/2021; accepted 1/26/2022

DOI: 10.47593/2675-312X/20223501eabc221

pressure of 130/70 mmHg. The patient used beta-blockers, aspirin, diuretics, rosuvastatin, and ticagrelor.

An ECG performed before the AMI showed normal ventricular repolarization, while the current test showed deep T wave inversion in the anterior wall (Figure 2A). New tests showed a normal blood count, renal function, and electrolyte, creatine kinase-MB, troponin, and lactate dehydrogenase levels. Echocardiography showed mild concentric left ventricular hypertrophy and normal valves and pericardium. Myocardial hypocontractility was present in the ADA territory, but this vessel had prominent predominant diastolic flow with normal Doppler velocity (Figure 3A). As this coronary artery was patent and the patient had no relevant symptoms, a DSE with simultaneous noninvasive CFVR assessment was proposed. The patient was informed of the benefits and risks of this procedure, which was programmed after his consent.

On DSE, dobutamine was administered in continuous intravenous infusion at doses of 10, 20, and 30 μcg.kg^{-1}.min^{-1} in three-minute stages, with atropine 0.5 mg being administered in the third stage and reaching maximum heart rate (HR) (220 - age in years). At this point, the test was concluded and a bolus of 3 mg of esmolol was administered intravenously and later repeated to return the HR to baseline levels.[1, 2] ADA flow was checked intermittently to reach a diastolic velocity twice as high as that at baseline to determine a normal CFVR ($\geq$2).[3-5] It should be noted that this normal coronary reserve was obtained early (HR = 98 bpm), i.e., at only 61% of the maximum test HR (Figure 3B). During DSE, the contractile response became normal (Video) without complications or symptoms. During the test, ECG showed T wave polarity normalization (Figure 2B).

Discussion

The demonstration of post-infarction ischemia can be challenging in specific conditions, especially in the absence of relevant clinical signs, showing the need to rule out differential diagnoses to improve safety regarding life risk or restrictions on the patient's daily activities.

Laboratory test findings were incompatible with myocardial injury, and no pericardial involvement was identified on echocardiography. Increased wall thickness can indicate a noticeable ventricular repolarization abnormality such as in asymmetric septal hypertrophy, apical hypertrophy, or Fabry disease; however, in this case, the hypertrophy was concentric and mild.

DSE is a safe and well-established test for coronary heart disease diagnosis and prognosis. Dobutamine also acts as a potent vasodilator, enabling a validated CFVR assessment. This is obtained by simply dividing the peak diastolic velocity obtained during stress by the one recorded at rest in the ADA flow, with a cutoff point $\geq$ 2 being the normal value. CFVR is highly accurate at indicating a good prognosis or the absence of ischemia, particularly if it is obtained early (before DSE completion).[3, 5-7]

The greatest proportion of myocardial thickening is determined by the contraction of its inner third in the endocardium.[8] Consequently, an injury with less significant necrosis can determine ventricular wall hypokinesia on echocardiography, even after the ischemic event. However, an expressive contractile reserve is expected after physical or pharmacological stimulation in cases of minor injury. The patient reported here was reperfused within one hour of the AMI onset, which could justify the mild injury and the excellent contractile response during DSE.

The diagnosis of ischemic memory is unusual, but we consider its application adequate for the case presented here, as we have no elements other than previous ischemia to justify these marked ventricular repolarization changes. In fact, some facts substantiate the term ischemic memory in this case: first, the absence of a clinical presentation compatible with coronary insufficiency at rest or even during

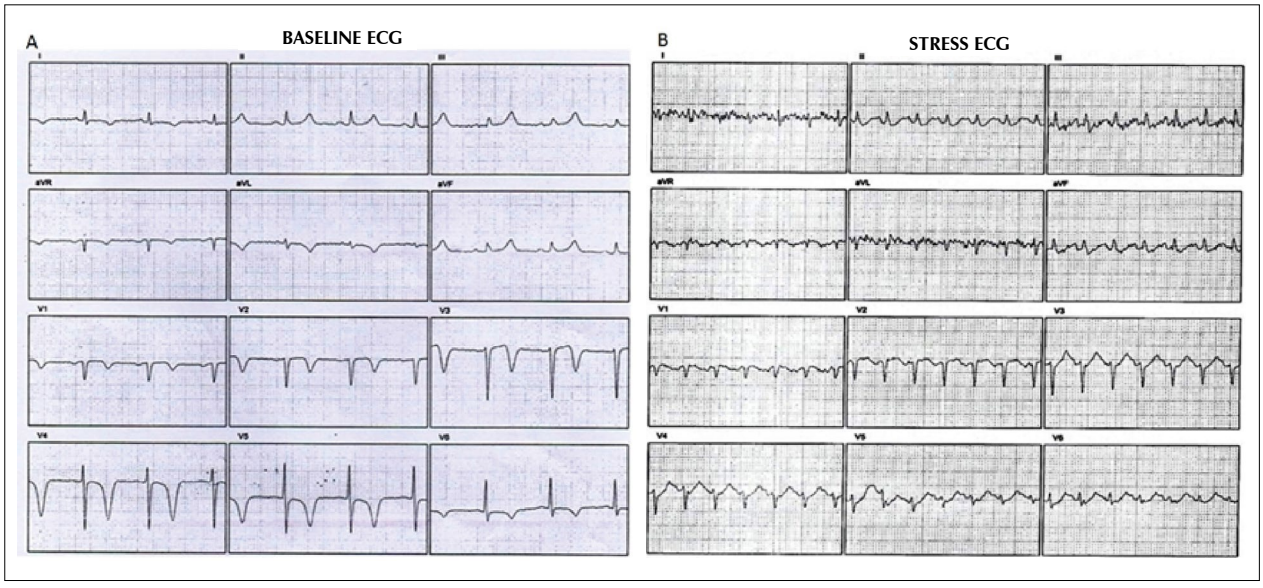

Figure 2 – *Electrocardiogram performed 40 days after the acute myocardial infarction showing an anteroseptal inactive zone and deep T wave inversion in the anterior wall (A). T wave polarity is normalized during stress echocardiography (B).*

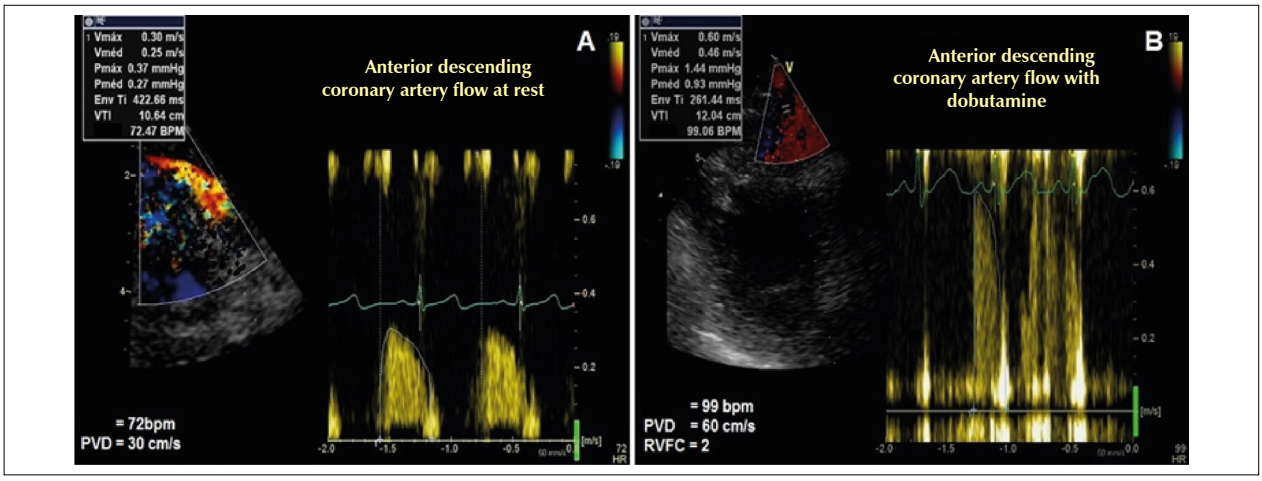

Figure 3 – *Baseline Doppler showing a normal PDV in the left ADA (A). A normal CFVR (≥2) is achieved during stress echocardiography at only 61% of maximum HR for age (B). CFVR, coronary flow velocity reserve; PDV, peak diastolic velocity*

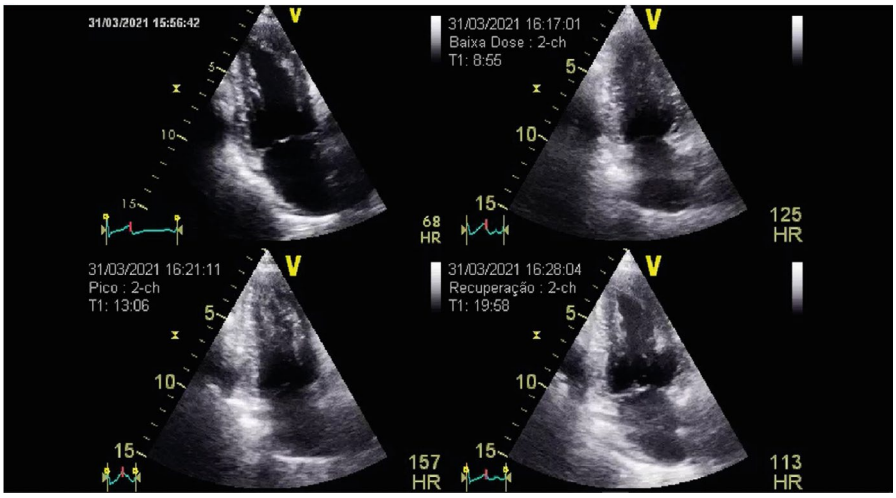

Video 1 – *Apical two-chamber view on stress echocardiogram showing normal inferior wall contraction and hypokinesia of the anterior wall at baseline (upper left frame). During stress, the absence of ischemia is observed at maximum heart rate represented by the excellent contractility of both walls (bottom left frame).*

DSE at maximum HR; second, the excellent contractile response of the myocardium during the test; third, the confirmation that the stress ECG showed no ischemia; and fourth, the ADA was patent with good basal flow, showing normal coronary reserve early.

The term "cardiac memory" has been used in cases that show diffuse T wave ECG inversions that may appear after ventricular tachycardia, intermittent left bundle branch block, or Wolff-Parkinson-White syndrome. We initially could not unquestionably rule out the possibility that the patient had previously presented any of these conditions. However, even in the most severe cardiac memory presentations, ECG presents positive or biphasic T wave polarity in the DI lead and positive polarity in the aVL lead.[9, 10] In this case, the T wave inversion extended to the entire anterior wall, so the possibility of cardiac memory was unlikely.

The exact mechanism of post-infarction ischemic memory is unclear, but it is common to see patients with adequate myocardial reperfusion showing significant ventricular repolarization changes. Considering the isolated ADA disorder, demonstrating its patency in a resting condition corroborates the possibility of DSE assessing the coronary reserve and myocardial contractile reserve, defining the diagnosis and prognosis and avoiding additional tests.[11]

Conclusion

In the presence of a patent ADA, the demonstration of normal CFVR and myocardial contractility during DSE favor a good prognosis despite the presence of inverted and deep T waves in the anterior wall on ECG in the post-infarction period.

Authors' contribution

Conception and design of the research: Abreu MEB and Abreu JS; Writing of the manuscript : Abreu MEB and Abreu JS; Analysis and interpretation of the data: Abreu MEB and Abreu JS; Acquisition of data: Pinheiro TCD, Guimarães AAL and Abreu JS; critical review of the manuscript for important intellectual content: Pinheiro TCD, Guimarães AAL and Abreu JS.

Conflict of interest

The authors have declared that they have no conflict of interest.

References

1. Pellikka PA, Arruda-Olson A, Chaudhry FA, Chen MH, Marshall JE, Porter TR, et al. Guidelines for Performance, Interpretation, and Application of Stress Echocardiography in Ischemic Heart Disease: From the American Society of Echocardiography. J Am Soc Echocardiogr. 2020;33(1):1-41.e8. doi: https://doi.org/10.1016/j.echo.2019.07.001
2. Abreu JS, Pinheiro TC, Abreu ME, Farias AG, Carneiro MM. Análise da segurança e exequibilidade do ecocardiograma sob estresse com dobutamina em dez mil e seis exames de uma população geral. ABC., Imagem Cardiovasc ; 33(4): eabc110, 20200000
3. Matsumura Y, Hozumi T, Watanabe H, Fujimoto K, Sugioka K, Takemoto Y, et al. Cut-off value of coronary flow velocity reserve by transthoracic Doppler echocardiography for diagnosis of significant left anterior descending artery stenosis in patients with coronary risk factors. Am J Cardiol. 2003;92(12):1389-93. doi: https://doi.org/10.1016/j.amjcard.2003.08.042
4. Forte EH, Rousse MG, Lowenstein JA. Target heart rate to determine the normal value of coronary flow reserve during dobutamine stress echocardiography. Cardiovasc Ultrasound. 2011;9:10. doi: https://doi.org/10.1186/1476-7120-9-10
5. Abreu JS, Rocha EA, Machado IS, Parahyba IO, Rocha TB, Paes FJ, et al. Prognostic value of coronary flow reserve obtained on dobutamine stress echocardiography and its correlation with target heart rate. Arq Bras Cardiol. 2017;108(5):417-26. doi: https://doi.org/10.5935/abc.20170041
6. Meimoun P, Sayah S, Tcheuffa JC, Benali T, Luycx-Bore A, Levy F, et al. Transthoracic coronary flow velocity reserve assessment: comparison between adenosine and dobutamine. J Am Soc Echocardiogr. 2006;19(10):1220-8. doi: https://doi.org/10.1016/j.echo.2006.04.028
7. Pelletier-Galarneau M, Ferro P, Patterson S, Ruddy TD, Beanlands RS, deKemp RA. Comparison of myocardial blood flow and flow reserve with dobutamine and dipyridamole stress using rubidium-82 positron emission tomography. J Nucl Cardiol. 2021;28(1):34-45. doi: https://doi.org/10.1007/s12350-020-02186-1
8. Myers JH, Stirling MC, Choy M, Buda AJ, Gallagher KP. Direct measurement of inner and outer wall thickening dynamics with epicardial echocardiography. Circulation. 1986;74(1):164-72. doi: https://doi.org/10.1161/01.cir.74.1.164
9. Shvilkin A, Ho KK, Rosen MR, Josephson ME. T-vector direction differentiates postpacing from ischemic T-wave inversion in precordial leads. Circulation. 2005;111(8):969-74. doi: https://doi.org/10.1161/01.CIR.0000156463.51021.07
10. Nakagawa T, Yagi T, Ishida A, Mibiki Y, Yamashina Y, Sato H, et al. Differences between cardiac memory T wave changes after idiopathic left ventricular tachycardia and ischemic T wave inversion induced by acute coronary syndrome. J Electrocardiol. 2016;49(4):596-602. doi: https://doi.org/10.1016/j.jelectrocard.2016.04.001
11. Cortigiani L, Rigo F, Gherardi S, Bovenzi F, Molinaro S, Picano E, et al. Coronary flow reserve during dipyridamole stress echocardiography predicts mortality. JACC: Cardiovascular Imaging. 2012;5(11):1079-85.

Incidental Finding of Iliac Vein Compression Syndrome

Achado Incidental de Síndrome de Compressão da Veia Ilíaca

Marcelo Bellini Dalio[1], Milton Sérgio Bohatch Júnior[1], Tércio Ferreira de Oliveira[1], Maurício Serra Ribeiro[1], Edwaldo Edner Joviliano[1]

University of São Paulo, Ribeirão Preto Medical School of Medicine[1], Ribeirão Preto, São Paulo, Brazil.

A 49-year-old woman presented with a progressive history of bilateral buttock and calf intermittent claudication, reaching a walking distance of 10 m. She was a smoker and had hypertension. She had no history of venous thrombosis, leg edema, varicose veins, or signs of chronic venous disease. Her femoral pulses were absent. Computed tomography angiography showed occlusion of the infrarenal aorta with recanalization of both iliac arteries. Interestingly, the right common iliac artery compressed the left common iliac vein, which was enlarged (Figure 1). Left-sided dilated pelvic collaterals were observed: uterine and gonadal veins (Figure 2). There was no compression on the left renal vein.

She underwent an aorto-bi-iliac bypass with Dacron without complications. The left common iliac vein was distended and was tightly compressed when it passed behind the right common iliac artery (Figure 3). As the patient had no venous symptoms, the vein was left undisturbed. The postoperative course was uneventful, and the patient had no thrombotic events.

Iliac vein compression syndrome, also known as May-Thurner syndrome or Cockett syndrome, is a condition in which the left common iliac vein is compressed by the right common iliac artery against the vertebrae.[1] The compression causes intimal hyperplasia, inner webs, and spurs, which can lead to thrombosis.[2] Three clinical stages were described: I, asymptomatic; II, spurs without thrombosis; and III, thrombosis.[3]

The diagnosis requires the demonstration of a stenotic or occlusive venous segment on imaging. Computed tomography and magnetic resonance are helpful. Venography has been performed as the gold standard.[4] Recently, intravenous ultrasound has shown improved sensitivity and is becoming widely used in diagnosis.[5,6] Treatment is not recommended for asymptomatic patients. Symptomatic patients may benefit from self-expanding stents.[1]

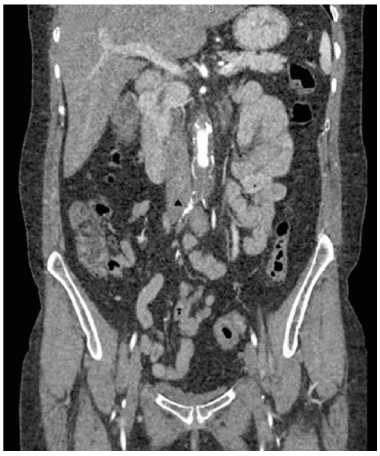

Figure 1 – *Computed tomography angiography of coronal sections showing occlusion of the infrarenal aorta with recanalization of both iliac arteries. The right common iliac artery compressed the left common iliac vein, which was enlarged (black arrowhead).*

Keywords

Iliac vein compression; syndrome, May-Thurner; Cockett; Asymptomatic Diseases.

Mailing Address: Marcelo Bellini Dalio •
Av. Bandeirantes 3900, 9º andar, Campus Universitário - Bairro Monte Alegre, Ribeirão Preto, São Paulo, Brazil. CEP: 14048900
E-mail: mbdalio@usp.br
Manuscript received 6/7/2021; revised 10/7/2021; accepted 12/8/2021

DOI: 10.47593/2675-312X/20223501eabc225

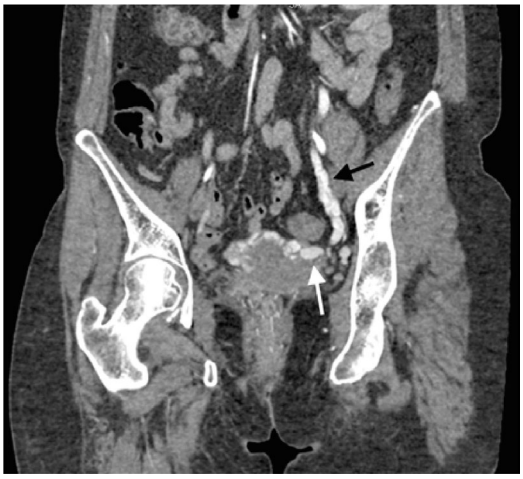

Figure 2 – *Computed tomography angiography in coronal section showing left-sided dilated pelvic collaterals: uterine veins (white arrow) and gonadal vein (black arrow).*

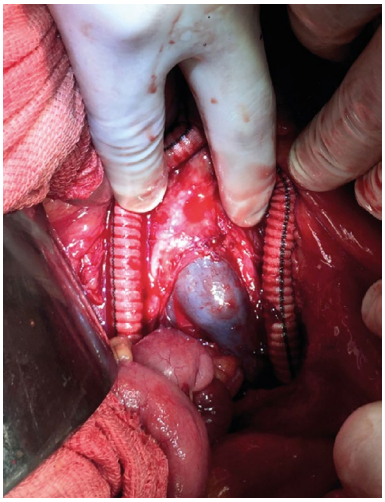

Figure 3 – *Intraoperative image of aorto-bi-iliac bypass procedure. The left common iliac vein was distended and tightly compressed when it passed behind the right common iliac artery.*

In our case, iliac vein compression was an incidental image finding confirmed during the procedure performed to treat another condition. Iliac vein compression is found in approximately 20% of patients without any venous symptom.[3] The patient received no specific treatment other than routine thrombosis prophylaxis. She did not receive therapeutic anticoagulation.

This study is in concordance with the institutional ethics committee and required consents were obtained. The patient agreed to the publication of the case and images.

Authors' contribution

Conception and design: Dalio MB, Bohatch Júnior MS, Oliveira TF; Analysis and interpretation: Dalio MB, Bohatch Júnior MS, Oliveira TF, Ribeiro MS, Joviliano EE; Data collection: Dalio MB, Bohatch Júnior MS, Oliveira TF; Writing the article: Dalio MB, Bohatch Júnior MS, Oliveira TF, Ribeiro MS, Joviliano EE; Critical revision of the article: Dalio MB, Bohatch Júnior MS, Oliveira TF, Ribeiro MS, Joviliano EE; Final approval of the article: Dalio MB, Bohatch Júnior MS, Oliveira TF, Ribeiro MS, Joviliano EE; Agreement to be accountable: Dalio MB, Bohatch Júnior MS, Oliveira TF, Ribeiro MS, Joviliano EE

Conflict of interest

The authors have declared that they have no conflict of interest.

References

1. Rehman ZU. May–Thurner and Paget–Schroetter Syndromes: A Review. Ann Vasc Dis. 2020;13:132–6.
2. Esposito A, Charisis N, Kantarovsky A, Uhl JF, Labropoulos N. A Comprehensive Review of the Pathophysiology and Clinical Importance of Iliac Vein Obstruction. Eur J Vasc Endovasc Surg. 2020;60:118–25.
3. Kibbe MR, Ujiki M, Goodwin AL, Eskandari M, Yao J, Matsumura J. Iliac vein compression in an asymptomatic patient population. J Vasc Surg. 2004;39: 937–43.
4. Zucker EJ, Ganguli S, Ghoshhajra BB, Gupta R, Prabhakar AM. Imaging of venous compression syndromes. Cardiovasc Diagn Ther. 2016;6(6):519-32.
5. Knuttinen M-G, Naidu S, Oklu R, Kriegshauser S, Eversman W, Rotellini L, et al. May-Thurner: diagnosis and endovascular management. Cardiovasc Diagn Ther. 2017;7(Suppl 3):S159-S164.
6. Joh M, Desai KR. Treatment of Nonthrombotic Iliac Vein Lesions. Semin Intervent Radiol. 2021;38(2):155-9.

Intermittent Aortic Intraprosthetic Failure

Insuficiência Intraprotética Aórtica Intermitente

Luciano H Melato[1], Daniela do Carmo Rassi[2], Rogério G Furtado[1], Ana Caroline R Oliveira[1]

[1]*Diagnostic Imaging Center – CDI, Goiânia, Goiás, Brazil.* [2]*School of Medicine, Federal University of Goiás, Goiânia, GO, Brazil.*

Intermittent mechanical prosthesis dysfunction is a rare and potentially serious complication[1–4] that can affect prostheses in the aortic[5] or mitral position. It causes obstruction or intermittent central regurgitation depending on the phase of the cardiac cycle in which the disk becomes stuck.[3] The most common cause of this dysfunction is pannus formation,[3,4] which may also occur due to thrombosis, mitral subvalvular tissue, suture material, vegetations, ventricular myocardium,[3] or mechanical failure.[2] Left untreated, transient mobility loss leads to permanent disk immobilization.[3] In this scenario, a patient in whom a size 21 Carbomedics® metallic aortic prosthesis was implanted 14 years prior was referred for echocardiography due to abnormal cardiac auscultation findings. Transthoracic and transesophageal echocardiograms showed significant intermittent central prosthetic regurgitant jet unrelated to arrhythmias (Figure 1; Videos 1 and 2). The mean prosthetic gradient was 29 mm Hg and the effective valve area was 1.08 cm^2. A refringent, periannular, fixed, sub- and supra-prosthetic image suggestive of pannus was also identified (Figure 2), which became the main etiological hypothesis for this unusual dysfunction presentation.

Authors' contributions

Data and images acquisition: LHM; Manuscript writing: DCR, LHM; Critical revision of the manuscript for important intellectual content: RGF e ACRO

Conflict of interest

The authors have declared that they have no conflict of interest.

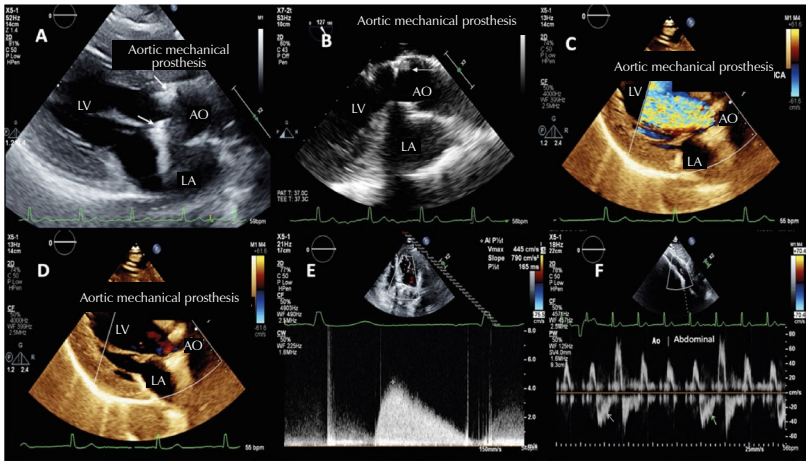

AO, aorta; LA, left atrium; LV, left ventricle.

Figure 1 – *Transthoracic echocardiography (A) and transesophageal echocardiography (B) images showing fixed (arrows) hyper-refringent sub- and supra-prosthetic images suggestive of pannus. Color flow mapping demonstrates significant aortic prosthetic regurgitation (C) with no signs of prosthetic regurgitation in the next cardiac cycle (D) on the same projection. Aortic prosthetic regurgitating jet with a pressure half-time of less than 200 msec (E). Presence of intermittent holodiastolic reversal flow in the abdominal aorta (F; arrows).*

Keywords

Heart Valve Prosthesis; Echocardiography; Prosthesis Failure.

Mailing Address: Luciano Henrique Melato •
Avenida R11, 1.035, apto. 401. CEP 74125-100 – Goiânia, GO, Brazil.
E-mail: lhmelato@hotmail.com
Manuscript received 1/23/2022; revised 2/1/2022; accepted 2/14/2022

DOI: 10.47593/2675-312X/20223501eabc284

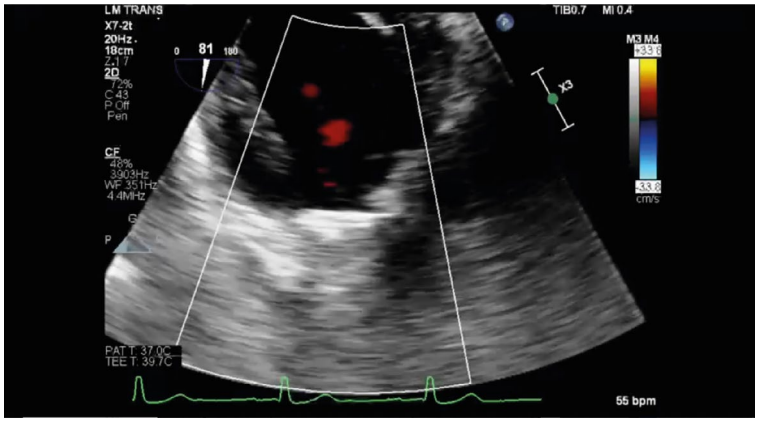

Video 1 – *Transesophageal echocardiography (trans-gastric view) showing intermittent aortic prosthetic regurgitation and a concomitant increase in left ventricular dimensions with a regular heart rhythm.*

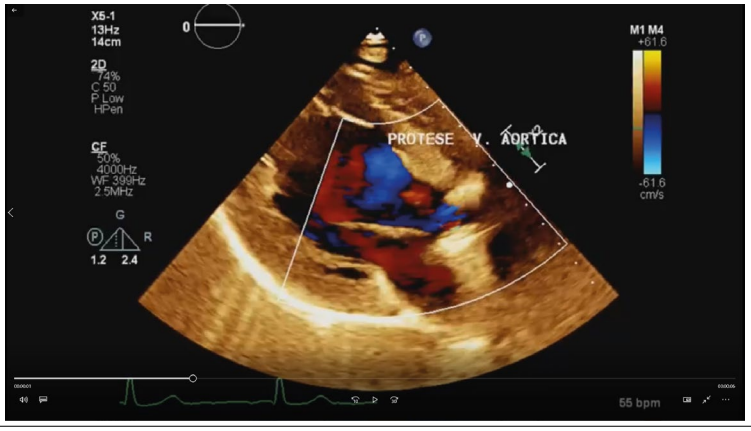

Video 2 – *Transthoracic echocardiography (longitudinal parasternal view) showing the intermittent intraprosthetic regurgitant jet of the mechanical aortic prosthesis with a regular heart rhythm.*

References

1. Melenovsky V, Al Hiti H, Lupinek P, Marek T, Veiser T, Skalsky I, et al. Intermittent cardiogenic shock in a man with mechanical prosthesis of the aortic valve. Circulation. 2011;124(1):e1-3. doi: https://doi.org/10.1161/CIRCULATIONAHA.110.012963
2. Eichinger WB, Hettich I, Bleiziffer S, Günzinger R, Hutter A, Bauernschmitt R, et al. Intermittent regurgitation caused by incomplete leaflet closure of the Medtronic ADVANTAGE bileaflet heart valve: analysis of the underlying mechanism. J Thorac Cardiovasc Surg. 2010;140(3):611-6. doi: https://doi.org/10.1016/j.jtcvs.2009.11.001
3. Fadel BM, Alassas K, Dahdouh Z, Pergola V, Galzerano D, Di Salvo G. Intermittent Malfunction of a Prosthetic Valve-A Diagnostic Challenge. Echocardiography. 2016;33(6):916-9. doi: https://doi.org/10.1111/echo.13210
4. Giroux SK, Labinaz MX, Grisoli D, Klug AP, Veinot JP, Burwash IG. Intermittent, noncyclic dysfunction of a mechanical aortic prosthesis by pannus formation. J Am Soc Echocardiogr. 2010;23(1):107.e1-3. doi: https://doi.org/10.1016/j.echo.2009.07.003
5. Galli CA, Muratori M, Montorsi P, Barili F, Polvani G, Pepi M. Cyclic intermittent aortic regurgitation of a mechanical bileaflet aortic valve prosthesis: diagnosis and clinical implications. J Am Soc Echocardiogr. 2007;20(11):1315.e5-8. doi: https://doi.org/10.1016/j.echo.2007.02.031